.

INFLUENCE OF MODIFIERS AND HEAT TREATMENT ON THE FATIGUE LIFE AND MECHANICAL PROPERTIES OF RECYCLED CAST ALUMINIUM ALLOYS

MICHAEL KAMAU NJUGUNA

MASTER OF SCIENCE
(MECHANICAL ENGINEERING)

JOMO KENYATTA UNIVERSITY OF

AGRICULTURE AND TECHNOLOGY

2007

.

INFLUENCE OF MODIFIERS AND HEAT TREATMENT ON THE FATIGUE LIFE AND MECHANICAL PROPERTIES OF RECYCLED CAST ALUMINIUM ALLOYS

MICHAEL KAMAU NJUGUNA

A thesis submitted in partial fulfilment for the Degree of Master of Science in Mechanical Engineering in the Jomo Kenyatta University of Agriculture and Technology

2007

DECLARATION

This thesis is my original work and has not been presented for a degree in any other University.

Signature ..... Date 05.11.2007

Michael Kamau Njũgũna

This thesis has been submitted for examination with our approval as the University Supervisors.

Signature ..... Date 12.11.2007

Dr. Eng. S. P. Ng'ang'a

JKUAT, Kenya

Signature ..... Date 12/11/07

Eng. B. O. Odera

University of Nairobi, Kenya

DEDICATION

To my dear wife Mũmbi; for your love, confidence, trust and immense patience. To our daughter Mũthoni; the limitless joy of our time.

ACKNOWLEDGEMENT

I would like to express my sincere gratitude to many people without whose selfless assistance this thesis would not have materialized. Much gratitude to my supervisors Dr. Eng. S. P. Ng'ang'a and Eng. B. O. Odera; without whose invaluable and professional advice, it would have been impossible to undertake and complete this work. Many thanks to Mr. T. O. Mbuya (University of Nairobi) for his tireless help in obtaining reference materials and sharing his deep insights on aluminium casting.

I am thankful to my colleagues and friends in the postgraduate programme; Mr. Kamau Hinga, Mr. Adika Adenya and Mr. Ondoro Otieno for the many useful discussions we had and the encouragement we continually shared. I cannot forget our 'elders' in the programme, namely Mr. Gĩtahi and Mr. Nderitũ for providing useful tips on the use of LaTex in report writing; many thanks.

Great thanks to the Chief Technician Mr. E. Kĩbiro too, for his assistance during use of computer laboratory and providing essential softwares; Mr. Michael Mwai and Mr. Richard Nyanjui for their patience, unreserved and dedicated help during the many hours of work at the foundry and during heat treatment; Mr. P. Waribu for his untiring assistance in fatigue testing and metallographic specimen preparation; Mr. Njue (University of Nairobi) for dedicating his time to assist me carry out microstructure examination and to many other members of staff in the Department of Mechanical Engineering as well as the Engineering Workshops for lending their help in various ways. I am most grateful to the Jomo Kenyatta University of Agriculture and Technology for sponsoring this work.

Special thanks to my wife, Mũmbi, for her encouragement and prayers. I also extend many thanks to my parents and family, friends and colleagues for all their support. Most important of all, to the Almighty, for availing this chance for study; I am eternally thankful.

TABLE OF CONTENTS

LIST OF FIGURES

LIST OF TABLES

NOMENCLATURE

AA	Aluminium Association
a	Fatigue crack size (μm)
$ASTM$	American Standards for Testing Materials
DAS	Dendrite Arm Spacing
DC	Directly Cooled
DCS	Dendrite Cell Size
$\%E$	Percent Elongation (%)
FCG	Fatigue crack growth
HCF	High Cycle Fatigue
HIP	Hot Isostatic Pressing
$HPDC$	High Pressure Die Casting
ISO	International Organization for Standardization
K	Stress Intensity Factor
LCF	Low Cycle Fatigue
$LEFM$	Linear Elastic Fracture Mechanics
LM	Light Metals
M	Modified
N	Number of fatigue life cycles
n	Strain hardening exponent
N_f	Number of fatigue cycles to failure
N_p	Fatigue Propagation Life (in cycles)
OES	Optical Emission Spectroscopy
PA	Peak aged
PEC	Precision Engineered Component
$PSBs$	Persistent Slip Bands
$SDAS$	Secondary Dendrite Arm Spacing
SEM	Scanning Electron Microscope

SSM	Semi-Solid Metal casting process
TEM	Transmission Electron Microscope
$T4$	Thermal treatment temper designation, solution heat treated quenched, and naturally aged to a substantially stable condition
$T6$	Thermal treatment temper designation, solution heat treated, quenched and then artificially aged
UA	Under aged
UM	Unmodified
UTS	Ultimate Tensile Strength (MN/m^2)
YS	Yield Strength (MN/m^2)
319	Aluminium Association (AA) designation for a casting alloy with Al-Si-Cu as the major constituents, (5.5-6.5%Si and 4-5%Cu)
332	AA designation for a casting alloy with Al-Si-Mg-Cu as the major constituents (8.5-10.5%Si, 0.7-1.3%Mg and 2.0-4.0%Cu)
355	AA designation for a casting alloy with Al-Si-Cu-Mg as the major constituents (5%Si and 1%Cu)
356	AA designation for a casting alloy with Al-Si-Mg as the major constituents (6.5-7.5%Si and 0.25-0.45%Mg)
380	AA designation for a casting alloy with Al-Si-Cu-Fe as the major constituents (7.5-9.5%Si, 1.3%Fe and 3-4%Cu)

σ	Stress (MN/m^2)
σ_{max}	Maximum applied stress (MN/m^2)
σ_{min}	Minimum applied stress (MN/m^2)
σ_a	Stress amplitude (MN/m^2)
ΔK	Stress intensity factor range ($MPa/m^{\frac{1}{2}}$)
ΔK_{th}	Threshold stress intensity factor range ($MPa/m^{\frac{1}{2}}$)
ΔK_{eff}	Effective stress intensity factor range ($MPa/m^{\frac{1}{2}}$)

ϵ	True plastic strain
K_q	Strength coefficient (MN/m^2)
Q	The quality index
q	Relative ductility parameter
U	Crack closure factor
$Y(a)$	Compliance calibration factor

ABSTRACT

Recycling aluminium provides metal at only 5% of the energy invested in producing primary aluminium from ore. Further, recycling aluminium alloys provides an alternative source of raw material to ores, in addition to ensuring that aluminium scrap is put to good use. Across the world, there is a renewed drive to explore new uses for recycled aluminium alloy products. To widen the scope of application for recycled aluminium alloy products, it is necessary to understand the whole range of properties that is possible to achieve, particularly when property influencing processes such as modification and heat treatment are used.

An investigation was carried out to determine the effects of modification and heat treatment on recycled cast aluminium alloys. The effects of these two processes on the fatigue life and mechanical properties of sand cast secondary foundry aluminium alloys were investigated. Selected scrap components mainly composing of pistons, cylinder heads, gearbox housings and oils sumps were used. Unmodified and sodium (Na) modified samples were subjected to the T6 and T4 heat treatment while others were tested in the 'as cast' condition. To investigate the influence of varying the heat treatment parameters on the mechanical properties, different sample sets were subjected to different solution treatment and ageing times. Constant amplitude, fully reversed fatigue tests under a stress ratio of R = -1 were carried out using a rotating bending machine at room temperature.

Increasing the sodium content to 0.025% was found to improve the tensile properties of the secondary alloys obtained. However, increasing the modifier content to 0.020%Na led to a reduction in the fatigue life properties of the recycled aluminium alloy, thus modification reduced the fatigue life.

Heat treatment to the T6 condition increased the ultimate tensile strength and the hardness of the secondary alloy when compared with the T4 temper condition. Increasing the ageing time was also found to increase strength properties

of the secondary aluminium alloys. Quality index charts for the aged recycled aluminium alloys were also developed. Compared with the 'as cast' samples, T6 heat treated samples had fatigue lives that were over 50% higher. T4 heat treated samples had fatigue lives close to those of the T6 condition.

The results indicate that the secondary aluminium alloys used in this study had chemical compositions that were very close to some existing primary commercial alloys especially AC 2A, LM22, LM16, LM4, 332 and 319. However, the fatigue life and mechanical properties were much lower.

Chapter 1

INTRODUCTION

1.1 Overview

In recent years, there has been a notable shift towards the use of low cost lightweight materials in a wide range of engineering applications. Due to its favourable properties, aluminium is widely used in the manufacture of critical parts and components for the automotive industry such as engine blocks, cylinder heads, pistons, wheels, suspension cross members, control arms, steering column housings, hydraulic system housings, crank shaft hubs, front knuckles and scroll compression air conditioning systems [1].

A wide range of aluminium alloys such as 319, 356 and 380 families are commonly used in casting engine blocks and cylinder heads. The increase in the use of aluminium alloy products coupled with the ease with which aluminium alloys can be recycled has led to an expansion of the cast secondary aluminium alloy industry worldwide. It is envisioned that the use of recycled cast aluminium will continue to increase and hence the need for a complete understanding of its properties in comparison to primary aluminium alloy products as well as other engineering materials.

Recycling of aluminium products has certain distinct advantages. The most distinct one is the reduced cost due to the fact that remelting aluminium scrap takes only about 5% of the total amount of energy required to produce the same tonnage of primary aluminium by the electrolytic reduction process [2].

However, recycling aluminium scrap can often be problematic. Aluminium easily oxidizes leading to contamination with an oxide layer. Each time aluminium is remelted, there is a consequent oxidation and resultant loss of aluminium to dross. Dross cannot be eliminated, but ways to minimize it have been suggested

[3]. Minor elements added in processing primary aluminium alloys for some specific purposes have been observed to impart some carryover effects. As an example, grain refiners like $TiAl_3$, TiB_2 and TiC have been demonstrated to provide some residual refining effect and small additions are enough to rejuvenate them to full potency. Modifiers may also carryover through the melt; antimony is able to reproduce its full modifying effect even after numerous remeltings, whereas sodium and strontium lose their effect more rapidly. Melt treatments like inert degassing and melt filtration (for example, ceramic foam filters) are recommended for use in processing secondary alloys in order to maintain the best possible quality [2, 4].

1.2 Statement of the Problem

Over the years, the use of aluminium alloy products has been on an upward trend all over the world. As an example, in 1900 the annual output of aluminium was one thousand tonnes, but by the end of the twentieth century the annual production had reached 32 million tonnes comprising 24 million tonnes of primary aluminium and 8 million tonnes from recycled metal [5]. In Kenya, once the useful life of an aluminium alloy product is over, some of the scrap is recycled locally while the remainder is shipped out of the country. The scrap is easily available from the automotive industry and is sold at reasonable rates. Previous studies have shown that the Kenyan foundry sector uses about 23% of its available capacity [6]. Reasons such as availability of only a limited range of cast products (that are of poor quality) which are poorly marketed and use of low level technology have been cited for this low level of capacity utilization. A study on the operations of the Kenyan foundry sector [7] focussed on the possible reasons for the above. Some of the noted shortcomings were; the use of low quality raw materials, lack of continued research in foundry and the use of low levels of casting and molding technology. Others include lack of cooperation

among the foundry stake holders and the lack of trained operators beyond the craft courses for the foundry industry.

The foundry sector has received a lot of attention in different parts of the world. A coordinated approach by industry, research institutions and government-funded institutions has led to major developments in foundry technology. In addition, this coordinated approach has made the dissemination of foundry knowledge and collective identification and solution of foundry sector problems much easier to achieve. As an example, in Australia, the Cooperative Research Centre for Cast Metals Manufacturing (CAST) coordinates research work in casting, dissemination of research knowledge and services that promote the casting industry. In the United States of America, the American Foundrymen Society (AFS) provides and promotes knowledge and services that strengthen the metal casting industry [4].

Aluminium scrap is purchased in various forms and compositions. Ideally, it should be sorted, blended, melted and alloyed to the required customer specifications. The secondary aluminium alloys will inevitably contain more impurities and in larger quantities than primary aluminium alloys. The levels and types of impurities present are expected to vary depending on the country of origin of the scrap. As an example, in Europe and Japan, antimony is used to control the eutectic silicon structure; the same antimony would act as an impurity in strontium modified Al-Si alloy castings produced in Australia and North America. Foundry shops in Kenya do not separate the scrap from different countries of origin. The result is that the scrap from different sources is mixed in the casting process. It is therefore expected that the different mix of trace elements and impurities will impart some deleterious effects on the properties of the resultant products.

It has been found that secondary alloys are almost equivalent in terms of chemical composition to several commercial Al-Si-Cu based alloys [8]. However, the mechanical properties do not correlate well with those of the equivalent commercial counterparts. Previous research has focussed mainly on alloy chemistry and process variables but no data has been generated on fatigue properties or influence of modifiers on mechanical properties [8]. It is therefore necessary to carry out further work on the secondary aluminium alloys with the aim of expanding the scope of available data on these alloys and comparing the results with those already documented. As regards locally recycled aluminium scrap, there is no known literature available on fatigue properties of the resulting melt. In addition, very little information is available regarding the properties of such melts after heat treatment.

It is clear from these observations that the study on locally processed secondary aluminium alloys has many gaps which need to be filled. It is necessary to understand the various aspects of the foundry process, the resulting products and their properties in full. This will go a long way in improving and widening the scope and breadth of the aluminium industry at large. These observations provide the motivation for this study on recycled aluminium alloys.

1.3 Objectives

The major objective of this study was to investigate the influence of modification and heat treatment on the fatigue life and the mechanical properties of recycled aluminium alloys.

Specifically, this work involved:

- Varying the modifier (sodium) content to investigate the influence of modification on the fatigue life, ultimate tensile strength, elongation and hard-

ness properties of the recycled aluminium foundry alloys.

- Heat treating the secondary foundry alloy to the T4 and T6 temper condition to investigate the influence of heat treatment on the fatigue life, ultimate tensile strength, elongation and hardness properties of the recycled aluminium foundry alloys
- Investigating the influence of varying the solution treatment time and ageing time on the mechanical properties of the recycled aluminium foundry alloys.
- Developing the Quality Index curves for the recycled cast aluminium alloys.

Chapter 2

LITERATURE REVIEW

2.1 Introduction

Aluminium is the second most commonly used metal in the world today, after Iron. Due to its attractive properties, aluminium has steadily grown in stature since it was first discovered almost two centuries ago and the popularity continues to increase as more research related to aluminium and its alloys is carried out. Aluminium occurs naturally, mainly as bauxite but also to a lesser extent as cryolite, alunite, leucite and alum shales. Alumina, an oxide of aluminium, is obtained from the aluminium ore by any of the various processing methods such as the bayer process or the pechiney system. Aluminium of varying purity levels is then obtained by a reduction process (mainly the Hall-Heroult process) before refining to commercially acceptable purity. Pure aluminium is a group III element, with atomic number 13, silvery white in colour with a high reflectivity for heat and light. Pure aluminium has a density of 2.699g/cm^3 and the melting point of 99.99% aluminium is 660.2^{o}C [9].

2.2 Aluminium Alloys

Pure aluminium is a relatively weak metal. To improve the strength and widen the scope of its application, pure aluminium is alloyed with metals such as copper, magnesium, manganese and zinc usually in combinations of two or more of these elements together with iron and silicon. A wide range of aluminium alloys have been developed to meet particular requirements. These alloys are identified by a series of national and international standards which specify the compositions and the average mechanical properties. These standards differ from country to country but for most alloys within particular groups, the compositions and mechanical properties are closely identical.

Table 2.1: The International Designation System for Wrought Aluminium Alloys [9]

Designation	Major Alloying Element
1XXX	Aluminium of 99.00% minimum purity
2XXX	Copper
3XXX	Manganese
4XXX	Silicon
5XXX	Magnesium
6XXX	Magnesium plus Silicon
7XXX	Zinc
8XXX	Other elements
9XXX	Unused series

The alloys covered by the standards are divided into two groups; namely those used for castings and those to be fabricated into wrought forms. There is an internationally agreed four digit system for the wrought alloys in which the first of the four digits in the designation indicates the major alloying element within the group as shown in Table 2.1 [9]. The designations of aluminium casting

Table 2.2: National Specifications of Some Casting Alloys [10]

USA AA/ASTM	Britain	ISO	France	Germany	Italy	Japan
150	LM0	Al99.5	A5	-	UNI 3950	-
384	LM2	Al-Si10Cu2Fe	A-S9U3-Y4	-	UNI 5076	ADC12
319	LM4	Al-Si5Cu3	A-SU3	G-AlSi6Cu4 (225)	UNI 3052	AC 2A
541	LM5	Al-Mg5Si1	AG6	G-AlMg5 (224)	UNI 3058	AC 7A
-	-	Al-Mg6	-	-	-	-
A413	LM6	Al-Si12	AS13	G-AlSi12 (230)	UNI 4514	AC 3A
A360	LM9	Al-Si10Mg	A-S10G	G-AlSi10Mg (233)	UNI 3049	AC 4A
222	LM12	Al-Cu10Si12Mg	A-U10G	-	UNI 3041	-
336	LM13	Al-Si12Cu	A-S12UN	-	UNI 3050	AC 8A
355	LM16	Al-Si5Cu1Mg	A-S4UG	-	UNI 3600	AC 4D
A413	LM20	Al-Si12Cu	A-S12-Y4	G-AlSi12(Cu) (231)	UNI 5079	-
-	-	Al-Si12CuFe	-	-	-	-
308	LM21	Al-Si6Cu4	A-S5U2	G-AlSi6Cu4 (225)	UNI 7369	AC 2A
319	LM22	Al-Si5Cu3	A-S5U	G-AlSi6Cu4 (225)	UNI 3052	AC 2A
A380	LM24	Al-Si8Cu3Fe	A-S9U3-Y4	G-AlSi8Cu3 (226)	UNI 5075	AC 4B/ADC 10
A356	LM25	Al-Si9Cu4Mg	-	-	UNI 3599	-
332	LM26	Al-Si9Cu4Mg	-	-	UNI 3599	-
390	LM30	Al-Si17Cu4Mg	-	-	-	-
712	LM31	Al-Zn5Mg	A-Z5G	-	UNI 3602	-

alloys in different countries is shown in Table 2.2.

Table 2.3 shows different cast aluminium alloys designed to meet specific requirements and applications. The aluminium silicon alloy castings are the most commonly used and constitute 85 to 90% of total aluminium cast product parts produced worldwide [4]. Due to their attractive properties, aluminium silicon alloys have found prominent application in the automotive industry for components such as engine blocks and cylinder heads. Other uses include chassis and steering components such as control arms, steering gear components, front strut support bearings and wheels [11].

Table 2.3: Typical End Use of Aluminium Silicon Castings [10]

USA AA/ASTM Specification	ISO Specification	Typical end use
150	Al99.5	Electrical, food and chemical plant
319	Al-Si5Cu3	General engineering, cylinder heads, crankcases, clutch cases, gearboxes, tool handles, household fitings, electrical tools, office equipment
355	Al-SiCu1Mg	Air compressor pistons, air craft supercharger covers, fuel pump bodies, water cooled cylinder heads, valve bodies, water jackets and cylinder blocks.
308	Al-Si6Cu4	General engineering, crankcases, clutch cases, tool handles, gear boxes, household fittings, electrical fittings and office equipment.
A356	Al-Si7Mg	Aircraft pump parts, nuclear energy installations, aircraft fittings, food equipment, chemical, marine, road transport, cylinder blocks, cylinder heads and wheels.
A380	Al-Si8Cu13	Engineering die castings, motor housings, doors, vacuum cleaners, floor polishers and motor frames
332	Al-Si9Cu4Mg	Pistons for petrol and diesel engines
A360	Al-Si10Mg	Marine on deck castings, water cooled manifolds, doors, chemical equipment, dye and food plant, motor housings, cover plates and instrument casings
384	Al-Si10Cu2Fe	Almost any die casting component
336	Al-Si12	Pistons for petrol and diesel engines, pulleys
A413	Al-Si12	Marine on deck castings, water cooled manifolds, doors, chemical equipment, dye and food plant, motor housings, cover plates and instrument casings
390	Al-Si17Cu4Mg	Die cast automobile engine blocks without piston liners, air compressors, pumps, pulleys and brake shoes.

Amongst the hundreds of the Al-Si alloys available, there are some which are very popular for particular applications as shown in Table 2.3. The chemical composition and hence mechanical properties differ from one specification to another depending on the desired application. The composition also differs

depending on country of origin of the alloy. Table 2.4 shows some of the more commonly used Al-Si alloys, particularly those of the 3xx.x series.

Table 2.4: Percent chemical composition of some common casting alloys [10]

Alloy	Element									
	Si	Fe	Cu	Mn	Mg	Cr	Ni	Zn	Sn	Ti
222	2.00	1.50	9.2-10.7	0.50	0.15-0.36	0.2-0.6	0.50	0.80	0.05	0.25
308	5.0-6.0	1.00	4.0-5.0	0.50	0.10	0.25	0.35	1.00	0.05	0.25
319	5.5-6.5	1.00	4.0-5.0	0.50	0.10	0.25	0.35	1.00	0.01	0.25
332	8.5-10.5	1.20	2.0-4.0	0.50	0.5-1.5	0.35	2.0-3.0	0.35	0.05	0.25
336	11.0-13.0	1.20	0.5-1.5	0.35	0.7-1.3	0.35	2.0-3.0	0.35	0.05	0.25
335	4.5-5.5	0.60	1.0-1.5	0.50	0.4-0.6	0.25	0.5-1.5	-	-	0.25
A356	6.5-7.5	0.20	0.20	0.10	0.25-0.45	-	-	0.10	-	0.20
A360	9.0-10.0	1.30	0.60	0.35	0.4-0.6	-	0.50	0.50	0.15	-
A380	7.5-9.5	1.30	3.0-4.0	0.50	0.10	-	0.50	3.00	0.35	-
384	10.5-18.0	1.30	3.0-4.5	0.50	0.10	-	0.50	3.00	0.35	-
390	16.0-18.0	1.30	4.0-5.0	0.10	0.45-0.65	-		0.10	-	0.20
A413	11.0-13.0	1.30	1.00	0.35	0.10	-	0.50	0.50	0.15	-
514	0.35	0.50	0.15	0.35	3.5-4.5	-	-	0.15	-	0.25
712	0.30	0.50	0.25	0.10	0.5-0.65	0.4-0.6	-	6.0-6.5	-	0.15-0.25

2.2.1 The Aluminium Silicon Alloy System

Aluminium alloys have increasingly gained popularity and applications for critical components and structures in sectors such as automotive, aerospace, agriculture and defence. The popularity of aluminium alloys results from their excellent properties with regard to castability, stability, high strength to weight ratio, good weldability, good tensile and fatigue properties, low coefficient of expansion and good corrosion resistance [3, 9, 12, 13].

Binary aluminium silicon alloys combine the advantages of high corrosion resistance, good weldability, and low specific gravity [3]. The main feature of the Al-Si binary system is that a eutectic is formed at 577^{o}C with 11.7wt.%Si, as illustrated in Figure 2.1. This eutectic constitutes of a solid solution of a limited amount of silicon in aluminium and practically pure silicon particles [12]. In hypoeutectic alloys (such as Al-7Si), the aluminium solid solution precipitates from the liquid as the primary phase in the form of dendritic network followed by the eutectic reaction. Silicon reduces the coefficient of thermal expansion, increases

corrosion and wear resistance and improves the castability and machinability characteristics of the alloy. Eutectic silicon in the unmodified 'as cast' state

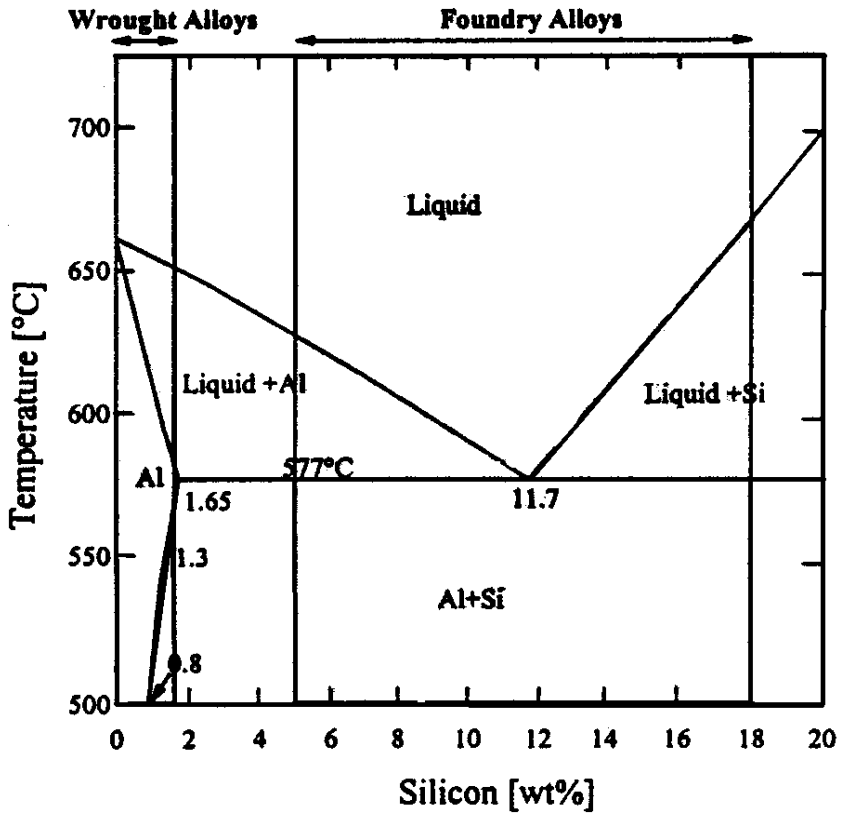

Figure 2.1: Binary Al-Si alloy equilibrium diagram [14]

exhibits a coarse, polyhedral particle structure and imparts poor mechanical properties to the casting. However, the morphology of the silicon particles can be altered by several methods. One method involves addition of small amounts of certain elements known as modifiers (such as sodium, antimony or strontium). The mechanical properties of the alloys are mainly governed by the structure, size and morphology of the eutectic phase, thermal modification and the cooling rate during solidification. All these can be used in combination to provide finer structural refinement and hence optimized mechanical properties. Al-Si alloys could also exist as hypoeutectic or hypereutectic alloys depending on the silicon content.

2.3 Casting

Casting can be generally defined as the process by which molten metal is poured into a cavity of a desired shape and allowed to solidify into the desired shape [11]. It is a popular production method that has been employed for a wide range of products of varying shapes and sizes, material composition, physical and chemical properties. Casting can be continuous or semicontinous [15]. There are different casting processes, classified according to the mould material (e.g. sand casting) or mould filling method (e.g. high pressure die casting, low pressure die casting, gravity die casting and squeeze casting). Another recent casting process is the semi solid casting which covers the Semi-Solid Metal(SSM) casting process and Thixomolding [15]. The selection of the casting process to use among the above methods depends on a number of factors. These include cost, mechanical properties desired, surface finish, level of technology available and the desired application, among others. Each one of the above casting processes has its advantages and disadvantages, which are well enumerated in a paper contained in the report by Dahle [15] on the casting and solidification of light alloys.

In sand casting, the pattern with the shape and dimensions of the final casting is surrounded by mould materials which consists of a mixture of refractory particles such as silica sand and a binder such as clay (bentonite) or thermosetting resin. The combination of sand, binder, moisture and other additives such as coal dust, lime, magnesia, etc., is properly mixed, tempered and conditioned. Clay is a necessary bond to the moulding sand, with small amounts of additives like lime, magnesia, iron oxide, soda, etc., being added to soften the sand. Coal dust, which imparts a characteristic black colour to used sand, helps to cool the mould after the molten metal has been poured. The mixing process should ensure a uniform distribution of clay, moisture and other constituents between the sand grains. During sand tempering, sufficient moisture is added to the sand

to achieve a sand mixture that will bond properly. Proper sand conditioning helps to accomplish uniform distribution of the binder around the sand grains, controls moisture content, eliminates foreign particles and aerates sand so that it flows readily and takes up the detail of the pattern. After a proper mix of the sand is achieved, the sand is rammed around the pattern in a mould box until the mould attains adequate strength to hold on its own. The mould is equipped with a properly designed pouring cup, sprues, gates and feeders.

There are specific rules for the design of proper metal flow and distribution (running system) as well as the feeding system [16–18]. The metal is poured into the mould where it takes up the shape of the cavity or impression left by the pattern in the mould. The mould sand is shaken out once the metal has solidified. Traditional sand casting is simple to carry out and results in castings which are of good quality depending on the application. Due to its nature, sand casting is prone to defects such as porosity, pinholes, oxide film entrapment and poor surface finish. It can thus only be relied upon in a limited range of applications where high integrity of components, high precision, high pressure tightness levels etc are not critical. In recent years, improvement in tooling design, mould materials and filling methods have led to a new sand casting method that can deliver high quality components. This recent method is called Precision Sand Casting and its adoption in producing parts such as automotive parts has advantages such as high productivity, flexibility and low costs.

In gravity die casting, molten metal is poured manually or by mechanical means from a ladle or pouring cup into a metal mould. Gravity is the driving force for metal flow. The die usually consists of two halves sometimes with sand cores located in the cavity to produce internal features. Die materials are usually die steel or grey iron. Die faces are coated with a thermally insulating coating. Mould filling time is in the order of a few seconds while solidification takes a

few minutes. Aluminium silicon alloys of the 3xx, 4xx and 6xx series are used in gravity die casting. Gravity die casting is suitable for a few hundred to a few thousand castings of parts such as taps, pipe parts and valves.

In low pressure die casting, molten metal fills the die under application of low pressure. Al-Si alloys of the 3xx and 6xx series are commonly produced using this method. Car wheels, oil sumps, brake drums, cylinder heads and engine parts are some of the parts cast by low pressure die casting method in the medium batch to large batch production range.

High Pressure Die Casting (HPDC) is a high precision casting method and involves injecting metal into a cavity at high velocities so as to produce near net shaped parts with good dimensional accuracy [4, 19]. Parts cast using HPDC are not heat treated as the porosity produced under high pressure is likely to cause expansion and hence produce a grossly disfigured surface. Examples of parts made using HPDC include automotive gear box housing, door handles and engine blocks. As a high cost production process, it is suitable for large production runs in the range of 10,000 parts and above.

In squeeze casting, the casting is subjected to substantial applied pressure for the duration of solidification. This produces castings free of micro and macro porosity as the applied pressure feeds the solidification shrinkage completely. The primary use of squeeze casting is in producing near net shape high integrity components. Parts produced by the method include brake callipers, master cylinders and premium road wheels and components of automobiles, trains, aircraft and aerospace vehicles requiring high specific strength, cryogenic toughness and reliability [20, 21].

In all the above processes, it is absolutely necessary that the highest possible integrity castings be obtained. The pouring, running, gating and feeding system

are optimized to reduce casting related defects. Melt integrity is critical to casting quality. Attention to the recommended composition levels for each material adds value to the integrity of casting obtained. The selection of the method to apply in a particular situation is limited by availability of the technology, cost, number of parts required and the expertise necessary to operate the technology successfully.

2.4 Modification

Modification refers to the morphological change observed in the silicon structure when aluminium silicon melts are treated with certain elements. The elements which have been known to effect this change from acicular silicon to fine globular silicon are sodium, strontium, potassium, rubidium, cerium, calcium, barium, lanthanum and ytterbium. Other elements like antimony, arsenic, selenium and cadmium act to produce lamellar silicon (a finer version of the coarse acicular structure). However, only sodium, strontium and antimony have found widespread commercial use. Modification was first observed by Aladar Pasc in 1921 [4]. Aluminium silicon alloys treated with sodium, strontium or antimony have been reported to have improved mechanical properties and machinability [22].

Since Pasc's observation on modification, further research has shed more light on what is actually responsible for the change in mechanical properties and machinability. Untreated alloy contains the silicon phase in the form of large plates with sharp sides and ends (acicular silicon). The addition of sodium causes eutectic silicon to solidify with a fine, apparently globular morphology [3]. This transition from acicular silicon to globular silicon is responsible for the improved properties of modified Al-Si castings. Figure 2.2 (a) and (b) illustrates typical unmodified and modified silicon eutectic structures respectively.

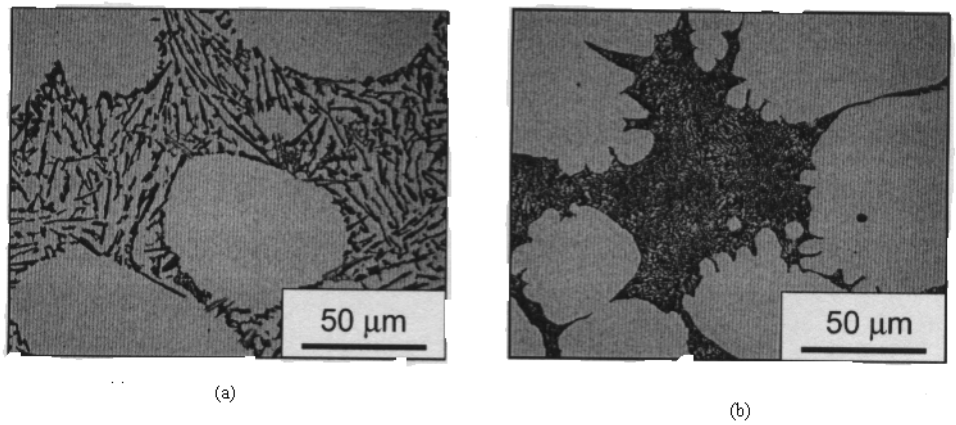

Figure 2.2: (a) Unmodified eutectic silicon and (b) Modified eutectic silicon [4]

Unmodified silicon solidifies in an unbranched flat plate morphology. The introduction of an impurity during the solidification of silicon introduces defects in the form of twins in the growing silicon, leading to frequent silicon branching. Studies by Transmission Electron Microscopy(TEM) have revealed that modified silicon fibres contain an order of magnitude more twins than do unmodified silicon plates. The efficiency of an element in modifying the silicon can be measured by the number of twins produced in the modified silicon fibres. Measured values of twin spacings are presented in Table 2.5 for five elements which are known to modify silicon.

Table 2.5: Measured Twin Spacings in Several Modified Systems [4]

Structure	Modifier	Twin spacings at constant freezing rate (nm)
Acicular	None	400
Fiber	Sodium	5
Fiber	Strontium	30
Fiber	Barium	30
Fiber	Calcium	100
Fiber	Ytterbium	50

The amounts of each element that will cause sufficient modification is dependent on the modifier itself and the composition of the alloy being modified. As an example, antimony, common in Japan and Europe, is sufficient in amounts of 0.1% or greater.

The use of each element as a modifier is dependent on the chemical and physical properties of the element. Sodium is highly reactive, as a result of which it is vacuum packed as elemental sodium in aluminium cans. It is added into the melt in the aluminium cans to minimize problems with oxidation and hydrogenation. Sodium has been traditionally used to spheroidize eutectic particles. However, despite its good modifying properties, sodium fades rapidly on holding and practically disappears after only a few remelts. Strontium has the advantage that its effect does not fade on holding and its use has become more widespread. However, since the dissolution of strontium is difficult, using it requires holding times at 750^{o}C, leading to increased gas pick up [4]. Compared to sodium, it is relatively easy to make strontium master alloys, and strontium is used in the form of master alloys. The commonly used master alloys are Al-10%Sr-14%Si, Al-10%Sr, 10%Al-90%Sr, Al-35%Sr [22]. Pure strontium reacts with water vapour and cannot be used effectively. The toxicity of antimony (which reacts with H_2 dissolved in liquid aluminium to produce deadly stibine gas) renders it difficult for the element to be added to the melt directly in the foundry.

In general, the melt treatment procedure is done by plunging the additive held in a perforated cup or bell below the surface of the melt. A gentle stirring action improves the dissolution rate but this should not be so severe as to unduly agitate the melt surface. Sodium reacts violently while the addition of Sr is quiescent and H_2 pickup is not a problem. Dissolution of sodium is complete within 5 minutes. Sodium has a high vapour pressure (0.2atm at 730^{o}C)and hence large amounts of Na which are added boil off immediately. Sodium recoveries in the

range of 20% to 30% are practical [22]. Strontium has a high recovery but has more complex dissolution characteristics. Modification with strontium is often less uniform than with Sodium while Antimony produces a lamellar and less fibrous structure. Modification does not result in a sharp change of structure and castings with an inadequate amount of either Na or Sr will exhibit a mixed structure. The structures obtained by modification fall into any of the six (6) classes observed to occur [4], namely;

- Class 1, Fully unmodified structures
- Class 2, Lamellar structures
- Class 3, Partial modification
- Class 4, Absence of lamellar structures
- Class 5, Fibrous silicon eutectic, and
- Class 6, Very fine structures.

The well modified structures fall into class 5, under modified into class 2 and the unmodified into class 1. However the exact structure that will form under modification is not always clear. This will depend on a number of variables such as type of modifier used, impurities present in the melt, amount of modifier used, freezing rate, silicon content and the cleanliness of the melt.

2.5 Heat Treatment

Heat treatment in its broadest sense refers to any heating and cooling operations performed for the purpose of changing the mechanical properties, the metallurgical structure or the residual stress of a metal product [23]. For aluminium alloys, the term is applied to specific operations employed to increase strength

and hardness of the precipitation hardenable wrought and cast alloys. The heat treatment of aluminium alloys is mainly carried out in three stages, namely; solution treatment, quenching and age hardening.

Solution heat treatment is the process by which alloying constituents are taken into solution and retained by rapid quenching. Subsequent treatment at lower temperatures, such as artificial ageing or natural ageing at room temperature allows for a controlled precipitation of the constituents, thereby achieving increased strength. The solution treatment temperature is critical to the success of the procedure, and it is desirable that the solution treatment is carried out as close as possible to the liquid temperature in order to obtain maximum solution of the constituents.

Quenching is done to ensure that the dissolved constituents remain in solution down to room temperature. The rate of quenching is important and the result can be affected by excessive delay in transferring the work to the quench medium. Generally, very rapid precipitation of constituents commences at around 450^oC for most aluminium alloys and the work must not be allowed to cool below this temperature prior to quenching. The usual quenching medium is water at room temperature.

After solution and quenching, hardening is achieved either at room temperature (natural ageing) or with precipitation heat treatment (artificial ageing). In some alloys, sufficient precipitation occurs in a few days at room temperature to yield stable products with properties that are adequate for many applications. These alloys are sometimes precipitation heat treated to provide increased strength and hardness in wrought and cast alloys. Other alloys with slow precipitation reactions at room temperature are always precipitation heat treated before being used. The artificial ageing or precipitation heat treatments are low temperature long time processes. Ageing temperatures and holding times range from 115 -

200^{o}C and 5 - 48 hours respectively.

Commercial alloys whose strength and hardness can be significantly improved by heat treatment include the 2xxx, 6xxx and 7xxx series wrought alloys and 3xx.0, 2xx.0 and 7xx.0 series casting alloys. Most of the heat treatable alloys contain combinations of magnesium with one or more elements such as copper, silicon and zinc.

T6 heat treatment entails heating the aluminium alloy at high temperature (solution treatment) of between 495^{o}C and 540^{o}C depending on the alloy, quenching in water at room temperature (sometimes in water at 70^{o}C to 80^{o}C temperature) and then artificially ageing by heating for 4 to 6 hours at temperatures of between 155^{o}C and 200^{o}C. In some cases, a pre-ageing stage is added before precipitation treatment during T6 treatment. The alloy is then left to age naturally for up to 16 hours before the precipitation treatment commences. In T4 treatment procedure, the alloy is subjected to solutionizing and quenching just as in the T6 procedure and then subjected to natural ageing until the alloy reaches a substantially stable condition.

2.6 Influence of Alloying and Impurity Elements in Al-Si Foundry Alloys

2.7 Introduction

Alloying elements are intentionally added in alloys to influence the properties and structure in a certain desired manner while impurity elements, whose effects are not desirous, are either present in the system from the initial processing stages or unintentionally added during processing. The major alloying elements in aluminium silicon foundry alloys include silicon itself, copper, magnesium and zinc, while the minor alloying elements include manganese, chromium, nickel, iron, titanium and tin [9,12]. According to Mondolfo [12], the composition limits

for various elements fall within the limits given in Table 2.6.

Table 2.6: Composition limits for alloying elements in cast Al-Si alloys [12]

Element	**Weight %**
Silicon	5 -- 25
Copper	0 -- 5
Iron	< 3
Magnesium	0 -- 2
Zinc	0 -- 3
Manganese, Chromium, Cobalt, Molybdenum Nickel, Berylium, Zirconium	Up to 3
Sodium, Strontium	< 0.025
Phosphorous	< 0.01

Whether an element is an impurity element or not is sometimes dependent on the particular alloy in question and its applications. As an example, in sand cast alloy 355, A356 or A357, Fe is an impurity element while in die cast alloy A380, 384 or 390, Fe is intentionally added to prevent die soldering in die moulds. These elements occur in various forms such as; solid solution in the aluminium phase, eutectic phase or intermetallic phase in the alloy. Their effects and the properties they impart into the alloy are as varied as the elements themselves. The effects of the alloying and impurity elements on the structure, physical, chemical and mechanical properties of the alloys formed have been the subject of intense research since the first aluminium alloys were made. An overall review of the subject is beyond the scope of this study and only a brief discussion of the pertinent issues will be presented.

2.7.1 Influence of Alloying Elements

Silicon is the second most abundant impurity of aluminium (after Fe) originating from the silica or silicate of bauxite. It is also one of the most common additions to aluminium alloys. Silicon imparts higher fluidity, higher corrosion resistance and increases resistance to hot cracking [12, 24]. The resultant alloys have excellent castability and are easy to weld. Increasing the silicon content increases the strength of the alloy with a corresponding marginal reduction in ductility [12]. During age hardening, silicon in combination with magnesium forms the strengthening magnesium silicide precipitate [3, 25]. It also provides a low coefficient of thermal expansion and high hardness for improved wear resistance.

Silicon content in aluminium alloys can vary from 0.2% to 25% [9]. Silicon containing aluminium alloys are classified as hypoeutectic (Si content less than 10%), eutectic (Si content between 10% and 13%) or hypereutectic (Si content between 13% and 25%). Aluminium silicon alloys constitute 85% to 90% of total aluminium parts produced worldwide and hence rank as the most popular of the aluminium alloys. In hypoeutectic and eutectic Al-Si alloys, silicon occurs in a coarse and polyhedral form (also reported to occur as thin platelets, needle like structures) in the interdendritic regions as the secondary phase. In this form, it imparts poor ductility to the alloy. Ductility can however be improved by either chemical modification through addition of Na, Sr, Ca or Sb elements during the melting process or thermal modification through heat treatment. The morphology and size of the eutectic Si is changed to finer, globular particles, hence achieving improved ductility [3, 24]. Calcium has also been reported to have a refining effect on the eutectic silicon leading to improved strength and ductility [26]. However, there have been reports of the modifiers leading to increased porosity in the castings [3, 4, 26], while others report no recognizable

increase in the same [27]. High Si content in hypereutectic Al-Si alloys leads to high strength, high hardness alloys of poor ductility. Addition of phosphorous in hypereutectic silicon alloys results in the nucleation of silicon to permit a fine distribution of hard primary Si particles, that impart high wear resistance and marginally improved ductility.

Shrinkage in solidification is appreciably reduced by the presence of silicon, but is only slightly affected by other alloying elements; it is in the order of 3-4% at 6-12%Si and only 1-2% at 20-24%Si [12].

Strontium, sodium, calcium and antimony are some of the more popularly used elements for modifying the structure of silicon in aluminium silicon alloys [4]. Unmodified silicon occurs in coarse and polyhedral structure. In this form, it imparts poor ductility and affects strength properties negatively. Modified silicon acquires a globular or spheroidized shape which marginally improves the strength, ductility and fatigue properties. Modified alloys contain Fe intermetallics in large numbers and sizes, in some cases twice as large as the Si particles [28].

Copper is added to increase strength and fatigue resistance without loss of castability, but at the expense of corrosion resistance. Copper also improves the elevated temperature properties through heat treatment [11, 12]. The copper free alloys are used for low strength to medium strength castings with good corrosion resistance while the copper bearing alloys are used for medium to high strength castings where corrosion resistance is not critical. Complex shaped castings with good properties can be obtained due to the excellent castability of the Si-Cu bearing aluminium alloys. Copper, if not in solution is present as $CuAl_2$. The amount of Cu in solution is reduced by Ni or Mn in favour of the Cu-Ni and Cu-Mn compounds.

Magnesium, especially after heat treatment, increases the strength substantially but at the expense of ductility. After heat treatment, magnesium precipitates as Magnesium Silicide (Mg_2Si), which is well distributed in the dendrites and leads to strengthening of the alloy. Magnesium, if not in solution is present as Mg_2Si.

2.7.2 Influence of Impurity Elements

Iron is the main impurity in aluminium alloys and the content should be maintained as low as is economically possible. It has deleterious effects on corrosion resistance and ductility. In sand castings and permanent mold castings, the upper limit is usually 0.6 - 0.7% Fe. However, in die castings, Fe is intentionally added (may contain up to 3% Fe) to prevent die soldering, for example, in some piston alloys. Cobalt, Chromium, Manganese, Beryllium, Molybdenum and Ni are sometimes added as Fe correctors, and their addition improves strength at high temperatures [12]. Beryllium addition tends to reduce the number of intermetallics present and improves their shape [29, 30]. Depending on the content, Fe forms intermetallics in combination with Al, Si and either Mn, Zn or Cu. The shapes of the intermetallic phases formed may range from platelets to chinese script morphology. In the absence of copper, Fe is usually in the form of Al-$FeSiAl_5$-Si eutectic as thin platelets interspersed with silicon needles or rods as shown in Figure 2.3 (a). For more than 0.8% Fe, primary $FeSiAl_5$ appear. In alloys with low Si content or those containing Mg, Cu or Zn, Fe_2SiAl_5 is formed as chinese script, as illustrated in Figures 2.3 (b) and (c). When Cu is present, Fe may be associated with it, probably as Al_7FeCu_2.

Iron forms $Al_{15}(FeMn)_3Si_2$ with manganese, often in the shape of chinese script, thus removing the embrittling effect of Al_5FeSi. The total content of Mn and Fe should not exceed 0.8% otherwise the $Al_{15}(FeMn)_3Si_2$ will form as primary

globules which will reduce the machinability of the alloy. Cobalt does not combine with silicon and is rated as the best corrector of Fe. Molybdenum has the same effect as Cobalt.

Zinc is a tolerated impurity in many alloys, often upto 1.5 - 2% Zinc because it has no substantial effect on room temperature properties. Zinc in amounts up to 1% is in solution and does not form any visible phases.

2.7.3 Influence of Alloying and Impurity Elements on Mechanical Properties

Mechanical properties that can be obtained in average castings are shown in Table 2.7. Alloys prepared by powder metallurgy exhibit greater strengths, especially at elevated temperatures. Ultimate Tensile Strengths of 200 - 400 MN/m^2 and elongation in the range of 2% to 20% are obtained in wrought products [12]. Poor casting technique may lower the properties although Al-Si alloys are among the most sensitive to variables such as gas content, design of castings, rate of cooling and feeding. High purity and special treatments can produce properties 10 - 20% better than average; conversely secondary alloys tend to have lower ductilities than do primary alloys.

From Table 2.7 it can be seen that increasing Si content increases strength at the expense of ductility, but this effect is not very marked. Modification by Na produces limited increase in strength but the increase in ductility is substantial especially for sand castings. At the higher cooling rates typical of gravity die castings, the silicon is already somewhat refined without modification and improvement from modification is reduced.

The effect of dendrite arm spacing (DAS) and cell size on mechanical properties is not very marked for Si$\geq$ 8%, but in lower Si alloys, in which Al dendrites predominate, there is hardly any effect. Iron may slightly increase strength,

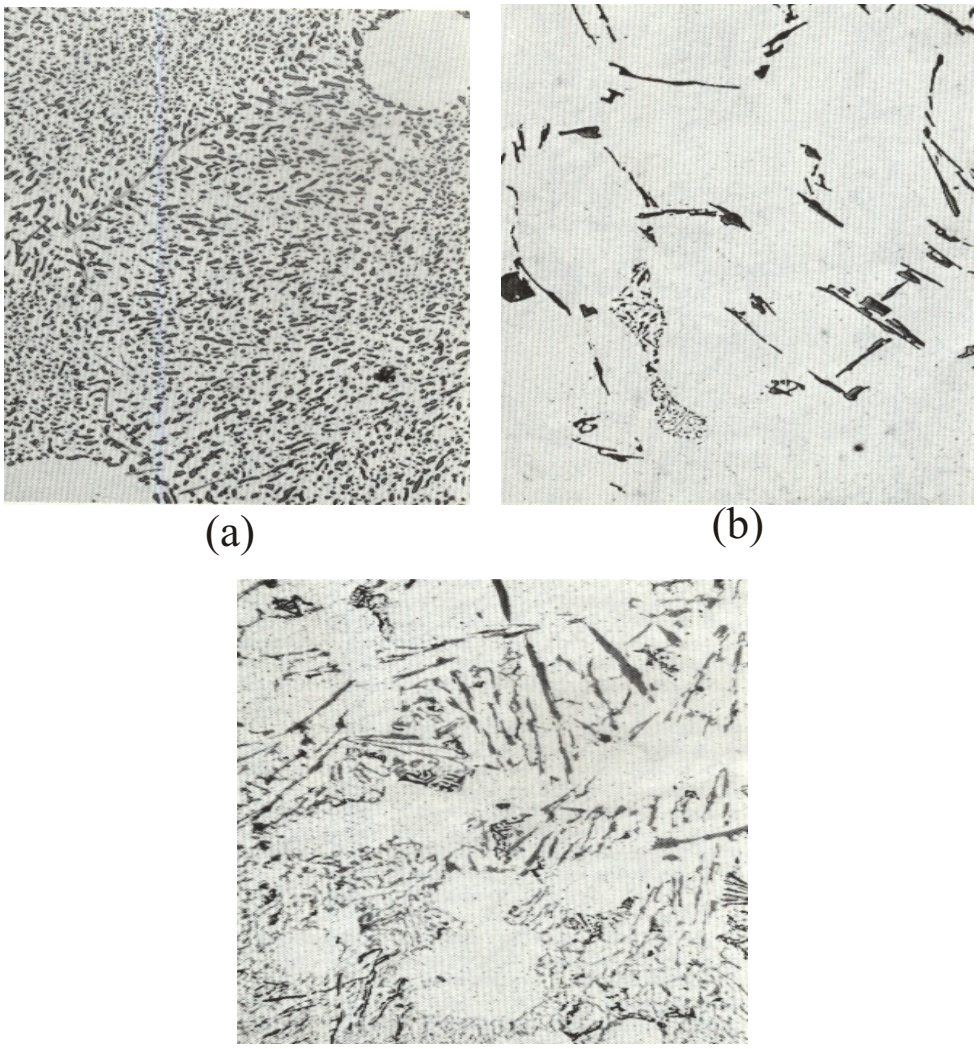

Figure 2.3: Micrographs showing (a) Sand cast modified alloy with 12%Si, 0.3%Fe showing light needles of $FeSiAl_5$ and darker globules of Si particles, (b) An alloy with 5%Si, 0.2%Fe, P-bearing showing coarse Si crystals and finely dispersed Al-$FeSiAl_5$-Si eutectic and (c) A metal mould cast alloy with 10%Si, 0.9%Cu, 0.6%Fe showing Iron as Fe_2SiAl_8 in coarse Si zone and as $FeSiAl_5$ in fine Si area [12].

but drastically decreases ductility (especially when Fe content is $\geq$0.7% and not corrected by manganese, cobalt etc).

Table 2.7: Typical Mechanical Properties of Aluminium Alloys [12]

	Sand Cast					Heat treated, artificially aged			
	Hardness (H_v)	**UTS (σ_{UTS}) (MN/m^2)**	**YS (σ_{YS}) (MN/m^2)**	**% Elongation**		**Hardness (H_v)**	**UTS (σ_{UTS}) (MN/m^2)**	**YS (σ_{YS}) (MN/m^2)**	**% Elongation**
Al-Si:5-7%Si									
Unmodified	400-500	80-140	40-60	3.0-5.0					
Modified	400-500	100-150	50-70	4.0-10.0					
Al-Si:9-12%Si									
Unmodified	600-700	100-150	50-80	1.0-5.0					
Modified	600-700	150-200	70-120	10.0-14.0					
AlSi5-10%Si-0.2-0.3%Mg	600-700	100-150	60-80	1.0-3.0		800-1000	250-320	200-250	1--6
AlSi>12%Mg-CuNi	700-900	100-150	40-70	0.0-3.0		1000-1600	200-300	150-250	3--0
AlCuSi: 2-6% Cu, 3-12%Si	600-800	150-200	100-150	0.0-3.0		800-1000	200-300	150-200	0--3
AlCuSi:3-12% Si, 2-6%Cu 0.5-1.5%Mg	600-800	150-200	100-150	0.0-3.0		800-1200	250-350	200-300	0--2

Be, Mn, Cr, Mo, Ni, Co and Zr all slightly increase strength; manganese, cobalt, nickel and molybdenum if needed to correct for the iron may also increase ductility, otherwise all of them tend to reduce it.

Copper and zinc also increase strength at the expense of ductility, but the most effective strengthener is magnesium especially after heat treatment. Grain refinement by addition of Titanium, Boron, or Zirconium has only a limited effect on ductility. Antimony, when in combination with magnesium, may reduce response to heat treatment.

Fatigue resistance is relatively low, especially if silicon is not modified or spheroidized by heat treatment [12, 31]. Fatigue strength values of the order of 50-70MN/m^2 are given for hypoeutectic alloys, with slightly higher values of 70-80MN/m^2 for copper bearing alloys and lower ones for hypereutectic alloys [12]. Be, Co and Mn may improve fatigue resistance [31]. Wear resistance of high silicon alloy arising from hard Si particles is 10 times better than plain steel and comparable with hardened steel.

2.8 Quality Index Curves for Al-Si Alloys

The Quality Index, Q, introduced by Drouzy et al. [32] has been commonly used as a tool for assessing the effect of changes in process variables such as degassing, modification of eutectic Si particles and heat treatment on the strength and ductility of Al-Si-Mg alloys [33–38]. An example of a quality index chart for the Al-7%Si-Mg alloy is shown in Figure 2.4.

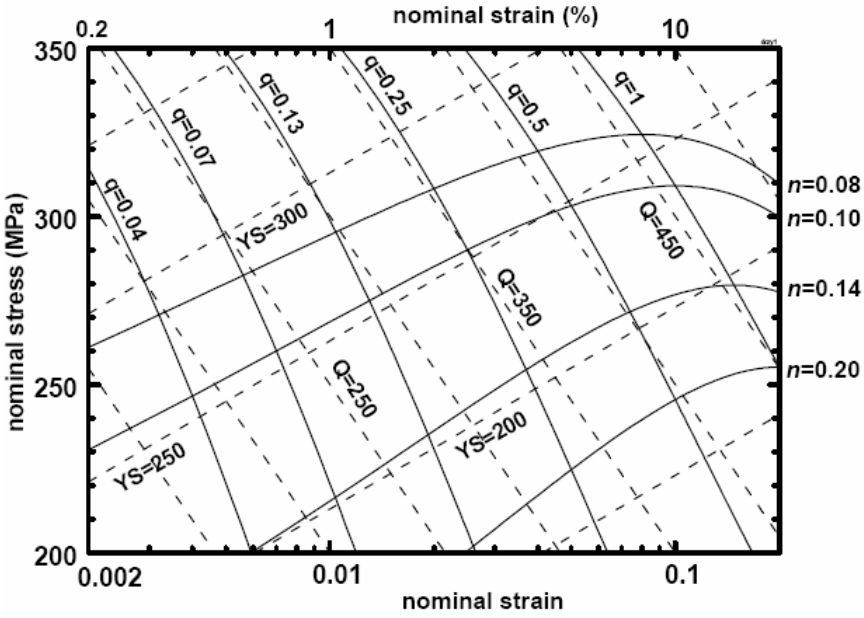

Figure 2.4: A quality Index chart for Al-7%Si-Mg alloy [38].

In Figure 2.4 the dashed lines represent the quality index chart as determined using Equations 2.1 and 2.2. The solid lines (flow lines identified by the n-value) have been calculated using Equation 2.4. Iso-YS lines are identified by the yield stress value, while Iso-Q lines are identified by the Q-value. Aside from the two main axes, nominal stress and nominal strain, the grid of dashed lines indicates the quality index, Q, and the yield strength, YS. Normally, nominal stress (or sometimes UTS) and nominal strain (or sometimes elongation to fracture) are plotted and Q and YS are read off the chart.

The practical value of the Quality Index chart stems from the fact that the

mechanical 'quality' of the alloy is expressed as a single numerical parameter, whose value can be read off a Quality Index Chart or calculated through a simple equation relating the elongation to fracture and the tensile strength of the material.

The quality index chart was initially mainly used for Al-7%Si-Mg [32, 34–36, 38] but it has since been used for other aluminium based alloys [37, 39, 40] as well as a Mg-based alloy [38]. Generally, the quality index charts have been found to be handy tools although slight modifications to the original formulations by Drouzy et al. [32] (Equations 2.1 and 2.2) are required for alloy systems other than Al-Si-Mg. Before the existing quality index charts can be used for all alloy systems, it is necessary to generate individual curves for any variant alloy system first in order to ascertain which parameters are best applied and hence the exact behaviour of the alloy's strength - ductility relationship. Further, according to Caseres et al. [37], extending the quality index concept to alloy systems other than Al-Si-Mg requires determining the behaviour of the strength - ductility relationships.

It was therefore deemed necessary to include the development of the quality index charts for secondary foundry alloys in this study. This is expected to provide a useful guide in the investigation and prediction of the mechanical properties of recycled aluminium alloys subjected to different ageing conditions. An analytical method of generating the quality index charts is discussed in the following section. In Section 4.5.2.5, the method is applied in the analysis of the experimental results obtained with the secondary foundry alloys studied.

2.8.1 An Analytical Model for the Quality Index

The Quality Index, Q, is an empirical parameter that is related to the tensile strength (UTS(MPa)) and the elongation to fracture (s_f) of the material by the

equation [32]:

$$Q = UTS + d\log(s_f). \tag{2.1}$$

The Q value can also be read off a quality index chart as shown in Figure 2.4. Lines generated using Equation 2.1 represent lines of constant alloy quality and are called Iso-Q lines, where the Q value is defined as the y-intercept at s_f = 1%. The lines identified by the yield stress are called probable yield stress lines and follow the relation

$$YS = aUTS - b\log(s_f) - c, \tag{2.2}$$

where YS (MPa) is the yield stress (0.2% off-set). The parameters a, b, c and d in Equations 2.1 and 2.2 are empirical constants whose values depend on the alloy system [32, 39, 40].

The analytical model assumes that the deformation curves of the material can be described with a constitutive equation of the form

$$\sigma = K_q\epsilon^n, \tag{2.3}$$

where σ is the true flow stress, K_q the strength coefficient of the material, ϵ the true plastic strain and n the strain hardening exponent. Ignoring the difference between the true and nominal strain, the nominal stress-plastic strain curve is approximated by the equation [33, 36, 38]

$$P \cong K_q s^n exp^{-s}, \tag{2.4}$$

where the engineering values of stress (P) and the plastic strain (s) in Equation 2.4 correspond to the true values of σ and ϵ in Equation 2.3 respectively. Equation 2.4 has been used to generate the flow lines in Figure 2.4 [33, 37].

The ductility of the material is measured against the necking onset strain by the relative ductility parameter, q, defined as the ratio between the actual elongation

to fracture, (s_f) and the strain hardening exponent, where

$$q = \frac{s_f}{n}. \tag{2.5}$$

Solving Equation 2.5 for n and replacing in Equation 2.4

$$P = K_q s^{s/q} exp^{-s}, \tag{2.6}$$

Equation 2.6 has been used to generate the Iso-q lines in Figure 2.4.

The gradient of the Iso-q lines in Figure 2.4 can be identified with the slope of the Iso-Q lines, i.e., the parameter d in Equation 2.1. Differentiating Equation 2.6 with respect to strain relates d in Equation 2.1 to K_q as

$$d = -\frac{dP}{ds} \cong 0.4K_q \tag{2.7}$$

(where, for the approximation, $q = 1$). The negative sign in Equation 2.7 keeps the current formulation consistent with Equation 2.1.

Combining Equations 2.4, 2.5 and 2.7, Equation 2.1 takes the form

$$Q = K_q[(qn)^n e^{-qn} + 0.4log(100qn)]. \tag{2.8}$$

The terms in the square bracket do not change much with n and a convenient approximation [38] for Equation 2.8 is

$$Q \approx \beta_q K_q, \tag{2.9}$$

where β_q = 1.12+0.22ln(q). When q = 1, Equation 2.9 becomes

$$Q = 1.11K_q. \tag{2.10}$$

The strength coefficient of the material relates to the YS as

$$K = YS(\frac{E}{\alpha YS})^n, \tag{2.11}$$

where E is Young's modulus and α is a scale factor of the order of 1.

Combining Equations 2.7 and 2.11 with Equation 2.1 leads to a most useful combination of experimental parameters

$$Q = UTS + 0.4YS(\frac{E}{\alpha YS})^n log(100s_f), \tag{2.12}$$

which makes explicit the relation between Q and YS [33, 38].

2.9 Fatigue Properties of the Al-Si Alloy system

2.9.1 Introduction

The study of the fatigue properties of Al-Si alloys has been driven by the upsurge in the applications of the alloys in critical components in areas such as automotive, aircraft and defence. These alloys have an array of attractive properties, such as high strength to weight ratio, good castability, good thermal conductivity and good resistance to corrosion [9, 11, 12]. Some of the components which are made of these high strength but lighter aluminium silicon alloys include pistons, crankcases, engine blocks, cylinder heads, clutch cases, gearboxes, fuel pump bodies, wheels, pulleys and brake shoes [13]. In most of these applications, the components are subjected to high load levels which are sometimes cyclic in nature, hence the need to fully understand the fatigue properties of these alloys. Almost all studies in the fatigue of Al-Si alloys agree on the dominance of casting defects over all other established factors. These defects come in the form of porosity (gas and shrinkage porosity), entrapped oxide films and sometimes intermetallic inclusions. However, casting porosity is the main culprit in negatively influencing the fatigue properties of the alloys. Other microstructural parameters such as the Dendrite Arm Spacing (DAS) and the silicon particle size, distribution and shape have also been variously found to influence the fatigue properties of cast aluminium alloys.

Fatigue life is composed of microcrack incubation, microcrack initiation, micro-

crack nucleation and coalescence and macrocrack growth or propagation to failure [41]. Microcrack initiation is the point in the component life when a crack is first detected using non-destructive examination techniques. Macrocrack propagation is defined as the process of crack growth which results in the ultimate failure of the component by fracture. Where a crack is found to exist in the form of a defect, the crack nucleation life is only a small portion (sometimes less than 1%) of the total fatigue life. In such cases, the fatigue life is dominated by crack propagation, and can be easily estimated by using the various approaches for analyzing crack growth and estimating fatigue life, that have been proposed by different researchers over time. In the sections that follow, a review of the fatigue properties of aluminium alloys is presented. This involves the influence of casting defects, microstructural parameters, heat treatment and modification. It also covers the approaches developed for estimating fatigue properties of the aluminium silicon alloys.

2.9.2 Effect of Casting Defects

It is widely acknowledged that casting defects substantially influence the fatigue properties of cast aluminium alloys. The major casting defects found in cast aluminium alloys are porosity and inclusions. It has proved pretty difficult to completely eliminate casting defects, but there has been commendable progress in developing methods of reducing the casting defect levels and hence their effects on mechanical properties such as tensile strength and fatigue. Casting porosity is the major fatigue controlling defect. Oxide inclusions, intermetallic phases and eutectic silicon particles have also been found to initiate fatigue cracks, particulary where; the size of pores have been reduced to certain critical levels, low porosity levels exist or the dendrite arm spacing is small.

The size, position and distribution of defects are important in considering the

effects of defects on fatigue life of cast alloys. As a general rule, bigger defects cause shorter lives, while a surface defect of a given size can be more damaging than a large internal one. Moreover, the presence of clusters of relatively small but numerous close pores also accelerates the failure process, not only by easier crack propagation but by collectively raising the stress concentration factor [3]. In the sections that follow, the effects of casting defects, modeling approaches and methods of controlling their effects is reviewed.

2.9.2.1 Effect of Porosity

Porosity is found in castings as; voids or cavities on the surface of the casting, voids within the body of the casting and as pinholes or pipes in the feeding channels of the casting. It is generally agreed that porosity in castings can be classified into two broad categories, namely gas porosity and shrinkage porosity. Depending on the category of porosity, the sizes may range from the micron to the millimeters range. Gas porosity is due to the presence of dissolved hydrogen in liquid aluminium, while shrinkage porosity is brought about by the lack of adequate feeding in the interdendritic channels to compensate for solidification shrinkage. Factors controlling porosity formation have been previously reviewed [42] and summarized as dissolved hydrogen content, the local freezing rate, the local temperature gradient, melt cleanliness(presence of inclusions, oxides and intermetallics), alloy treatments and grain refinement. Details of how these factors influence porosity formation are discussed in references [4] and [15].

Porosity is the most common casting defect that foundries must battle with and there has been concerted efforts in the past aimed at understanding porosity, its effects on mechanical properties, its control and how to model its effect on fatigue properties. That porosity is the major defect controlling the fatigue properties of cast aluminium alloys is not in doubt. Indeed, previous researchers have come

to the conclusion that porosity has the most detrimental effect on the fatigue properties of cast alloys, especially when pore size and amount exceed certain values. It is widely acknowledged that fatigue cracks easily initiate from pores located at or near the surface of a cast component or test specimen [13, 42–51].

Shrinkage porosity was found to overshadow the effects of heat treatment and mean stresses on the fatigue properties of a strontium modified Al-7Si-0.4Mg [43]. In this case, failure is initiated at interdendritic shrinkage defects. Reducing the size of pores increased the fatigue life but only up to the stage at which classical fatigue crack initiation from Persistent Slip Bands (PSBs) became operative.

The size, morphology and location of pores clearly play the major role in determining the fatigue crack initiation life as well as the fatigue strength of cast Al-Si alloys. Skallerud et al. [48] found that pores larger than 0.2mm resulted in a high stress concentration within the vicinity of the pore and resulted in a short initiation life which significantly reduced the total fatigue life in Al7Si0.4Mg alloy. Odegard and Pedersen [49] reported pores in the range of 200-300μm as the most active crack initiation sites in a cast 356-T6 alloy. Boileau and Allison [11] stress that it is the size and location rather than volume percent of pores that determine the crack initiation life. Large pores close to the surface are very detrimental to fatigue life as are small pores close to the surface, compared to large pores in the interior of the casting. Similar conclusions are made by other researchers [50, 52–54]. In Boileau and Allison [11], it was found that doubling the average initiating pore diameter from 449μm to 1005μm resulted in a 30% decrease(from 55MPa at 449μm to 38MPa at 1005μm) in run out stress(stress at which the fatigue test is stopped without specimen failure). Buffiere et al. [53] found that cracks initiated at pores by decohesion of silicon particles located near the convex part of the pores, which are located at or below the surface

of the specimen. Similar results are reported by Savelli et al. [55]. Other researchers have indicated that iron intermetallics encourage the nucleation of porosity(by providing pore nucleation sites) leading to a further deterioration of fatigue properties [56–58].

In the work of Jason and Frederick [52], fatigue life was assessed as a function of the defect size at various applied stresses and some of their results are illustrated in Figure 2.5. The effect of defect size on fatigue life was more severe in the low stress range than in the high stress range. However, at low stresses and long lives, a minimum defect size is predicted below which no further reduction in fatigue life exists (400μm when the S_{max} = 55.2MPa). The as cast surface specimens seem to have lower fatigue life than the polished specimen when compared at the same defect size in the low stress ranges.

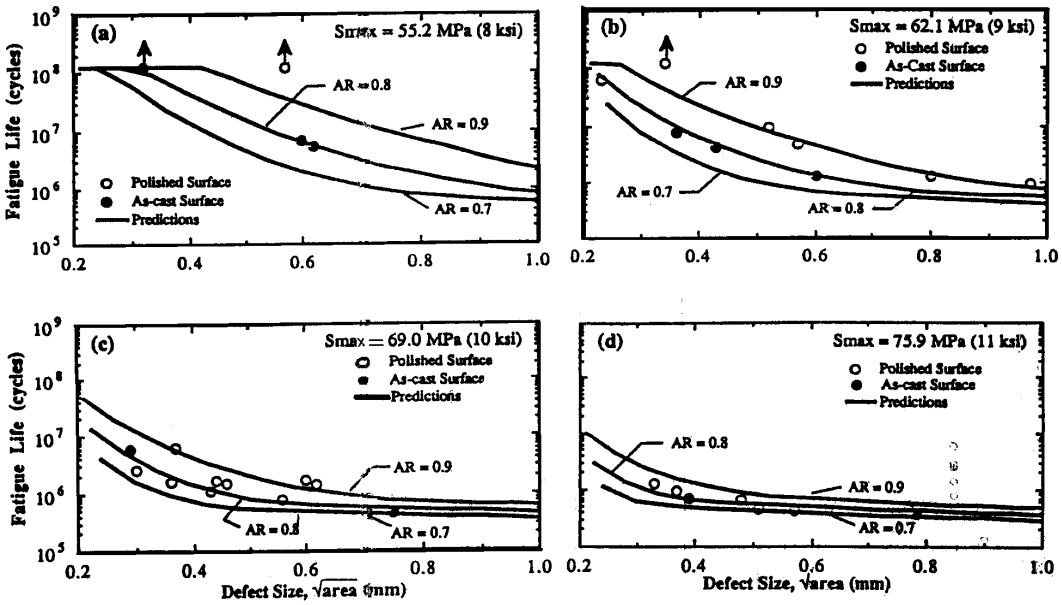

Figure 2.5: Fatigue life as a function of defect size for the AA319 alloy [52].

The degree of porosity also influences the fatigue behaviour of cast materials, with higher porosity containing alloys displaying a higher probability of containing large size pores and hence a lower fatigue life. In the study by Sonsino and Ziese [44], an increase of the degree of porosity from degree 0 to 4, and from 0

to 8 (as classified according to ASTM 155 guidelines [59]) reduced unnotched fatigue strength at 10^7 by 11% and 17% respectively. In the notched condition, the age hardened alloy displayed a reduction in fatigue strength of 7% while the non age hardened material displayed a drop of 20% due to its lower yield stress.

The presence of clusters of relatively small but numerous close pores also accelerates the failure process not only by allowing easier crack propagation but also by collectively raising the stress concentration factor [3]. This is also demonstrated by Skallerud et al. [48] who carried out an assessment of the fatigue life of aluminium casting alloys with casting defects. They tested the fatigue life of AlSi7Mg(0.4) cast alloy with T4 and T6 heat treatments, with and without shrinkage cavities. The test specimens were obtained from conventional cast car wheels (with shrinkage cavities) and from Directly Cooled or Chilled (DC) castings (with very low pore content). They found that pores with a maximum diameter larger than 0.2mm resulted in a significantly reduced fatigue lifetime. The shrinkage cavities resulted in a high stress concentration within the vicinity of the cavity and resulted in a short initiation life. In comparison to the total fatigue life, the resultant short fatigue crack initiation life could be considered as negligible, implying that the total fatigue life could be approximated by the crack propagation life.

Odegard and Pedersen [49] also investigated the fatigue life of cast A356 alloy, both free from and containing casting defects and heat treated to the T6 heat treatment condition. The specimens were obtained from low pressure die cast wheels and semi-continuously DC cast billets. The DC material was tested in both 'as cast' and extruded condition. The extrusion process, which results in a uniform distribution of silicon particles, was done before the T6 heat treatment. The percentage porosity in the direct chill materials was almost nil while the wheel material had about 1% maximum porosity. The average pore diameter

was 100μm while the maximum pore diameter was 140μm for the wheel material. The corresponding pore sizes found active at the surface crack initiation sites was 200μm and 300μm, in agreement with similar observations by Skallerud et al [48]. In the extruded material, cracks were seen to initiate at PSBs. By extruding the material, a homogenous Si-particle distribution was obtained causing both an increase in the number and a decrease in the length of the PSBs. The fatigue lifetime for the extruded material was higher compared to the directly chilled material. They also reached a similar conclusion to Skallerud et al. that the crack initiation life was negligible compared to the total fatigue life and could be ignored during total fatigue life modeling.

Jason and Frederick [52], in modeling the long life fatigue behaviour of a cast aluminium alloy tested the fatigue life of as cast and smooth specimens of AA319 aluminium alloy containing casting porosity. The tests were done mainly in the long life region (N$\geq 10^8$). Fatigue cracks were observed to initiate from near surface casting pores or from discontinuities resulting from the 'as cast' surface texture. The observed fatigue lives were strongly dependent on the size of square root of the area ($\sqrt{area}$)of the observed casting defects. The fatigue initiating defect was quantified by measuring the square root of its area projected on the plane normal to applied stress, i.e., the $\sqrt{area}$.

Stanzl-Tschegg et al. [50] found that cast voids (pores) were the major influence in determining the fatigue properties of an Al-Si11 aluminium alloy with 0.12-0.20% Mn and one with 0.05% Mn and increased H_2 content. The material inhomogeneities due to casting porosity lead to a reduction in the fatigue strength and hence early fracturing. Stanzl-Tschegg et al. were testing the fatigue strength of AlSi11 in the very high cycle regime, in the range of 10^8-10^9 cycles. Large voids significantly reduced the fatigue strength and were largely responsible for the early crack initiation. The two materials tested had different

porosity distribution as depicted in Figure 2.6 .

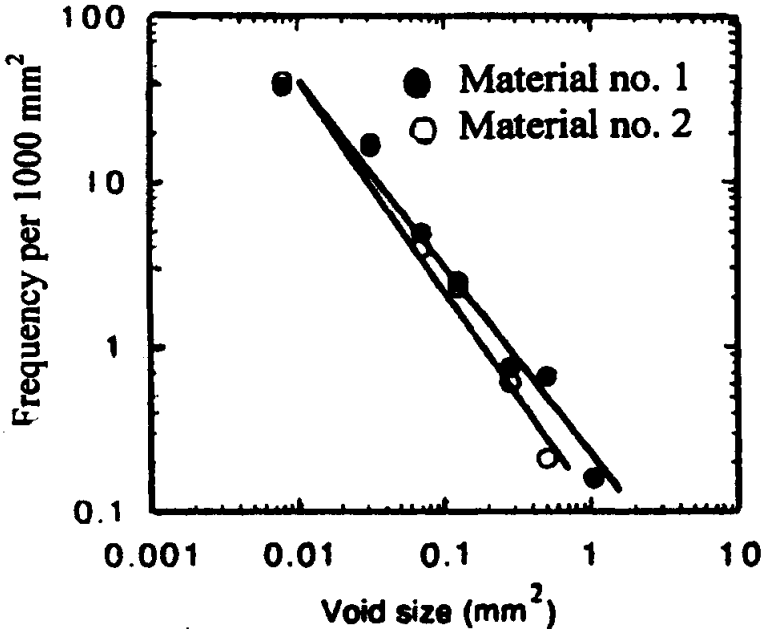

Figure 2.6: Distribution of voids in the two tested AlSi11 cast alloys [50].

The dependence of the number of cycles to failure on void size is illustrated in Figure 2.7 and shows that similar void sizes influence the number of cycles differently in the two materials. The number of cycles to failure is for example approximately 6 x 10^7 for material number 1 for load sequence with σ_{max}= 110MPa, if the void cross section is 0.5mm^2, while it is four times larger for material number 2 with identical void size. As observed by Skallerud et al. [48] and similarly in Stanzl-Tschegg et al's work, the crack initiation life time depends strongly on whether a void is located close to the surface or nearer to the center of the specimen. Since the location of voids in the test specimens was not considered in the work by Stanzl-Tschegg et al [50], part of the scatter in the plot of Figure 2.7 may be due to this effect.

Boileau and Allison [11] studied the effect of porosity size on the fatigue properties in a cast 319 aluminium alloy. They compared the sizes of porosity present in a Precision Engineered Component(PEC) and a wedge casting. They found

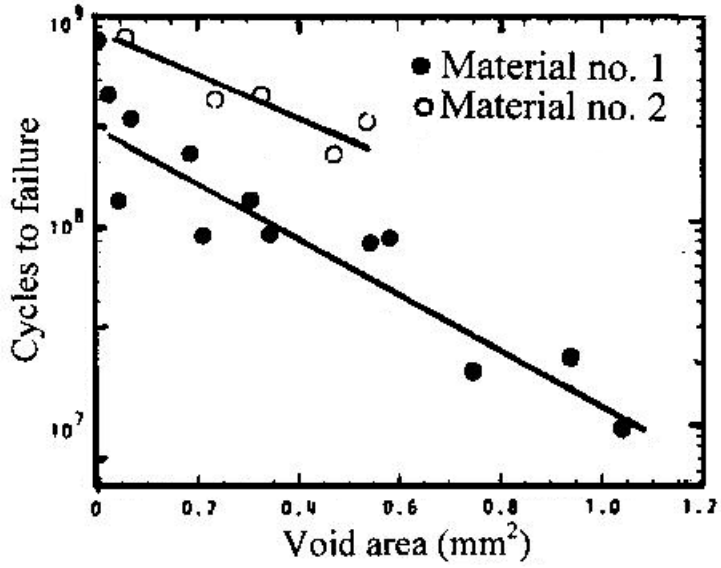

Figure 2.7: Dependence of number of cycles to failure on void size of two AlSi11 cast alloys [50].

that PEC samples had a lower run-out stress (38MPa) (stress at which the tests are stopped without fatigue failure of specimen) compared to the samples taken from the wedge (55MPa). This resulted from the change in the diameter of the pores that initiated the fatigue cracks. The wedge based samples had an average initiating pore diameter of 449μm while those from PEC sections averaged 1005μm. It was observed that doubling the average initiating pore diameter resulted in an approximate 30% decrease in run-out stress. It was also found that the correlation between the sizes of pores obtained from metallographic examination and fracture surfaces was very poor. Measurements made using conventional metallographic techniques substantially under-reported the average and maximum sizes of the crack initiating pores present in this alloy.

Gao et al. [54] investigated the effect of porosity on fatigue life of cast aluminium alloys, both experimentally and by using Finite Element Analysis(FEA). They found that pores close to the surface have high stress concentrations and easily lead to crack initiation. These failure dominant pores were primarily responsible

for fatigue failure in the A356-T6 alloy they tested.

In all these studies, it is noted that once a defect in the form of a pore exists, the total fatigue life can be approximated to the fatigue crack propagation life. This is justified through the argument that crack initiation life represents an insignificant portion of the fatigue life and can be neglected [48, 49, 52]. The initiating pore is assumed to be an initial crack and LEFM analysis is done to approximate the fatigue crack propagation rate, and hence the approximate fatigue life of the specimen or component. In most of these studies however, the initial crack sizes are obtained only upon carrying out fractographic examinations on the fracture surfaces to estimate the fatal fatigue crack initiating defect size. The study by Boileau and Allison [11] revealed a very poor correlation between the fatal defect sizes obtained from the metallographic surfaces and those obtained from fractographic examination on the fracture surfaces. Measurements made using conventional metallographic techniques severely under-reported the average and maximum sizes of the crack initiating pores present in the alloy. This therefore means that the fatigue lives obtained by using initial crack sizes from metallographic surfaces could severely overestimate the fatigue life. Further, this presents a strong case for the use of non-destructive examination methods (for example, technology in the level of high resolution X-ray tomography [53]) to obtain maximum defect sizes especially in highly stressed and critical areas for purposes of fatigue life prediction.

Stress level and small crack effects have also been found to influence fatigue crack propagation. At low stresses, cracks stopped at grain boundaries while at high stresses crack propagation was independent of such boundaries [53]. Caton et. al. [60] have also reported higher small crack propagation rates as opposed to lower long crack propagation rates, hence a small crack and stress level effect. These observations imply that to obtain accurate predictions using

LEFM analysis, one must consider the influence of small crack effect, stress level effect and defect size effect. Due to these varied effects, results obtained by fatigue life prediction methods vary greatly from alloy to alloy and casting method and also display a high level of scatter. Crack propagation mechanisms and especially crack blocking become an important consideration that cannot be ignored in fatigue life prediction.

In conclusion, it is clear from the literature reviewed above and from references [20, 61–63], that in almost all conditions, porosity remains the single most harmful defect in a casting. The porosity may be in the form of microporosity or gas porosity, macro porosity or shrinkage porosity or a combination of both. It is desirable that a casting should have as little porosity as possible or no porosity at all. Porosity can be eliminated or minimized in castings by adopting such practice as; a high cooling rate during solidification, maintaining the melt as clean as practically possible, using degassing techniques to reduce the level of dissolved hydrogen in a liquid melt and proper design of the pouring, runner, gate and feeding system to ensure a solidification process that does not encourage formation of shrinkage porosity. In certain cases, post casting treatment processes such as Hot Isostatic Pressing (HIP) has been employed with commendable degree of success in reducing and sometimes eliminating pores altogether [61, 63, 64]. However, as observed by Mashl et al. [64], Hot Isostatic Pressing is most successful in cases where there is no surface connected porosity such as in sand and investment casting. Hot Isostatic Pressing dramatically increased the fatigue life of cast components by eliminating pores as the sites for crack initiation, and instead, cracks initiated from eutectic particles or persistent slip bands. Figure 2.8 demonstrates the large gain in fatigue life attainable after HIP processing.

Pores close to and near the surface are the most detrimental in reducing the

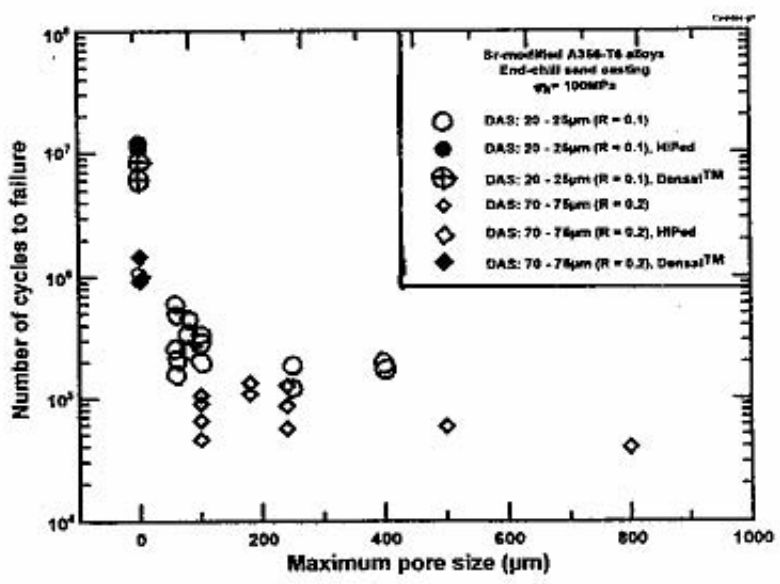

Figure 2.8: Fatigue behaviour as a function of maximum pore size for as cast, and for HIP and Densal processed A356 castings. All samples are in the T6 heat treated condition [64].

fatigue life of cast components due to the sharp increase in the stress intensity factor and hence a reduction in the crack initiation life. Castings have critical pore sizes below which pores will not initiate cracks. However, this pore size is a function of many variables such as solidification rate (and hence the dendrite arm spacing(DAS)), composition, casting process, post casting treatment processes and melt treatment. Below this critical pore size, other crack initiators such as oxide film, eutectic particles, intermetallic phases and persistent slip bands become dominant.

The existence of pores in castings has meant that their influence on mechanical properties remains an ever present reality. The need to use cast components in critical applications has added impetus to the search for a means of predicting the influence of porosity on the mechanical properties and particularly fatigue. Models have been developed which treat existing pores as initial cracks and employ LEFM to predict the crack propagation life and hence the fatigue life of

the components at hand. In almost all approaches developed, the crack incubation period is considered negligible when compared to the total fatigue life, hence the justification to approximate the fatigue life using the crack propagation component only. In the following section, some of the various approaches used to estimate fatigue life are reviewed.

2.9.2.2 Crack Propagation Life Modeling

Defects in cast aluminium in the form of pores, oxide films and other inclusions initiate cracks when subjected to cyclic loading. The cracks mainly initiate at the points where the defect has a sharp end or where eutectic silicon particles can easily decohere due to high stress concentration. To predict fatigue life and fatigue strength, the defects are treated as initial cracks. This simplification enables the use of LEFM to predict the fatigue properties of cast components containing defects. Experiments have shown that cracks easily initiate from defects, and that the crack initiation life is small compared to the total fatigue life. Odegard and Pedersen [49] found that crack initiation life from surface cracks comprised only 1% of the total fatigue life in specimens of a wheel material (WM-T6) heat treated to the T6 condition. As a result, LEFM has been used to predict fatigue life by using models based on treating casting defects as initial cracks and the crack propagation life as the approximate fatigue life to failure with a reasonable degree of accuracy [43, 45, 48, 49].

The number of cycles required to grow a crack from an initial size, a_i, to a final size, a_f, can be readily computed from a growth rate equation, the Paris-Erdogan law, of the form:

$$\frac{da}{dN} = C(\Delta K)^m \tag{2.13}$$

where;

- K = the Stress Intensity Factor, which expresses the severity of the loading at a crack or defect.
- C, m = Paris Law region constants.

The stress intensity factor range, ΔK, can be approximated by the equation

$$\Delta K = Y(a)\sigma_a\sqrt{a\pi} \tag{2.14}$$

where;

- σ_a = the applied stress amplitude
- $Y(a)$ = compliance calibration factor.

To cater for crack closure effects, equation 2.13 can be written as;

$$\frac{da}{dN} = C(\Delta K_{eff})^m \tag{2.15}$$

where ΔK_{eff} is the effective stress intensity factor which is equal to $U.\Delta K$. U is the crack closure factor and is obtained from crack closure measurements.

Couper et al. [43] used these simplifying and other assumptions to obtain the number of cycles to propagate a crack to failure ($N_p = N_f - N_i$) using equation 2.16 as:

$$a_i N_p = [\frac{1}{CY(a_i)\sqrt{\pi}^m U_R(a_i)^m(\Delta\sigma)^m}] \tag{2.16}$$

The constants C and m used in the above analysis were obtained from previous work by Couper et al. [43] on alloy CP601 as $10^{-10.2}$ and 4 respectively, and were observed to be insensitive to heat treatment. The equivalent crack sizes, a_i, were obtained from measurements on fracture surfaces. The results obtained

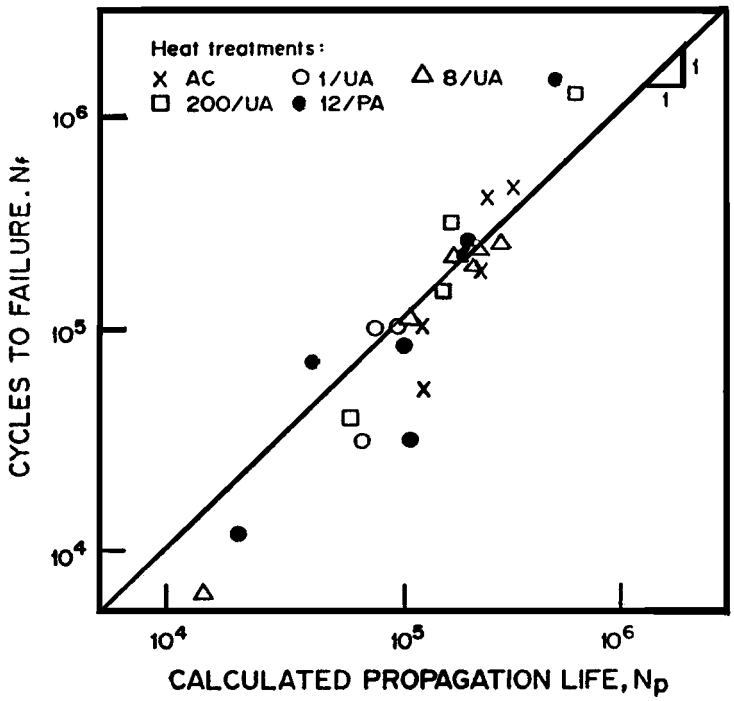

Figure 2.9: Comparison of actual fatigue life(N_f) with the estimated propagation life(N_p)of cast CP601 for tests at R = -1 [43].

were compared with stress-life test results (at $R = -1$) and are illustrated in Figure 2.9.

The model gives reasonable agreement with the test results, with the results being within a factor of 2.4 of the relation $N_f = N_p$. The authors, in obtaining some of the factors in equation 2.16, for example the closure factor, $U_R(a_i)$, and the compliance factor, $Y(a_i)$, assumed that crack closure occurs during the compressive half cycle only. Their results are thus influenced by these assumptions and the authors noted that these assumptions needed to be experimentally verified.

Skallerud et al [48], while investigating the fatigue life of aluminium alloys with casting defects observed different defects and classified the most important as;

- a single cavity at or near the specimen surface

- a series of shrinkage cavities at the surface
- a gas pore at the surface

These defects initially had complex geometries. However, upon growth these defects quickly developed into simplified shapes. Based on these observations, they used simplifying assumptions to approximate the complex shapes as semi-elliptical shapes and embedded circular cracks. Examples of typical defect geometries and how they were simplified in the analysis are illustrated in Figure 2.10.

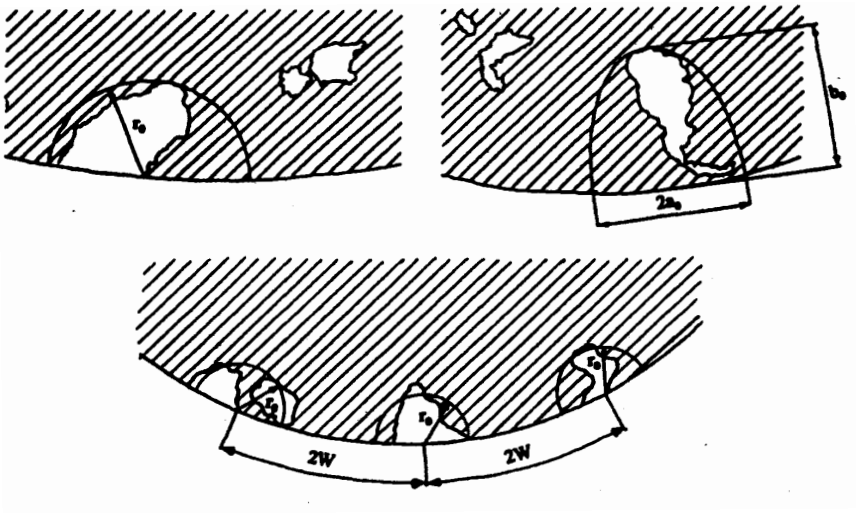

Figure 2.10: Typical defect geometries and how they are simplified [48].

As a result, they developed the modified Paris-Erdogan law as:

$$\frac{da}{dN} = C[(\Delta K)^m_{eff} - (\Delta K)^m_{th,eff}], \tag{2.17}$$

where $(\Delta \mathrm{K})^m{}_{th,eff}$ is the effective threshold stress intensity factor

and $(\Delta K)_{eff} = (\sigma_{max} - \sigma_{open}) F \sqrt{a\pi}$,

F is the geometrical factor suitable for the observed initial crack shapes simplified as appropriate. Calculations for obtaining the values of F, $\frac{da}{dN}$ and ΔK for the

irregularly shaped cracks are discussed in Skallerud et al. [48]. This model took crack closure into account and simplified the initial complex shapes. The model gave satisfactory results, which were found to agree with experimentally obtained test results.

Wang et al [45] also used a modified version of the Paris-Erdogan equation to obtain an equation for estimating the fatigue propagation life, N_p, as

$$a_i N_p = B(\Delta\sigma)^{-m} \tag{2.18}$$

where;

$B = [\frac{m-2}{2} CY(a_i)^m U_R(a_i)^m \pi^{\frac{m}{2}}]^{-1}$

and m is a constant. This equation was found to adequately describe the test results for A356-T6 alloys.

Apart from porosity, there are other factors that affect the fatigue behaviour of cast aluminium alloys, some of which relate to the alloy itself, processing method etc. Therefore, any attempt to model the fatigue behaviour of the alloys based on porosity only cannot be truly accurate. However, models developed by various researchers have closely approximated the fatigue life of the materials when compared to experimental results. It is evident that the fatigue life can be reasonably approximated by the crack propagation life in instances where a material is found to have a pre-existing defect in the form of a shrinkage pore, gas pore or folded oxide film. In such cases, the portion of life spent in initiating the crack is small and can be neglected [43, 45, 48, 49]. Despite all the efforts made towards modeling the fatigue life of cast aluminium components, it has proved difficult to come up with a universally accepted threshold pore size above which, fatigue properties would be porosity controlled.

2.9.2.3 Effect of Oxide Films

Aluminium alloys form self protecting, and hence coherent oxide films, when their surfaces are exposed to an atmosphere containing oxygen [16, 65–67]. This film, when continuous on the surface of a melt, is helpful in preventing further oxidation and contamination of the melt. However, if proper control of the melt during pouring and mould filling is not exercised, the melt's advancing front becomes unstable and could lead to entrainment of the film in a folded oxide dry-side to dry-side orientation in the body of the casting or component. Such folds essentially constitute cracks in the solidified castings [16].

Considerable effort has been expended by various researchers in trying to establish the effects of the oxide films on the tensile strength [67, 68] as well as the fatigue properties of aluminium alloy castings [45, 65, 66, 69]. These researchers have established that after porosity, oxide films rank next in detrimentally influencing the mechanical properties of cast aluminium alloys.

Campbell [16] and Nyahumwa et al. [66] have drawn a distinction between old and new (or 'young') oxide films. Old oxide films are formed during the melting process when the melt is still held in the furnace, or during the transfer of the melt to the mould using a ladle. Young oxide films are formed during the melt transfer process from the ladle to the mould cavity through the running system. Old oxide films are mainly thick chunks of refractory oxide, sometimes high in magnesium because of the development of the spinel structure with time (time is important in determining how thick the oxide film becomes). New oxide films are essentially thin and are finely folded during the pouring process. The new oxide films are mainly associated with pores and are formed from substantially pure aluminium oxide [66]. Further, old oxide films are usually trapped inside dendrites while young oxide films are generally located along

grain boundaries [65].

Nyahumwa et al. [66] used turbulent and quiescent mould filling to investigate the effects of entrapped oxide films on the fatigue life of a cast Al-7Si-Mg alloy. Turbulently filled castings had lower fatigue lives than the quiescently filled castings. Fatigue cracks in the turbulently filled castings initiated at a mixture of young and old oxide film defects and pores associated with oxide films. Competing mechanisms of fatigue crack initiation in the quiescently filled castings were old oxide film defects and near surface slip. It is therefore necessary to control the mould filling process if one is to obtain castings that have acceptable mechanical properties. Quiescent, filtered, bottom gated filling systems are preferred as one way of controlling the filling process to ensure that the amount of oxide films entrained during the filling process is closely controlled [16].

The importance of oxide films in fatigue crack initiation has also been demonstrated by other researchers [45, 69]. The study by Wang et al. [45] suggested that the effect of oxide films was of the same order of magnitude as large phase constituents in the alloy. They further reported that compared with materials that failed from porosity, the fatigue life of specimens in which fatigue cracks initiated from oxide films was almost 4-5 times longer. Wang et al. also reported a critical oxide film size of 50μm for A356 alloy tested under a stress amplitude of 100MPa and a stress ratio of 0.1. Below this size, the fatigue life was found to be comparable to samples that were free from oxide films. Figure 2.11 presents fatigue lives as a function of oxide film size at different sizes of SDAS as reported by Wang et al. [45].

In the work of Campbell et al. [65], it was proposed that the effects of oxide films may in reality be underrated. They suggested that the cracking of intermetallics which is conventionally attributed to their brittleness and eutectic particle/matrix interface debonding, may actually be due to a non-bonded

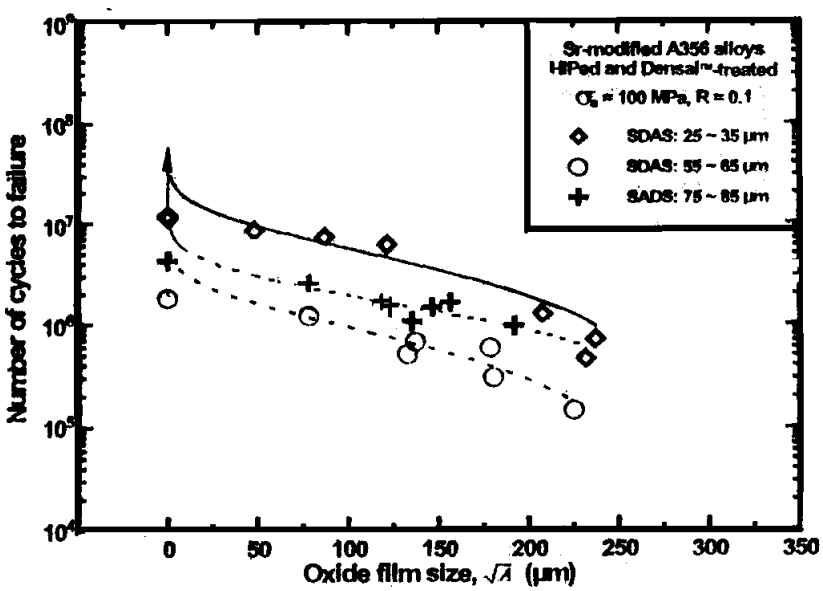

Figure 2.11: Fatigue life of a Sr-modified A356-T6 alloy as a function of oxide film size for various SDAS values [45].

oxide inter layer. This is a very interesting proposition given the widespread interpretation of the mechanisms of fatigue failure by cracking of intermetallic particles and eutectic particle/matrix interface debonding that is reported in the literature. Further research on their proposition is undoubtedly required.

2.9.3 Effects of Microstructure and Alloy Chemistry

2.9.3.1 Introduction

In the preceding sections, the effects of porosity and oxide inclusions on the fatigue properties of cast aluminium alloys have been discussed. The overriding aspect is that failure of cast aluminium alloys through fatigue or other fracture modes is caused by cracks initiated from prominent defects. If these defects are minimized or altogether eliminated, performance is improved. The mechanical properties are then limited by the next family of defects. When the prominent defects are removed or tightly controlled, larger intermetallic compounds or other brittle phases commonly consisting of Fe and Mg may cause failure. If

these large compounds and phases exist at low levels (or small sizes), component failure is dictated by the microstructural characteristics of the material such as slip resistance; once slip is initiated, slip distance will depend on dendrite arm spacing [47].

Therefore, microstructural features become an important influence on the fatigue properties once the casting defects have been eliminated or reduced below certain critical levels or sizes. These critical sizes are dependent upon many factors such as processing methods, local freezing conditions, loading conditions and alloy chemistry. The microstructure of aluminium alloys consists of aluminium dendrites, eutectic particles, intermetallic phases and inclusions. Depending on alloy chemistry and post treatment procedures (heat treatment), other features such as Mg_2Si precipitates may play a key role in influencing the fatigue properties. The study of the effects of microstructure and alloy chemistry has focussed on; the effect of DAS, Si particles, Si particle modification and Iron. Heat treatment has also been found to affect the structure of the Al-matrix as well as the morphology and size of Si particles, and hence to influence the fatigue properties of the alloys. These issues are reviewed in the following subsections.

2.9.3.2 Effect of Dendrite Arm Spacing

Spear and Gardner [70] discussed the importance of the Dendrite Cell Size (DCS) as a means of quantitatively expressing the microstructural refinement of an aluminium alloy casting. In the same paper, they identified Dendrite Arm Spacing (DAS) and Dendrite Cell Interval (DCI) as the two other possible parameters of expressing the microstructural refinement of the same alloys. They concluded that the DCS is the most appropriate way to undertake this task. However, since then, secondary dendrite arm spacing (SDAS) has taken over as the preferred means of expressing the microstructural refinement in aluminium alloys, where

SDAS is defined as the distance between the secondary dendrite arms in a cast aluminium alloy.

Solidification rate and alloy composition are the major factors influencing the DAS. However, the solidification rate is a more prominent factor and the DAS of aluminium casting alloys is usually primarily related to the solidification rate. In early studies on Al-Si alloys [71], the DAS was related to the local solidification time, t_f and found to be inversely proportional to the local solidification rate, where for alloy Al7SiMg, A = 11μm x sec$^{1/3}$ and

$$DAS = A(t_f)^{1/3}. \tag{2.19}$$

Zhang et al. [13] found that the total fatigue life of A356.2-T6 aluminium casting alloy was affected by the cooling rate during solidification, as quantified by the secondary dendrite arm spacing (SDAS). They found that at SDAS less than ≈30μm, the fatigue life varies slightly with SDAS under low- and high-cycle axial and bending loading conditions. As the SDAS increases beyond ≈30μm, fatigue life drops by ≈3 times under low-cycle and ≈100 times under high cycle fatigue at R = 0.1. Fatigue cracks initiate at or near the eutectic regions when SDAS is less than ≈27μm. When SDAS is greater than ≈30μm, porosity becomes the dominant crack initiation site. A SDAS of ≈30μm corresponds to a critical pore size of ≈80-100μm. They concluded that in the absence of oxide inclusions, pore size may be used as a parameter to predict the fatigue behaviour of this casting alloy.

Wang et al. [72] found that for SDAS values less than 60μm, fatigue life decreased with increasing SDAS values, whereas for SDAS values larger than 60μm, increasing the SDAS did not decrease the fatigue life as reported in literature.

Kumai et al. [25] studied the effects of the silicon particle size and the dendrite

cell size in AC4CH aluminium alloy. In this study, it was difficult to isolate the effects of dendrite cell sizes and silicon particle size due to the fact that the cooling conditions which refine the dendrites also lead to finer silicon particle sizes. In this work, the effects of the silicon morphology were observed to override those of the dendrite cell size in influencing the fatigue behaviour. It was reported that due to the higher monotonic and cyclic strain hardening in coarse needle-like silicon particles, the unmodified silicon led to lower crack growth rates at low stress intensity factor ranges. At high stress intensity factor ranges, a higher crack growth rate was observed.

Further, large roughness induced closure effects are observed in the materials. However, since the crack closure effects are comparable in all the tests, it can be concluded that the effects observed are due to the dendrite cell sizes and the silicon particle morphology. Coarse and needle-like unmodified eutectic Si particles act as stress raisers and easily crack or decohere to provide multiple cracks and accelerate crack growth at high ΔK. In the low ΔK range, the unmodified cast structure showed a lower crack growth rate due to the larger proof stress observed at this condition which reduces the cyclic crack opening displacement [25].

2.9.3.3 Effect of Si and Eutectic Modification

Aluminium silicon alloys form a structure composed of aluminium dendrites, eutectic silicon and intermetallic phases on solidifying. The nature of the microstructure is influenced by the local solidification rate, the chemistry of the alloy, the melt treatment and post-treatment procedures (such as heat treatment). Previous work has shown that the morphology, size and distribution of the eutectic silicon particles have a significant role to play in determining the ultimate mechanical properties of the aluminium alloy, particularly once the cast-

ing defects and inclusions have been eliminated or significantly reduced [25, 73]. Eutectic silicon particles ordinarily solidify in a coarse, polyhedral needle-like structure. This eutectic silicon shape has been found to provide a weak link in the microstructure that negatively affects the mechanical properties. However, research has shown that the morphology of the eutectic silicon can be changed from needle-like form to fibrous form through chemical modification by use of modifiers such as sodium, strontium, calcium or antimony [4, 22, 46, 61], and further to rounded finer particles by thermal modification through heat treatment procedures [43, 74, 75]. Modification can improve the ultimate tensile strength and the percent elongation. In some studies, it has been claimed that eutectic modification results in poorer fatigue properties [46], while in other cases eutectic modification has been reported to result in improved fatigue properties [72]. Currently, in the commercial manufacture of most aluminium silicon alloys, use of modifiers has emerged as a standard procedure.

Eutectic modification by the use of strontium has been reported to cause an increase in gas porosity, thereby negatively affecting the fatigue properties. Zhang et al. [46] concluded that A356.2 without Sr modification shows better fatigue properties due to less porosity. According to Wang et al. [72], pore free modified A356/357 show improved fatigue properties. The overall fatigue lives of modified alloys are longer compared with those of unmodified alloys. The general behaviour with SDAS is however different for the unmodified and modified alloys. Modified alloys show a decreasing fatigue life with increasing SDAS for SDAS $<60\mu$m and increasing fatigue life with SDAS for SDAS $>60\mu$m. In unmodified alloys, fatigue life decreases with SDAS in both fine and coarse microstructures. At intermediate SDAS (40-60μm), fatigue life remains constant with SDAS.

In the work by Lee et al. [76], the effects of the size and morphology of eutectic silicon particles on the fatigue crack growth characteristics of an Al-Si-Mg cast

alloy were studied under the constant load amplitude condition. It was noted that refining the eutectic silicon size and change in shape to globular eutectic silicon leads to improved fatigue crack growth resistance. Size, morphology and content have also been observed to control crack initiation and growth in an Al-Si-Cu-Ni-Mg alloy [77].

Lados and Apelian [73] studied the effects of different silicon contents (1%, 7% and 13%) for both modified and unmodified Al-Si-Mg alloys. Figure 2.12 illustrates some of the results they obtained. They observed that the Si content of the alloy also plays an important role in the fatigue crack growth behaviour of both modified and unmodified Al-Si-Mg alloys. The lower the Si content, the better the fatigue crack growth resistance.

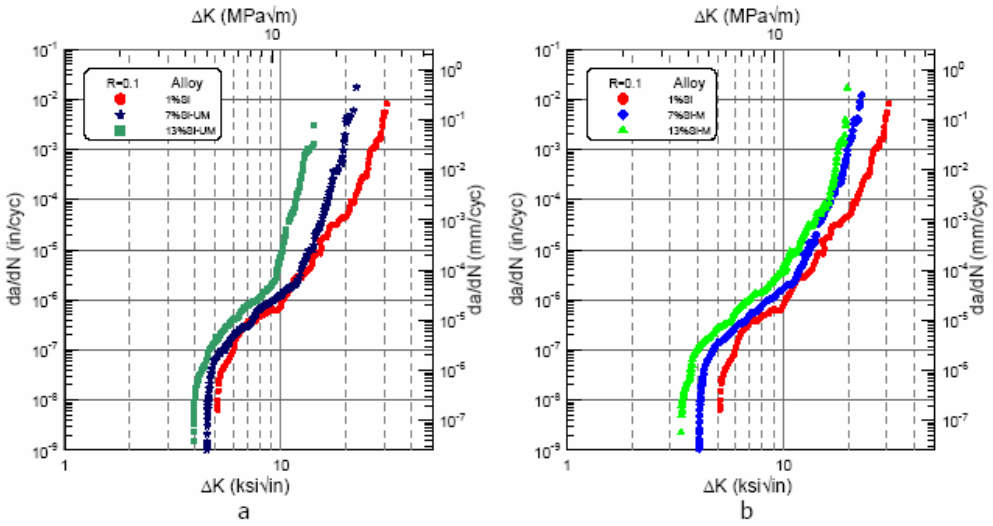

Figure 2.12: Effect of Si content on FCG behaviour of (a)unmodified (b) modified alloys under R=0.1 [73]

As seen in Figure 2.12, the dendritic alloy (1%Si, all in solid solution, no eutectic) has the highest threshold and pseudo-fracture toughness. It also has the lowest crack growth rate, followed by the A356 (7%Si) alloys and finally the eutectic (13%Si) alloys.

In alloys where all other fatigue initiating mechanisms have been eliminated, silicon particle decohesion contributes to crack initiation [55]. Once the crack has been initiated, it's propagation then becomes a function of the local microstructure especially at low stresses. Crack branching, crack deflection and crack blocking then determine the rate of propagation of the crack. Savelli et al. [55] observed three types of crack blocking, namely; intragranular, intergranular and triple point blocking. This implies that crack propagation mechanisms and especially crack blocking become an important consideration that cannot be ignored in fatigue life prediction.

The mechanisms of fatigue crack initiation associated with Si particles could be silicon particle/matrix interface decohesion or particle fracturing/cleavage. These mechanisms could be both present in an alloy undergoing fatigue failure but at least one must be dominant over the other for a given microstructure and fatigue failure case. This may depend on the stress intensity factor range, ΔK, the stress amplitude, the stress level and Si particle morphology. In modified alloys, the Si particles mainly decohere or pull out from the surrounding aluminium matrix during fatigue crack propagation. Finer particles exhibit higher strength than the stress required for their cracking, resulting in their decohering. Hence, in this regard, modified alloys are more resistant to fatigue crack growth than unmodified alloys [76].

2.9.3.4 Effect of Mg Content

Magnesium, in combination with silicon, age hardens heat treatable aluminium silicon alloys through the precipitation of magnesium silicide (Mg_2Si) in the aluminium dendrites [9, 12]. A study by Wang et al. [72] found that alloys high in magnesium content (e.g. A357) exhibited a shorter fatigue life especially at intermediate and large SDAS. The behaviour for unmodified alloys has three distinct

sections: At low SDAS(<40μm), the fatigue life is usually long and decreases with increasing SDAS, while at intermediate SDAS(40-60μm), the fatigue lives of both A357 and 356 alloys are independent of SDAS whereas in very coarse microstructures, the fatigue lives decrease with increasing SDAS. Increasing the Mg content increases the eutectic particle size, particularly in the Sr modified alloy due to the formation of large Mg-containing Fe-rich intermetallic phase. The increase in eutectic particle size leads to more particle fracture and thus short fatigue lives. Magnesium content also determines the size, number and shape of Fe phases [29].

2.9.3.5 Effect of Fe Content

Iron is not intentionally added as an alloying element to most aluminium alloys, but it is always present as the dominant impurity in commercial grades and is still a major impurity in purer grades. It forms large inclusions that are difficult to dissolve and are not modified by heat treatment. A significant reduction in mechanical properties (particularly fracture toughness and ductility) and corrosion resistance caused by an increase in the iron percentage has been observed and in critical applications, the maximum iron content is kept as low as economically possible [3].

Increasing the Fe content from 0.08% to 0.14% in A357 alloy decreases the fatigue life especially at very coarse microstructures. However, this influence of Fe is not very significant. In the work of Wang et al. [72], the characteristic fatigue life of low Fe A356 was found to be 8.35 x 10^5 cycles, while that of high Fe-containing alloy was 6.75 x 10^5 cycles. When the Fe content was increased from 0.13% (in A356) to 0.47% (in 356), the size and amount of the porosity increased from 420μm and 0.4% to 600μm and 1.5% respectively; the length and area percent of the iron intermetallics increased from 6μm and 0.5% to 25μm

and 2% respectively [56]. In the same study, the tensile ductility decreased by 60% while the Ultimate Tensile Strength (UTS) dropped by a marginal 8%; the Low Cycle Fatigue(LCF) strength dropped from 187MPa to 159MPa while the High Cycle Fatigue (HCF) strength decreased from 68MPa to 64MPa. Tan et al [58] also reported that in high Fe containing A357, intermetallic compounds initiated fatigue cracks while in low Fe containing A357, eutectic Si particles were the sites of fatigue crack initiation. In Hot Isostatically Pressed Al-Si-Cu-Mg alloy castings, Fe intermetallic compounds with needle shape were observed to act as the fatigue crack initiation sites [57].

The amount and size of the iron intermetallics formed is a function of the rate of solidification and the alloy chemistry. In the presence of other elements such as Mg, Al and Si, Fe forms intermetallics that degrade tensile ductility, the UTS and the fatigue strength. Fe also affects castability by interfering with interdendritic feeding and thus promoting increased formation of porosity. Some of the intermetallics formed may take the following forms depending on the elements present [29, 78]:

- Al_5SiFe (β- phase); thin platelets or rod like morphology especially for Magnesium content below 0.35% to 0.40%.
- When manganese is present, $Al_{15}(FeMn)_3Si_2$ (α - phase) in the chinese script morphology.
- When magnesium is present, $Al_8FeMg_3Si_6$ (π - phase) is formed (this has a chinese script morphology too if formed during eutectic reaction but globular if it forms as a primary precipitate from the liquid)

Elongated Fe compounds encourage early crack initiation and also accelerate crack propagation. The increase in interconnected shrinkage porosity in the

high Fe secondary 356 alloy is mainly related to the increasing size and amount of α and β phases, which reduce the permeability of the mushy zone and thus increase the propensity for the formation of interconnected shrinkage porosity. In addition, a change in the solidification sequence may lead to the nucleation of eutectic Si on intermetallic platelets and hence decrease the permeability of the interdendritic network. Addition of Beryllium to high iron containing alloys has been found to lead to a change in morphology of intermetallic compounds from acicular $FeSiAl_5$ to comparatively harmless spherical iron bearing compounds, hence removing the embrittling effect of the acicular shape compounds [58]. Beryllium also reduces the number of iron bearing compounds.

2.9.3.6 Effect of Heat Treatment

Heat treatment of aluminium silicon alloys has the double effect of strengthening the aluminium dendrite phase, through the precipitation of magnesium silicide (Mg_2Si) and the refining of the eutectic silicon phase. Thus the heat treatment procedure has the potential of increasing the tensile strength of the alloy. Heat treatment may also increase the fatigue strength of a defect free alloy through reduction of the stress raising effect of the eutectic silicon (by changing the shape from acicular to the less harmful refined and spheroidized shape). This is however possible only in cases where the defect level has been significantly reduced, and the adverse effects of the residual stresses introduced during the heat treatment procedure eliminated.

In certain cases, attempts to investigate the effects of heat treatment on fatigue have been completely frustrated by the presence of more dominant casting defects [43]. Investigations have shown a clear influence of heat treatment on fatigue properties of wrought aluminium alloys, but the influence has not been exhausted in the case of cast aluminium alloys. Couper et al. [43] reported that

the S-N properties of CP601(A356) are remarkably insensitive to heat treatment condition, in contrast to the behaviour of wrought alloys in which the fatigue resistance is usually closely related to the yield stress or the tensile strength. The influence of heat treatment on cast alloys is further complicated by the different heat treatment procedures that the alloys can be subjected to. In one test by Wang et al [72], it was observed that the soft matrix produced by two under-aged heat treatments resulted in a lower fatigue life compared with a sample having a T6 near peak aged heat treatment. In this case, longer T6 solution treatment (12h) produced an optimum combination of small Fe rich and silicon particles leading to T6 treated alloys A356/357 having adequate fatigue lives.

Solution heat treatment results in a material that has a higher yield strength and ultimate tensile strength while the ductility is reduced [3]. Precipitation of magnesium silicide (Mg_2Si) after heat treatment is the most effective strengthener of the Al-Si-Mg alloys. Treatment T6 led to a certain improvement in the fatigue performance of the alloy, although this positive effect was almost completely hidden by the stronger one associated with porosity. It is therefore necessary to exclude this more marked influence to reveal that owing to heat treatment [3].

In conclusion, heat treatment changes both the size and morphology of phases like the eutectic Si, improves both the tensile and yield strength, reduces segregation and relocates residual stresses. Fatigue life is therefore also affected by heat treatment. The influence of heat treatment does not depend on the heat parameters alone, but also on casting conditions, alloy chemistry, and casting sizes and geometries. However, specific information relating to the effect of heat treatment on fatigue life of casting aluminium alloys is unavailable in the literature.

2.9.3.7 Effect of Yield Strength

The influence of yield strength of a cast aluminium alloy on the fatigue properties has not been specifically studied. However, heat treatment affects the yield strength of the alloys, and thus the influence of yield strength on fatigue properties of cast aluminium alloys can be deduced from heat treatment studies. This influence can be presented differently depending on the approach used and is thus not easy to interpret. Couper et al [43] showed that in contrast to wrought aluminium alloys, the S-N properties of a cast aluminium alloy CP601(A356) did not respond to heat treatment. This suggests that the fatigue life of these alloys was not dependent on yield strength or tensile strength since heat treatment significantly increased these properties in the cast alloy. However, in this case, the fatigue cracks were observed to have originated from casting pores. According to fracture mechanics theories, increasing the yield strength results in lower threshold stress intensity factors, ΔK_{th} and expedites the growth of microstructurally small cracks during the initiation period [47]. On the other hand, increasing the yield strength reduces the number and size of local plastic deformation zones in the material. This decreases the possibility of forming microcracks in front of the main fatigue crack. In addition, increasing the yield strength increases the matrix resistance to dislocation movement within dendrite cells, leading to fewer dislocations moving towards the cell grain boundaries to interact with the eutectic particles [72]. This decreases the long crack growth rate during propagation period due to reduced micro crack damage in the material.

2.9.4 Influence of Residual Stress

The main processes used to heat treat aluminium involves heating to a temperature of 540^{o}C and then quenching in water at room temperature or in water at about 70^{o}C to 80^{o}C. When treated in this manner, residual stress is inevitably

introduced into the casting. Residual stress can be defined as self equilibrating locked in or internal stresses remaining in a material that is free of applied (external) forces, external constraints or temperature gradients [79]. In most cases, residual stresses are an undesired result of processing and they persist in the material unless eliminated by subsequent stress relieving techniques. Residual stresses are found in all alloy systems; aluminium alloys, super alloys, titanium alloys and steels. Accurate non destructive measurement of residual stress levels in materials is a rarity using currently available measuring techniques. Only X-ray diffraction technique comes close to this, but it is limited by the fact that it is applicable only at the surface. Despite the difficulty in obtaining accurate data relating to residual stress level, determining its presence, magnitude and distribution is vital for correct interpretation of fatigue crack growth experimental data and implicitly, real life applications.

The effect of residual stress on fatigue properties of cast Al-Si-Mg alloy has been presented by Lados et al. [47]. They report that when residual stresses are high, they mask the effect of microstructure, with all alloys with different microstructure (modified, unmodified, different Si levels - 1%, 7% and 13%) having similar and high thresholds (9-10MPa$\sqrt{m}$)(as shown in Figure 2.13(a)). When the residual stress level was reduced, the microstructure/roughness of the alloys become operative and a threshold ranking at a lower range (3.5-5.5MPa$\sqrt{m}$) is observed (as shown in Figure 2.13(b)from [73]).

The effect of residual stress on crack growth is most pronounced at low ΔK levels (ΔK_{th}) where the applied stresses are low and the ratios of residual stresses to applied stresses are high. Fracture toughness is also affected by residual stresses, but due to high applied stresses, the effect is considerably diminished relative to the impact on ΔK_{th}.

Lados and Apelian [80] developed mathematical models to quantify adequately

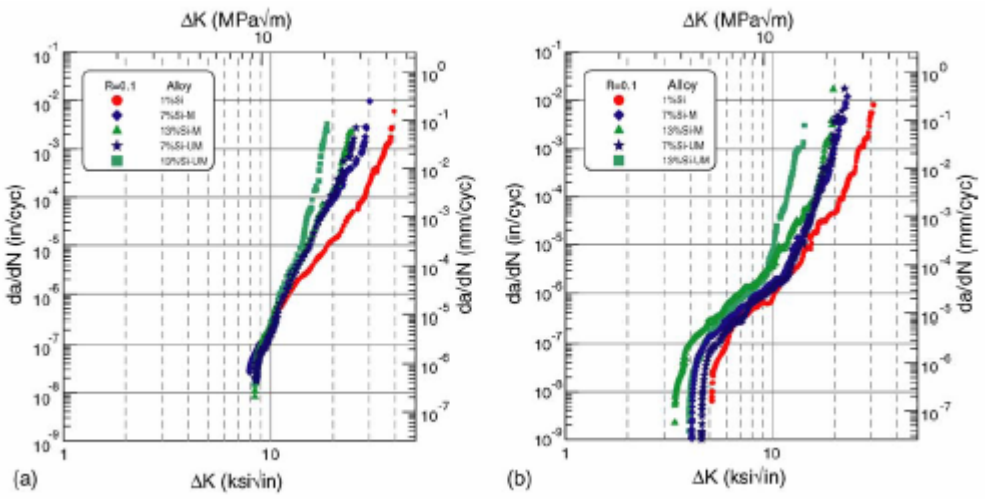

Figure 2.13: Fatigue crack growth behaviour of alloys for R = 0.1 (a) with residual stress (b) without residual stress [73]

the effect of residual stress on the fatigue crack growth data. The corrective methods used by the researchers apply to specimen geometries where notch clamping can be measured as well as cases where residual stress distribution is symmetrical; compression on the surface and tension on the interior.

Residual stresses can have a positive or negative impact on the fatigue behaviour, depending on whether the stresses are compressive or tensile. The increase in thresholds is explained by considering that the tip of the notch is subjected to compressive residual stresses, which at high levels create crack closure. Higher closure implies less effective driving force and hence lower growth rates, which for a given stress gives higher ΔK [80]. Due to the higher closure, less of the applied force actually acts on the crack tip (i.e., there is sheltering of the crack tip) and therefore a greater cyclic force will be required to reach the threshold and propagate the crack. In contrast, if the notch is found in a tensile stress field (centre crack tension specimen) the opposite effect is expected. In this case, the thresholds are lower than the residual stress free thresholds considering that the crack is open at all times, and the crack tip is exposed to the whole applied load

range. The two effects for compression and tension specimens are illustrated in Figure 2.14, where the effects of the compressive and tensile residual stresses on fatigue crack growth behaviour are presented.

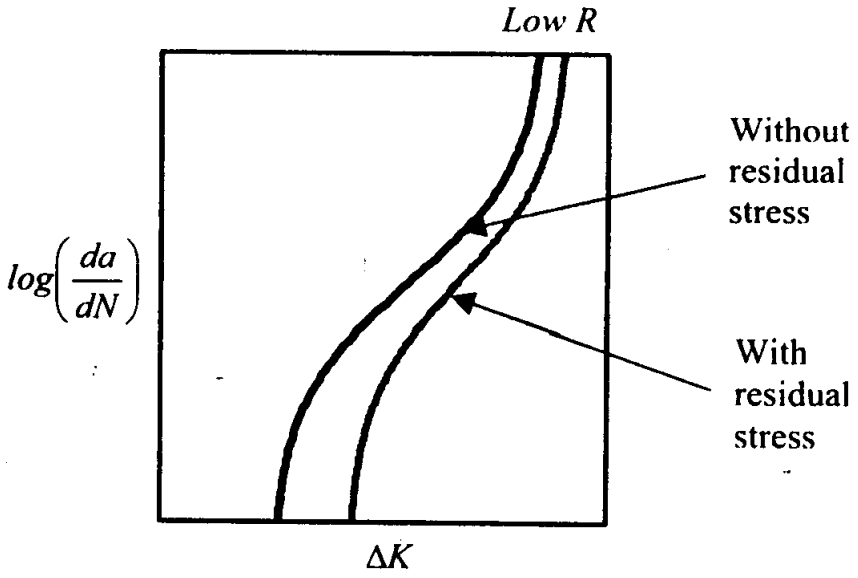

Figure 2.14: Influence of the residual stress on the fatigue crack growth (FCG) behaviour of cast aluminium alloys [47]

Residual stresses have traditionally not been given much attention in studying the fatigue behaviour of heat treated aluminium alloy castings. However, as seen in the preceding discussion, their effects can be significant and need to be taken into account where they are established to be present. There are several ways to eliminate residual stresses, such as thermal annealing, mechanical deformation and thermo-mechanical (also called up-hill quench). According to Lados et al. [47], thermo-mechanical (or up-hill quench) is the most successful one for aluminium alloys, in terms of both eliminating the residual stresses and also preserving the shape and mechanical properties of the part. The work presented by Lados and Apelian [80] presents a significant development in dealing with residual stress in cast products and presents useful ways of mathematically and experimentally accounting for it.

2.10 Comments on the Literature Review

It is evident from the literature that to achieve superior and reliable aluminium alloy castings, great care must be taken to control the entire preparation and casting process from selection of materials to design of the pouring, running, gating and feeding systems, mould making, melt handling, melt treatment and pouring. The type of casting process used and the actual processing conditions are also paramount to the casting quality. This complex interaction of parameters and practise determines the final structure and integrity of the casting. The resultant casting microstructure and soundness determine the mechanical properties, which in turn determine the suitability of the casting for the desired application.

With the development of appropriate technologies and procedures for casting and handling aluminium alloys, the popularity of secondary aluminium alloys for domestic, transport and industrial applications will continue to increase. In the developed countries, proper systems for segregating and grading scrap aluminium alloys using company specific recycling procedures ensure that high grade secondary aluminium alloys are possible. It is standard procedure to use spectrometers to control the quality of the scrap being recycled. As a result, it is easy to produce components and products from recycled aluminium that are within the set standard specifications. It is therefore expected that the castings obtained will have properties that are consistent with the established standards.

However, in certain cases, such as for the secondary aluminium sector in a developing country like Kenya, the level of technology, skill and knowledge does not allow foundries to have such strict controls on the aluminium recycling procedures. As a result, the castings in such foundries may not have compositions and properties that are consistent with the expected values for recycled aluminium

elsewhere. It is therefore important to establish and document the properties and expected composition limits for locally recycled aluminium alloys while at the same time setting the pace for the establishment of procedures necessary to achieve the same. In the pursuit of this very important development for the Kenyan foundry sector, this study adds a new dimension to the emerging interest in local foundry research work. As a result, this study on the recycling of cast aluminium scrap was guided by the following objectives;

- To determine the influence of modifiers on the microstructure, fatigue life and other mechanical properties (ultimate tensile strength, percent elongation and hardness) of cast alloys obtained from an assortment of scrap components
- To determine the influence of T4 and T6 heat treatment procedures on the microstructure, fatigue life and the mechanical properties of cast alloys obtained from an assortment of scrap components
- To determine the percent compositions of the alloys obtained on recycling these assorted scrap components.

Chapter 3

EXPERIMENTAL METHODOLOGY

3.1 Introduction

The major objectives of this study were; to investigate the influence of modifiers and heat treatment on the microstructure, fatigue properties and other mechanical properties of recycled cast aluminium alloys and to generate the quality index charts for the recycled aluminium alloys. Aluminium alloy scrap mainly composing of pistons, cylinder heads, gearbox housings and oils sumps were cast in two stages. The first stage involved casting small sized ingots which weighed between 4 and 7Kgs. In the second stage, these ingots were melted in batches of 25Kgs, given different melt treatments in respect of modifier levels, fluxing, degassing and grain refinement and cast to obtain the final casting blocks. The cast blocks obtained were machined into 220mm x 20mm x 20mm. This was the minimum size from which tensile specimens (according to DIN 50125 standard) for the Shimadzu Universal Tensile machine could be machined. These pieces were then heat treated as appropriate before being machined to size for fatigue and tensile testing. Samples for microstructure, composition and hardness testing were also prepared. Details of the experimental procedures adopted for the study are detailed in the following sections.

3.2 Scrap Selection and Sorting

Assorted aluminium alloy scrap was purchased in lots from a scrap dealer in Nairobi. The available scrap was mainly from motor vehicle components. The most common components were pistons, cylinder heads, gearbox housings, alternator covers, oil sumps and axle housings, among other smaller parts. Results from a previous study on recycled cast aluminium alloy scrap indicated that there were insignificant variations in compositions of the alloys when cast sep-

arately by component type and when mixed together and melted as assorted scrap [8]. Hence no attempt was made to sort the scrap into categories save from ensuring that the melts used composed of pistons, cylinder heads, gearbox housings and oil sumps only.

3.3 Mould Design

It was paramount that the mould design be carried out in such a manner that the possibility of oxide film entrainment and foreign matter inclusion in the main casting be minimized. An optimized quiescent bottom gated system designed according to the recommended best practice was used; this was done to achieve a non-turbulent melt flow into the mold cavity with minimal chances of entrainment of gases and oxide film inclusion. Practical guidelines suggested by previous researchers [16–18, 81–84] were used as far as practically possible. Locally made filters, made using silica sand and sodium silicate as a bonding agent were incorporated in the running system. This was done to trap and filter away large inclusions and oxide films before they could find their way into the mould cavity. Other researchers have used ceramic foam filters coupled with real time X-ray radiography to observe melt behaviour in the running systems during mould filling and also computer modeling software such as MAGMAsoft to optimize the performance of the running system. This practice where the facilities are available is highly recommended. In this study, however, such advanced pouring control facilities were not available. The nomogram shown in Figure 3.1 was used to arrive at the initial dimensions but changes were made on carrying out several trials. This design approach followed a trial and error method of designing the filling system recommended by Campbell [16].

The major objectives in designing the running system were to ensure;

- that there is no splashing of the melt on its arrival in the mould cavity;

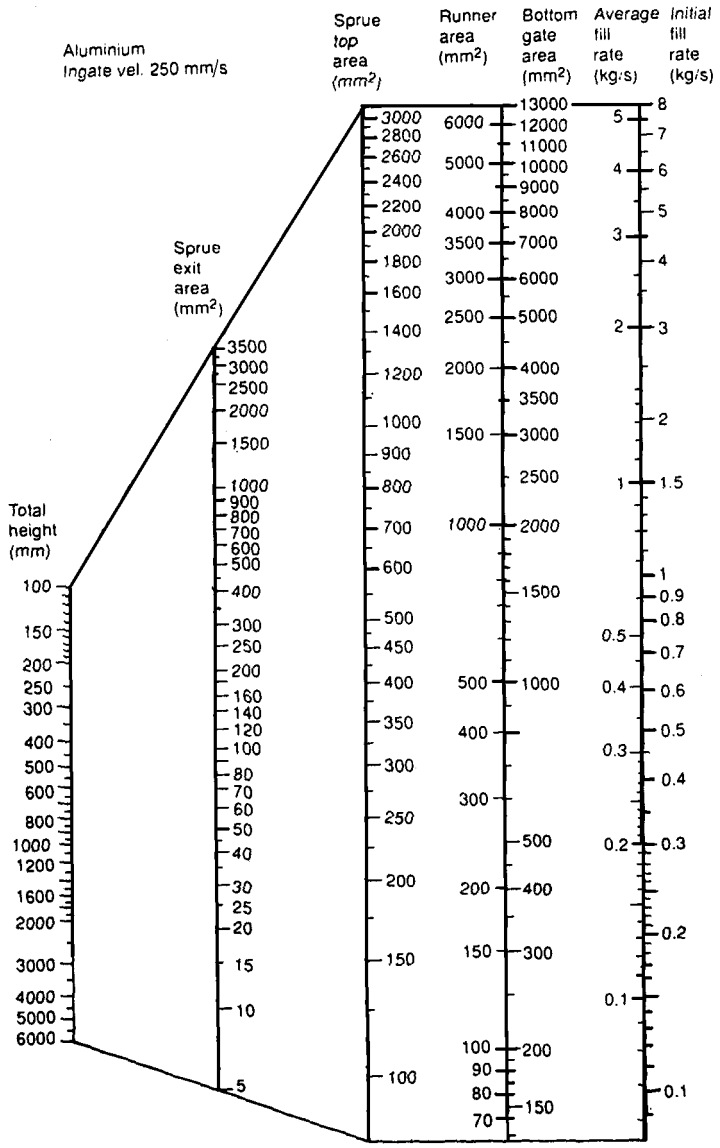

Figure 3.1: A nomogram for the calculation of running systems for aluminium alloys [16].

- an uphill flow of the melt in the runner, ingate and mould cavity;
- an ingate melt flow velocity of less than 0.5m/s.

The quiescently filled bottom gated system shown in Figure 3.2 was finally adopted after several trials. The sprue had an entrance area of 800mm^2, exit area of 640mm^2 and a height of 100mm.

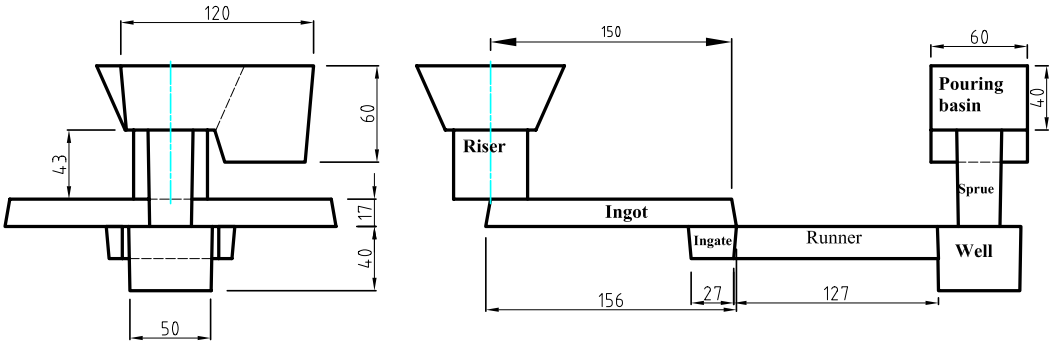

Figure 3.2: A schematic illustration of the running system used and the respective dimensions (in mm).

3.4 Scrap Melting, Melt Treatment and Pouring

Selected scrap lots were initially cleaned, melted and cast into small ingots. Cleaning was done using gasoline to remove oils, greases and other dirt to avoid contaminating the melt with dirt. During the transfer of the melt from the crucible to the ladle, care was taken to ensure that only about 80% of the melt was cast; the bottom 20% was thought to contain much of the iron and other contamination and hence unsuitable for the purpose of casting integrity products. In the second stage of casting, the ingots were charged in 25Kg lots into an industrial oil fired crucible furnace and melted under Coverall 11, which is a fluxing agent that acts as a flux to protect the melt from oxidation and hydrogen pickup during melting. At a melt temperature of about 750^{o}C, an inoculant was added into the melt and allowed to completely dissolve before Degasser 190 tablets were added for hydrogen removal. The inoculant tablets were added to refine the aluminium grains. Finally, a sodium modifier (Navac), was added. The quantity of the modifier was varied in different melts to investigate the effects of the different quantities of modifier on the microstructure and properties of the castings. The sodium content was varied between 0.00% and 0.025%. The melts were poured into the moulds at temperatures of between 730^{o}C and 750^{o}C.

3.5 Heat Treatment

Heat treatment was carried out using the air circulated electric resistance furnace at the Foundry Workshop, Jomo Kenyatta University of Agriculture and Technology. A photograph of the heat treatment furnace used in this work is shown in Figure 3.3. The specimens were heat treated before being machined to size. The T6 heat treatment procedure composed of; solution heat treatment at 540^{o}C for 8 hours, quenching with water at room temperature, pre-ageing at room temperature for 16 hours and precipitation treatment (artificial ageing) at 155^{o}C for 5 hours. The T4 heat treatment procedure composed of; solution heat treatment at 540^{o}C for 8 hours, quenching with water at room temperature and natural ageing for 96 hours before machining.

Figure 3.3: A photograph of the air circulated electric resistance furnace used for heat treatment.

To further investigate the effect of heat treatment on the UTS, elongation and hardness, three sets of the same alloy (modified with 0.005%Na and containing a high content of Cu and Mg) were subjected to three different heat treatment

procedures. The first set was solutionized for different times (4h, 10h, 14h, 18h, 24h and 32h) at a temperature of 500^{o}C, quenched in water at room temperature and artificially aged for 5 hours at 160^{o}C. No pre-ageing was done. The second set was solutionized for different times (4h, 8h, 10h, 15h, 20h and 24h), quenched in water, pre-aged for 16h at room temperature and then artificially aged for 5h at 160^{o}C. The third set was solutionized for 8h at 500^{o}C, quenched, pre-aged for 16 hours at room temperature and artificially aged (4h, 8h, 12h, 16h, 24h and 32h) at 160^{o}C. The heat treatment parameters were selected based on recommendations of previous work by Wang et al. [85] and Moustafa et al. [86]. A solution temperature of 500^{o}C is recommended for Al alloys containing above 2%Cu to prevent incipient melting of some of the Fe-Cu-containing phases within the alloy [85].

3.6 Fatigue Testing

Fatigue testing was carried out using Ono's High Temperature Rotating Bending Machine available in the Materials Testing Laboratory in the Mechanical Engineering Department, Jomo Kenyatta University of Agriculture and Technology. The fatigue tests were carried out in accordance with the rules and specifications set out in the Japanese Industrial Standards (JIS), JIS Z 2273-1978 [87] and JIS Z 2274-1978 [88]. The fatigue specimens had a maximum diameter of 12mm, minimum diameter of 9mm and a length of 90mm. A photograph of the fatigue testing machine used in this work is shown in Figure 3.4. The fatigue specimens were machined to size after T6 and T4 heat treatment and care was taken when machining to ensure that the specimen temperature did not rise by more than a few degrees. After machining, the specimens were carefully polished to eliminate any surface roughness. Constant amplitude, fully reversed fatigue life tests under a stress ratio, R = -1 and a frequency, f = 33Hz were carried out under room temperature conditions. The results of the tests were presented

Figure 3.4: A photograph of Ono's high temperature rotary bending machine used for fatigue testing.

using stress - life (S - N) curves as illustrated in Section 4.6.

3.7 Mechanical Property Testing

Specimens for tensile tests were machined to the dimensions specified in the German Standard DIN 50125 A12x60. The tensile specimens had a maximum diameter of 15mm, minimum gauge length diameter of 12mm and a length of 180mm. Three tensile specimens were obtained from plate castings for each modifier amount. For each level of modifier addition, 'as cast', T4 and T6 heat treated specimens were machined. For each set of tensile tests, an average of the three results obtained was taken to represent the respective property required. The tests were undertaken at the Materials Testing Laboratory, Kenya Bureau of Standards.

Hardness values, tested in accordance with the requirements of the British Standard for the testing of Brinell Hardness for Metals [89] were obtained using the Brinell Hardness Tester. Indentation measurements of five different indentations

were taken and an average obtained. The Brinell Hardness Number (BHN) for a load of 10Kg was then obtained from the relevant reference table (Table B.1) [89].

3.8 Composition Analysis

Specimens for composition analysis were tested at Booth Manufacturers Limited, Thika. The analysis was done using the Optical Emission Spectroscopy (OES) method.

3.9 Microstructure Analysis

Specimens for microstructure examination were obtained from 'as cast', T4 heat treated and T6 heat treated samples for all the modifier levels tested. This was necessary to establish the influence of modifier variation as well as heat treatment and non-heat treatment on the microstructure of the castings obtained. The specimens were ground to a smooth surface finish using a series of silicon carbide abrasive papers and copious amounts of water. The grinding was done using the abrasive papers in this order; 220, 240, 400, 500, 800 and finally 1200 grade. A polishing cloth was then used to polish the specimens to a mirror-like finish before etching. An aqueous solution of 25% Sodium Hydroxide in distilled water (25g of NaOH in 100ml of distilled water) was used as the etchant while a strong solution of Nitric Acid was used to remove the smut after etching. The microstructure was then observed using a light optical microscope under different magnifications. The micrographs were taken using a camera that was attached to the microscope.

Chapter 4

RESULTS AND DISCUSSION

The main objective of this study was to investigate the effects of sodium (as a modifier) and heat treatment on the fatigue, microstructure and other mechanical properties of recycled cast aluminium alloys. The results of microstructure examination, composition analysis, mechanical properties and fatigue life properties are presented and discussed in the following sections.

4.1 Microstructure Analysis

Figures 4.1 - 4.5 show the microstructure of the different scrap samples obtained on casting. The microstructure reveal a close similarity among the different samples. The micrographs show microstructure that mainly consist of Fe-rich intermetallics (chinese-script , marked A), eutectic silicon particles (marked B, D), Al-dendrites, Cu-containing phases (marked C), porosity (marked G), and Mg_2Si particles (marked E).

The microstructure for unmodified 'as cast' specimens in Figure 4.1 (a) predominantly shows a chinese script Fe-rich intermetallic, $Al_{15}(FeMn)_3Si_2$ within the Al matrix, elongated Si eutectic particles, Cu containing phase as flat plates and dark Mg_2Si particles. Similar phases are observed in T4 (Figure 4.1 (b)) and T6 (Figure 4.1 (c and d)) heat treated samples. However, the heat treatment process appears to have changed the distribution and size of the different phases within the microstructure. The Fe intermetallics are smaller and less conspicuous than in the 'as cast' microstructure and the silicon eutectic particles are more globular in the heat treated samples. The difference in the shape of the Fe-bearing intermetallics may be due to the effect of solution treatment in the presence of magnesium. This encourages the formation of π-phase $FeMg_3Si_6Al_8$ as chinese script. The eutectic silicon particles in the 'as cast' microstructure of

sand cast specimens are usually large and acicular in shape, which was the case in all the unmodified samples such as Figures 4.1 (a), 4.2 (a) and 4.3 (a). Prolonged heating tends to spheroidize the eutectic silicon. The spheroidising is faster in modified alloys and results in a coarsening of the silicon to a size very close to that of non modified material, e.g. Figures 4.2 (b and c) and 4.6 (a and b).

High iron contents ($> 0.7\%$wt.) and long solidification times favour the formation of the β-phases. The presence of a high Manganese content (between 0.168% and 0.233%) possibly led to the formation of $Al_{15}(FeMn)_3Si_2$ in the shape of chinese script. In some cases, however, primary Al_5FeSi exist as thin platelets. The presence of copper in combination with Mg, Fe and Si leads to the formation of Cu-containing phases which could be Al_2CuMg, $Al_5Cu_2Mg_8Si$, Cu_2FeAl_7 and $CuAl_2$.

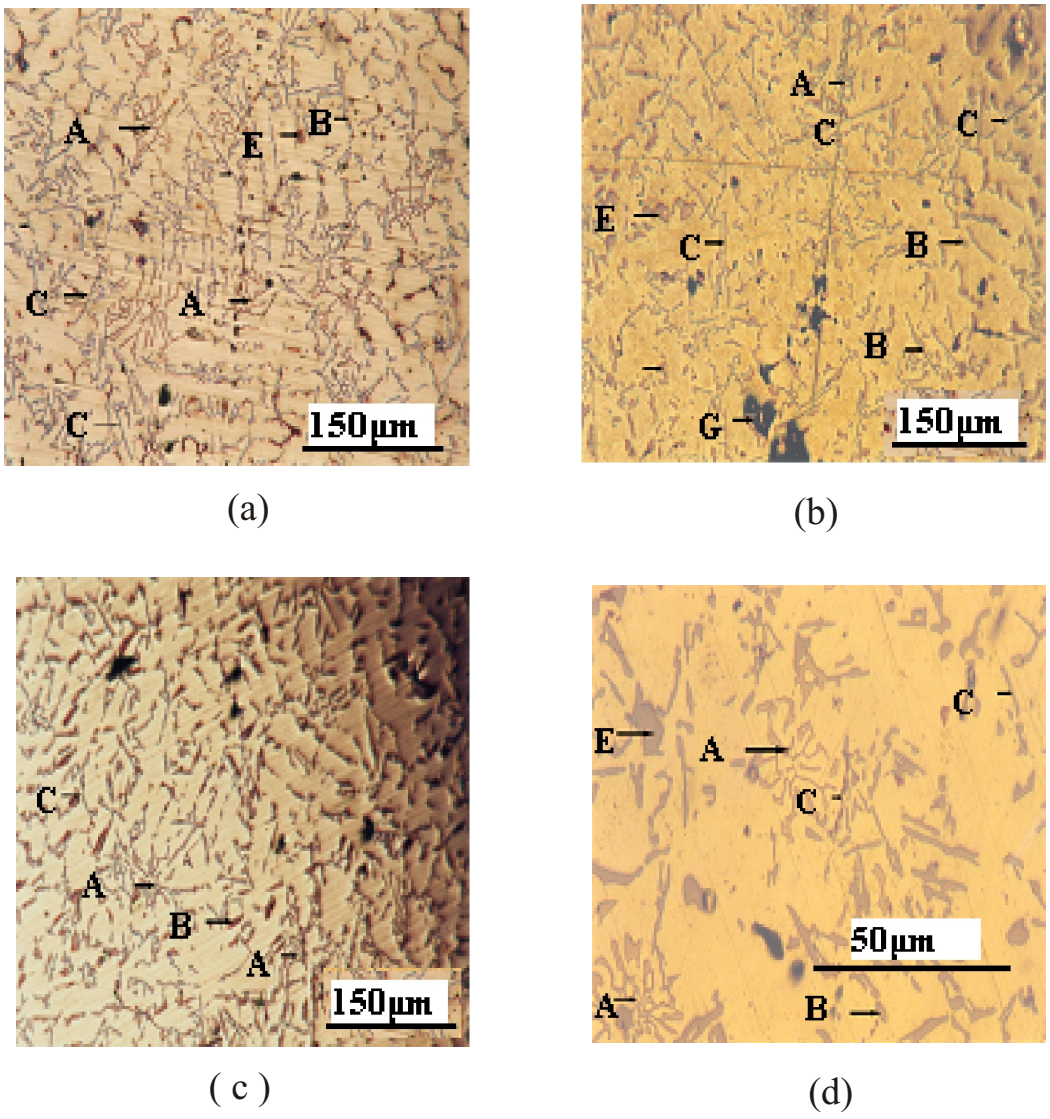

Figure 4.1: Micrographs (a) - (d) showing microstructure for unmodified recycled cast aluminium alloy specimens with Cu 3.88%, Fe 0.843%, Mg 0.318% and Si 7.359%; (a) 'as cast' condition (b) T4 (c) and (d) T6 temper condition. A-Fe-rich intermetallics, B-eutectic Si, C-Cu containing phases, E-Mg_2Si particles and G-porosity.

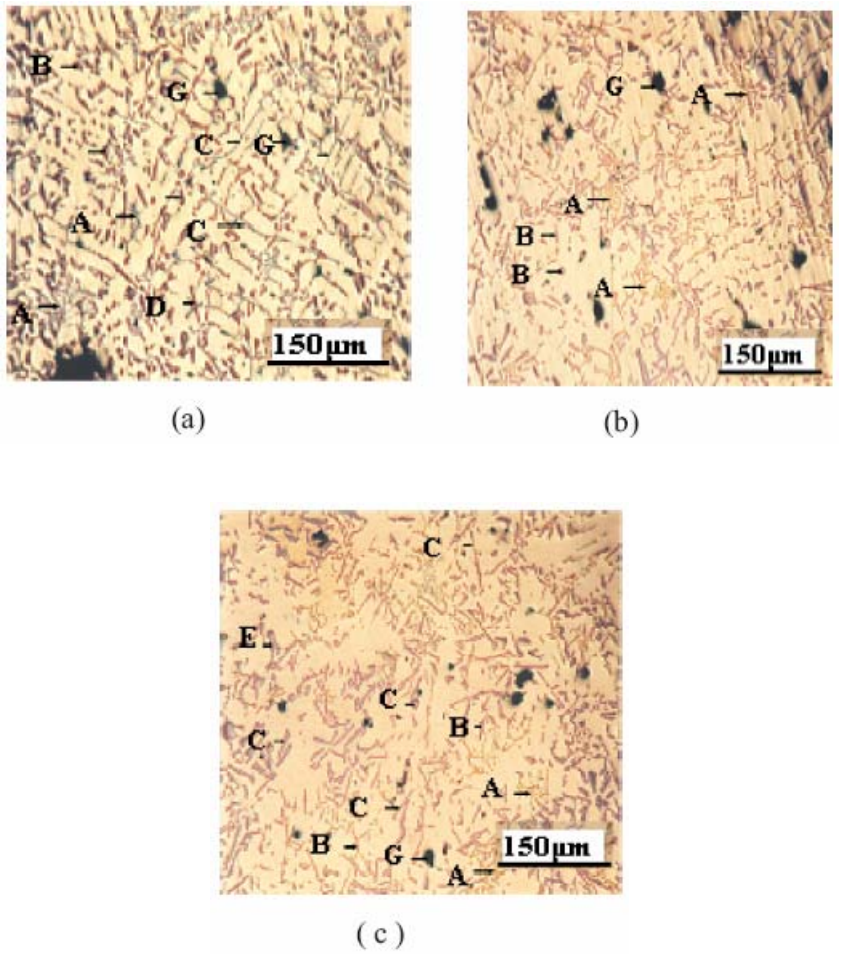

Figure 4.2: Micrographs (a) - (c) showing microstructure for 0.013% Na modified recycled cast aluminium alloy specimens with Cu 3.854%, Fe 0.760%, Mg 0.425% and Si 6.279%; (a) 'as cast' condition (b) T4 and (c) T6 temper condition. A-Fe-rich intermetallics, B-eutectic Si, C-Cu containing phases, D-Fe platelets, E-Mg_2Si particles and G-porosity.

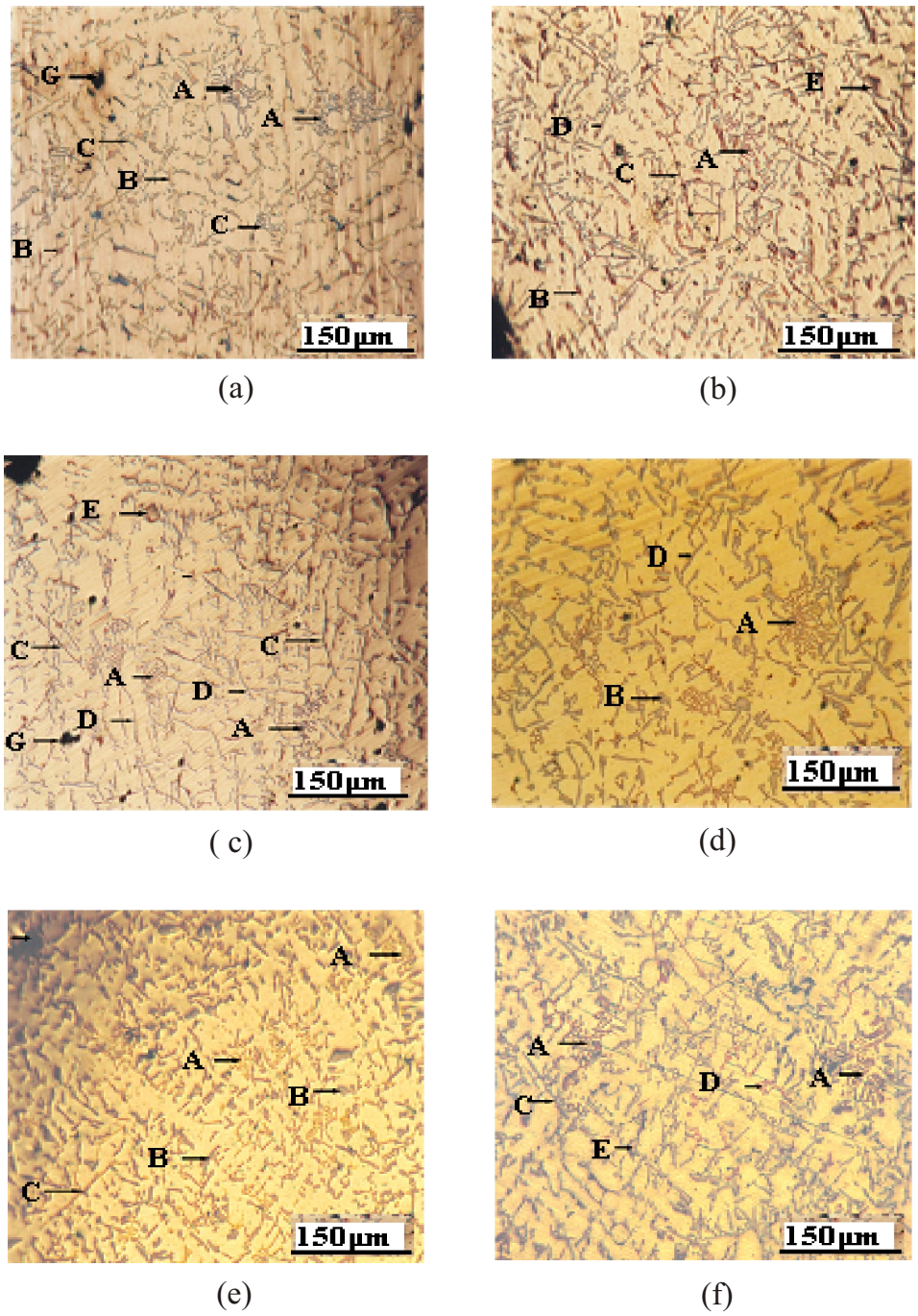

Figure 4.3: Micrographs (a) - (f) showing microstructure for 0.005% Na modified recycled cast aluminium alloy specimens with Cu 3.493%, Fe 0.739%, Mg 0.325% and Si 7.107%; (a) 'as cast' and (b) naturally aged. The rest were solutionized for 8h at 500^{o}C and artificially aged for (c) 4 (d) 14 (e) 18 and (f) 24 hours without pre-ageing.

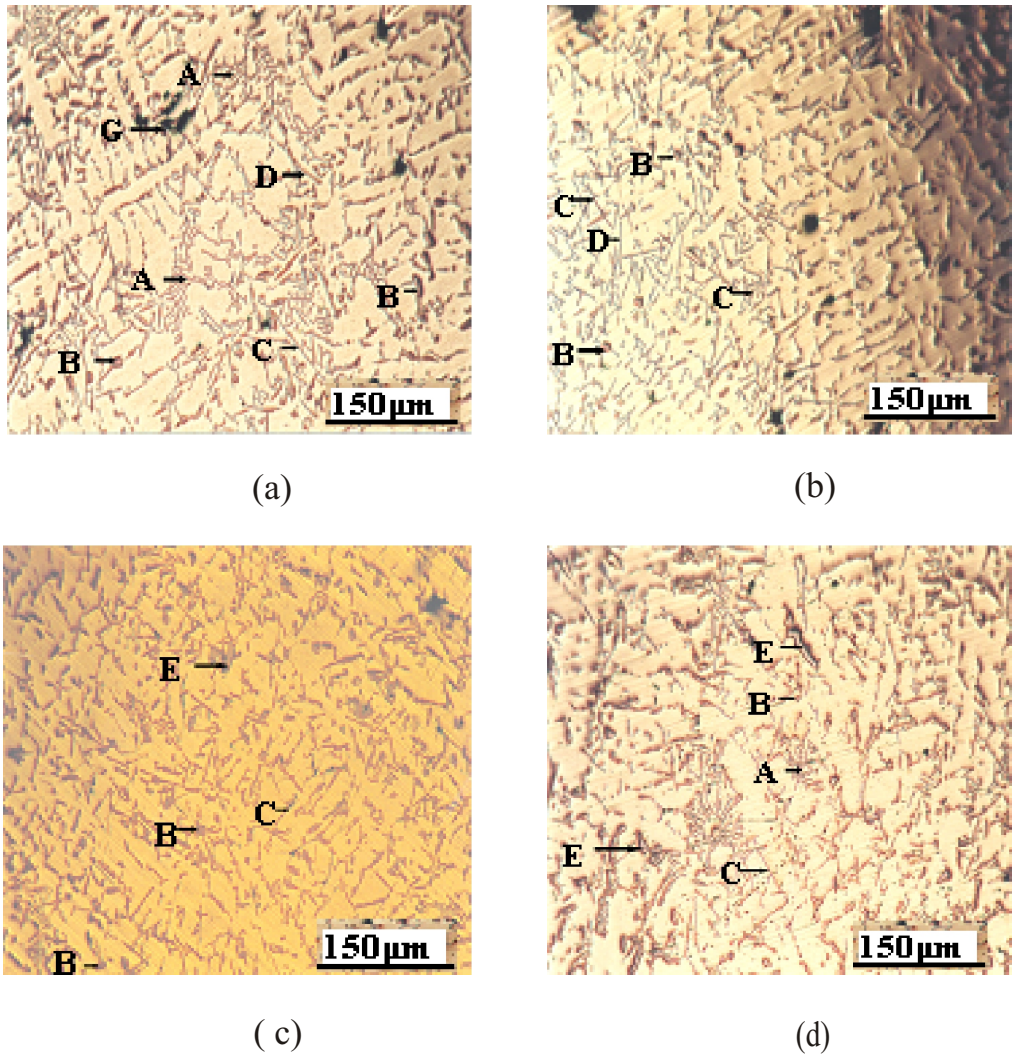

Figure 4.4: Micrographs (a) - (d) showing microstructure for 0.005% Na modified recycled cast aluminium alloy specimens with Cu 3.493%, Fe 0.739%, Mg 0.325% and Si 7.107%; solution heat treated at 500^{o}C for (a) 4 (b) 8 (c) 10 and (d) 24 hours, water quenched, pre-aged for 16 hours at room temperature and artificially aged for 5h at 160^{o}C. A-Fe-rich intermetallics, B-eutectic Si, C-Cu containing phases, D-Fe platelets, E-Mg_2Si particles and G-porosity.

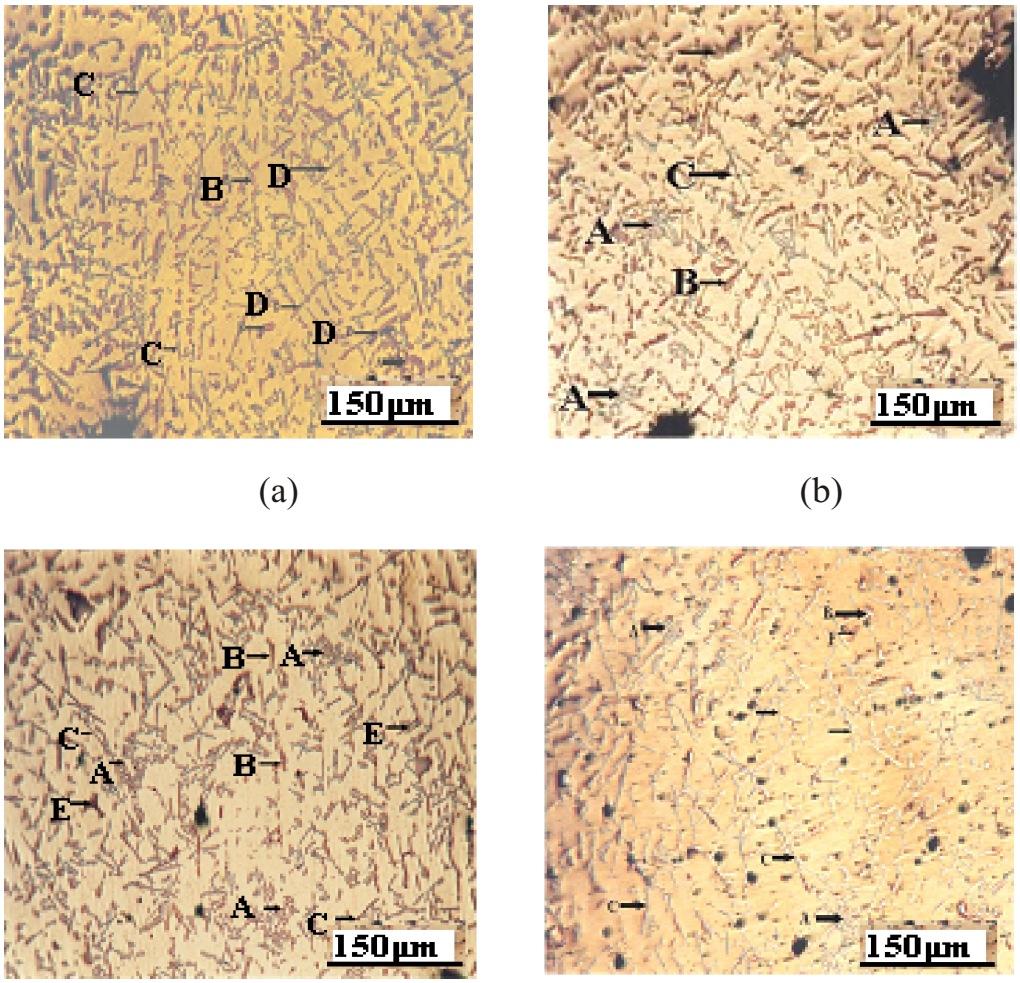

(a) (b)

(c) (d)

Figure 4.5: Micrographs (a) - (d) showing microstructure for 0.005% Na modified recycled cast aluminium alloy specimens with Cu 3.493%, Fe 0.739%, Mg 0.325% and Si 7.107%; artificially aged for (a) 8 (b) 24 (c) 32 hours at 160^{o}C and (d) overaged for 24 hours at 280^{o}C after solutionizing and pre-ageing. A-Fe-rich intermetallics, B-eutectic Si, C-Cu containing phases, D-Fe platelets, E-Mg_2Si particles and G-porosity.

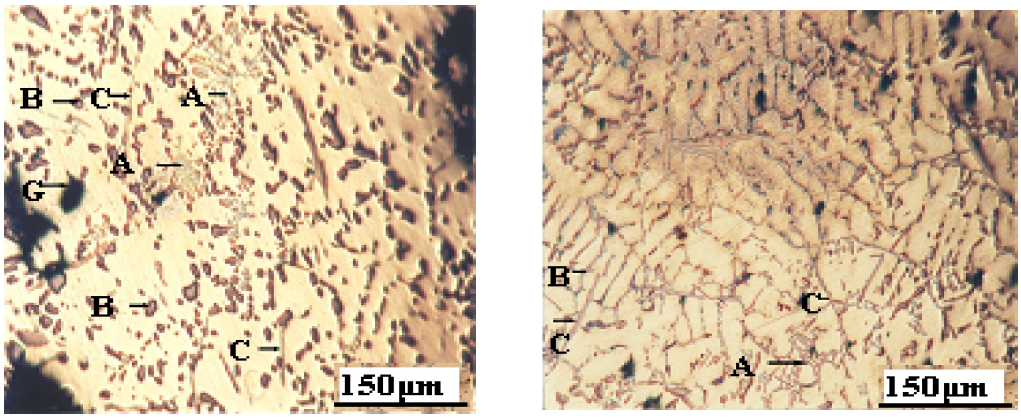

(a) (b)

Figure 4.6: Micrographs (a) - (b) showing microstructure for 0.020% Na modified recycled cast aluminium alloy specimens with Cu 4.800%, Fe 0.850%, Mg 0.588% and Si 6.647%; (a) T6 temper and (b) T4 temper. A-Fe-rich intermetallics, B-eutectic Si, C-Cu containing phases and G-porosity.

4.2 Effect of Modification and Heat Treatment on the Microstructure

The micrographs shown in Figures 4.1, 4.2 and 4.6 show the microstructure of the unmodified, 0.013%Na and 0.020%Na modified 'as cast' and heat treated cast samples. When unmodified, the eutectic silicon is acicular and contains large brittle plates of silicon which are known to cause the alloys to exhibit poor ductility. The presence of sodium, and in other cases strontium, changes the silicon morphology to a fine fibrous structure. Microstructural examination was carried out using optical metallography. An alternative would have been to carry out a complete quantitative analysis using a metallurgical microscope equipped with an image analyzer. This would have made possible the measurement of such parameters as area, perimeter, size and number of identifiable parts of observable images, however, this facility was not available. In the absence of the image analyzer, optical metallography was considered adequate for this study.

Nonetheless, in some of the micrographs, a change in the morphology of some of the constituents as a result of heat treatment and modification is observed. Figure 4.6(a), shows 0.020%Na modified eutectic silicon particles that have spheroidised and coarsened as a result of T6 heat treatment, which is in contrast to microstructure of the 'as cast' 0.013%Na modified alloy in Figure 4.2(a). An examination of the microstructure of 0.020%Na modified alloy in Figure 4.6 and the unmodified alloy in Figure 4.1 shows that the eutectic silicon particles have undergone a morphological transformation from acicular to fibrous and spheroidized shape as a result of modification and heat treatment. Solution treatment has been reported to cause a substantial degree of spheroidisation in both unmodified and modified eutectic phases [24]. Paray and Gruzleski [24] found that the presence of strontium leads to a more rapid spheroidisation of the silicon eutectic at an early stage of solution treatment and the modified silicon substantially coarsens with solution time. A combination of heat treatment and modification results in a more rapid spheroidisation process during heat treatment. This may be the reason for the observed microstructure in Figure 4.6(a). This observation is in agreement with the work of other researchers on the influence of modification and heat treatment on the microstructure of Al-Si alloys [24, 90].

4.3 Material Composition

The chemical composition for the secondary aluminium alloys used in this study are shown in Table 4.1. The samples were cast and tested in five sets, namely; M00 samples (not modified), M005 samples (modified with 0.005%Na), M13 samples (modified with 0.013%Na), M20 samples (modified with 0.020%Na) and M25 samples (modified with 0.025%Na).

In solidified aluminium alloys, elements (alloying, impurity and trace) can be

Table 4.1: Compositions of alloys tested.

Sample	Material composition in element percent (%)												
Code	Zn	Mn	Cu	Sn	Fe	Ni	Pb	Al	Mg	Si	Ti	Cr	Others
M00	0.902	0.233	3.880	0.180	0.843	0.228	0.135	85.754	0.318	7.359	0.105	0.021	0.042
M005	0.943	0.168	3.493	0.143	0.739	0.287	0.104	86.588	0.325	7.107	0.090	0.013	0.000
M13	0.963	0.186	3.854	0.125	0.760	0.276	0.127	86.861	0.425	6.279	0.130	0.014	0.000
M20	1.005	0.195	4.800	0.180	0.850	0.319	0.165	84.446	0.588	6.647	0.132	0.022	0.637
M25	0.960	0.169	3.528	0.135	0.778	0.288	0.140	86.335	0.328	7.205	0.098	0.028	0.008

present in a variety of forms; in solid solution in the primary aluminium phase, as a constituent of another solid solution phase or eutectic, or as a constituent of an intermetallic compound. Some of the elements could also exist as surface active elements present at the boundary between phases, as constituents of a non metallic inclusion trapped during solidification and in some cases as gaseous phases [2]. It is in light of these possibilities that the content and effects of the various elements in the five sets of cast alloys tested are subsequently discussed.

4.3.1 The Silicon Content

The silicon content was found to be in the range of 6.279wt.% to 7.359wt.%. This implies that the aluminium scrap selected for recycling were obtained from hypoeutectic aluminium alloys which contain silicon content below 11.7wt.%. The Al-Si equilibrium phase diagram in Figure 2.1 illustrates the silicon content limits for wrought and foundry Al-Si alloys. The silicon content for wrought aluminium - silicon alloys is below about 1.3wt.% Si while that of foundry Al-Si alloys is limited to between 5wt.% and 18wt.% Si [14].

The addition of silicon is usually a trade off between beneficial and harmful effects on the casting process and the resultant components' performance requirements. Silicon is a popular addition to aluminium alloys due to its many

advantages; it imparts fluidity during casting, improves corrosion resistance, reduces hot shrinkage and increases the hardness, yield strength and tensile strength of the alloy [12, 91]. Due to its low density, silicon may be added to aluminium without increasing the weight of the aluminium alloy. The coefficient of thermal expansion of aluminium is appreciably reduced by the addition of increasing amounts of silicon [91].

The influence of silicon on the mechanical properties depends on the distribution and shape of silicon particles rather than the content. Alloys with small round and evenly distributed silicon particles are more ductile. Alloys with faceted and acicular silicon particles are much less ductile but exhibit slightly higher strength. Silicon expands as it solidifies, and the expansion compensates for part of the solidification shrinkage of aluminium. Hence Al-Si alloys have low solidification shrinkage.

Silicon content in the composition range of 6.279wt.% - 7.359wt.% indicates an alloy that has excellent castability, machinability, tensile strength and reasonable hardness. The ductility will not only depend on the size and shape of the silicon alloy but also on the presence or absence of embrittling Fe-rich intermetallics.

4.3.2 The Copper Content

The copper content was found to be in the range of 3.493wt.% to 4.800wt.%. Copper is added to aluminium alloy castings to increase hardness, yield strength and fatigue resistance without loss of castability. Copper is found either dissolved in the matrix or forming intermetallics such as $CuAl_2$ (when Mg is not present). Alloys with dissolved copper have the largest increase in strength and retain substantial ductility. When copper is present as a continuous network at grain boundaries, the alloys do not show appreciable increase in strength, but rather a loss in ductility. When spheroidised evenly distributed $CuAl_2$ particles

are present, the strength of the alloy becomes a function of the mean free path between the particles [12, 91].

In Al-Si-Cu alloys, copper improves hardness, strength, fatigue, creep resistance and machinability. Copper and magnesium have also been found to improve the surface finish on machining, and to reduce the tendency of the alloy to build up on the cutting tool's edge. The optimum content of Cu in Al-Si-Cu alloys is usually between 4 and 5wt.% when hardness, yield strength, fatigue strength, creep resistance, heat treatment response and machinability are optimum. In contrast, copper contents in excess of 5wt.% degrade mechanical properties and encourage the formation of shrinkage porosity.

An Al-Si foundry alloy with copper content of between 3.493wt.% and 4.8wt.% is expected to have improved hardness, yield strength (at both ambient and elevated temperatures), fatigue strength and heat treatment response. However, the alloy would have reduced ductility, poor corrosion resistance and possibly increased amounts of shrinkage porosity due to poor feedability.

4.3.3 The Magnesium Content

The magnesium content was found to be between 0.318wt.% and 0.588wt.%. In some die casting alloys, such as 380, 413 and C443, magnesium is specified to be below a certain level, a maximum of 0.1wt.% in the USA. This could be due to the strong tendency of magnesium to react with other elements to form inclusions and intermetallics. Magnesium can easily oxidise in the melt to form MgO. At high holding temperatures (>745^{o}C) magnesium easily forms spinel, a complex Al-Mg oxide that grows rapidly as inclusions in the melt. Magnesium, especially when present in amounts exceeding 0.45% may also form complex intermetallics with other elements such as $Al_8FeMg_3Si_6$ and $Cu_2Mg_8Si_6Al_5$ [12,91–93]; all these reduce fluidity and affect other properties, hence the limit on composition.

Magnesium is also one of the few elements that lower the modulus of elasticity of aluminium and gives Al-Si alloys a very strong heat treatment response especially by enhancing the response of alloys containing up to 0.45% Mg to T6 and T5 tempers [92]. On solution treatment, magnesium and silicon dissolve in aluminium. Upon ageing, Guinier Preston (GP) zones or highly dispersed Mg_2Si micrometre scale size particles precipitate in the matrix. This increases the tensile strength, yield strength and elongation of the alloy. In sand castings, 5-11wt.% magnesium reduces ductility and increases strength and hardness.

The magnesium content in several commercial hypoeutectic Al alloys such as 332, 336 and 339 is specified to be below 1wt.%. The secondary aluminium alloy samples in this study had between 0.318wt.% and 0.588wt.%Mg. Hence magnesium is not expected to impart detrimental properties to the alloy. However, with the high Cu content, the alloys are expected to display severely reduced ductility.

4.3.4 The Manganese Content

The manganese content was found to be between 0.168wt.% and 0.233wt.%. At low manganese contents, the phase in equilibrium with Al is $MnAl_6$. Solubility of manganese in Al is reduced by the presence of Fe and Si leading to the formation of compounds such as $Al_{15}(FeMn)_3Si_2$ and $(FeMn)_3Al_6$. Manganese is usually added to wrought alloys as a hardener, to enhance the strength of these alloys by work hardening and as a corrector for Fe. In aluminium casting alloys, where work hardening is not employed, manganese offers no significant strengthening effect. The presence of manganese in Al-Si alloys may slightly improve the alloys' high temperature properties, enhance its fatigue resistance and reduce its shrinkage. Manganese and zinc in secondary alloys improve corrosion resistance to a level that is comparable to primary alloys. Manganese

may compensate for the negative effects of Fe by favouring the formation of the compound $Al_{15}(FeMn)_3Si_2$ in the shape of Chinese script, hence minimizing the formation of embrittling needle shaped phase Al_5FeSi. Manganese may absorb iron and form compounds such as $(FeMn)Al_6$. Manganese content is controlled to correct the iron only partially and not to allow the formation of the primary $Al_{15}(FeMn)_3Si_2$ crystals.

Manganese is usually added in the range of about 0.2wt.% and 0.6wt.% to reduce the harmful effects of iron. In the secondary casting alloys obtained in this study, Manganese content is between 0.168wt.% and 0.233wt.%. This content is sufficient to arrest the deleterious effects of Fe by encouraging the formation of chinese script $Al_{15}(FeMn)_3Si_2$ in place of the needle shaped Al_5FeSi.

4.3.5 The Iron Content

The iron content was found to be between 0.739wt.% and 0.850wt.%. The limits of iron set for sand and permanent mould castings are between 0.6wt.% - 0.7wt.%. However, in die castings, up to 3wt.% Fe may be tolerated. The alloy used in this study was sand cast while the aluminium scrap used is likely to have been cast by the high pressure die casting process. The higher iron content observed in this study may have arisen out of the higher iron content specification for high pressure die castings. Further, iron is always present in commercial aluminium alloys; mainly arising from the use of steel tools during melting and casting and use of remelting materials containing rust. Iron is intentionally added in die casting alloys to prevent die soldering.

Where the iron content in sand and permanent mould castings is more than 0.8wt.%, primary Al_5FeSi crystals appear. The effects of iron on the properties of aluminium alloys is largely dependent on the morphology of the iron bearing phases. In commercial casting alloys, due to non-equilibrium solidification, one

may find alloys in which $FeAl_6$, $FeAl_3$, $FeSiAl_8$, $FeSiAl_5$ and $FeSiAl_4$ coexist with one another and with silicon. In Al-Si alloys when copper is present, Al-$FeSiAl_5$-Si eutectic forms as thin platelets. Fast cooling tends to shift the eutectic towards higher iron contents and to disperse the $FeSiAl_5$ crystals. The nature and type of iron rich phases present (after solution treatment) depends on the magnesium content. When magnesium is below 0.35wt.% to 0.4wt.%, the majority of Fe rich phase are small α-phase ($FeSiAl_5$) platelets. For higher magnesium contents, large π-phase, $FeMg_3Si_6Al_8$ may form as Chinese script (when it is eutectic) or as globules (when it is primary). Iron forms as $Al_{15}(FeMn)_3Si_2$ with manganese often in the shape of chinese script thus removing the embrittling effect of the needle shaped $FeSiAl_5$ [12].

In commercial castings, iron bearing phases may appear as chinese script, needles (platelets) or angular globules and sometimes in the form of plate like particles. The size of the phases are smaller at faster cooling rates. Chromium and nickel may also correct the iron but $(CrFe)_4Si_4Al_{13}$ or $(CrFe)_5Si_8Al_2$ and $FeNiAl_9$ compounds may form. These compounds are elongated in shape and can cause brittleness. The best iron corrector is probably cobalt; it does not combine with silicon and the number of extraneous particles formed in the alloy is limited.

The iron content of between 0.739wt.% and 0.850wt.% obtained in the secondary foundry alloys is high enough to degrade the alloys' mechanical properties. However, the contents of manganese and nickel are sufficient to encourage the formation of less harmful iron intermetallics, hence significantly reducing the deleterious effects of the high iron content.

4.3.6 The Zinc Content

The zinc content was found to be between 0.902wt.% and 1.005wt.%. When zinc is present in amounts less than 1.0wt.%, it is usually in solution in aluminium

and does not form any visible phases. Zinc amounts up to 2.0wt.% have no effect on the room temperature properties and can thus be tolerated. In Al-Si alloys, zinc decreases the high temperature strength, increases tendency for hot tearing and improves the alloy's machinability. In secondary alloys, zinc and manganese compensate for copper and nickel and enhance the alloy's resistance to corrosion.

4.3.7 The Nickel Content

The nickel content was found to be between 0.228wt.% and 0.319wt.%. Nickel slightly increases the alloys' strength at both room and elevated temperatures and may slightly increase the ductility when acting as an iron corrector.

4.3.8 The Minor Elements

Ti, Cr, Pb and Sn were present in small quantities. Titanium and boron are added into aluminium alloys as grain refiners. The quantities added do not exceed solid solubility limits and thus do not form any separate phases. Tin and lead, if present, tend to enter into the Mg_2Si phase, decrease high temperature strength and improve machinability. Tin has a deleterious effect on the corrosion resistance.

4.4 Comparison with Commercial Alloys

The composition of the different sets of secondary alloys obtained in this study was found to be closely similar, the variations in composition being insignificant. The secondary alloys obtained are almost equivalent to some of the existing commercial Al-Si alloys as illustrated in Table 4.2. These are mainly the commercial aluminium alloys that are used in the manufacture of pistons (332, LM16) and cylinder heads (LM16, AC 2A). Others like 319 are mainly used for the manufacture of automotive components such as cylinder heads, gearbox and rear

axle housings, among others. Since the scrap components used in the recycling process were obtained from only a limited group of selected parts, it would be expected that the resultant alloys should not deviate too much from the parent alloy combinations as seen in Table 4.2.

Table 4.2: Comparison of scrap samples with equivalent commercial alloys.

Alloy code	**Equivalent commercial alloys**	**Composition range of the equivalent commercial alloys**
M00, M005, M13, M20, M25	AC 2A, LM22, LM16, LM4, A319, W319, 319, 332	2-4.0Cu, 4.0-8.0Si, 0.3-1.3Fe, 0.008-0.07Cr, 0.05-0.6Mg, 0.009-3.0Zn, 0.1-0.6Mn, 0.01-0.3Ni, <0.1Pb, 0.05-0.1Sn, 0.12-0.2Ti

4.5 Mechanical Properties

The results obtained in this study for hardness (BHN), Ultimate Tensile Strength (UTS) and percent elongation for the various secondary alloys used are summarized in the Appendix as Tables A.1, A.2, A.3 and A.4, while Figures 4.7 - 4.13 show the various trends for the different test conditions. The observations discernible from these results are presented and discussed in this section.

4.5.1 Hardness

Figure 4.7 shows the variation of hardness with ageing time while Figure 4.8 shows the variation of hardness with solution treatment time for the 0.005%Na modified recycled aluminium alloy. In Figure 4.7, the curve SP-A shows the variation of hardness for samples that were solution treated for 8 hours at 500^oC, quenched in water, pre-aged for 16 hours at room temperature and artificially aged for different durations (4, 8, 12, 16, 24 and 32 hours) at 160^oC. The curve shows a gradual increase in hardness with increase in ageing time.

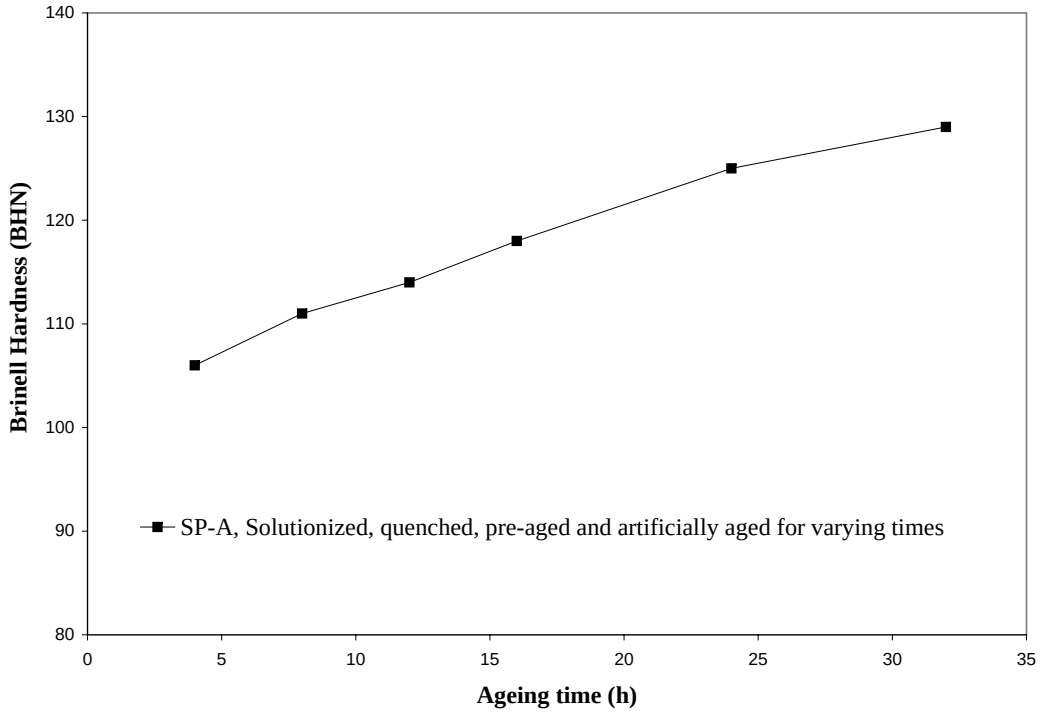

Figure 4.7: Influence of varying ageing time on the hardness of 0.005%Na modified secondary Al alloy.

In Figure 4.8, the SA curve represents the variation of hardness for samples that were solution treated for different times (4, 10, 14, 18, 24 and 32 hours) at 500^{o}C, quenched in water and artificially aged for 5 hours at 160^{o}C. In this case, the samples were not subjected to pre-ageing. The curve shows a gradual increase in hardness with increase in the solution treatment time. This trend is similar to that depicted in Figure 4.7. Though the trends are similar for the two cases, the values of hardness for the SA samples were always less than those of the SP-A samples except for the solution heat treatment time of 4 hours.

The SPA curve (Figure 4.8) represents the variation of hardness for samples that were solution treated for different times (4, 8, 10, 15, 20 and 24 hours) at 500^{o}C, quenched in water, pre-aged for 16 hours at room temperature and artificially aged for 5 hours at 160^{o}C. Table 4.3 shows the tensile and hardness properties for two more sets of samples that were subjected to different heat

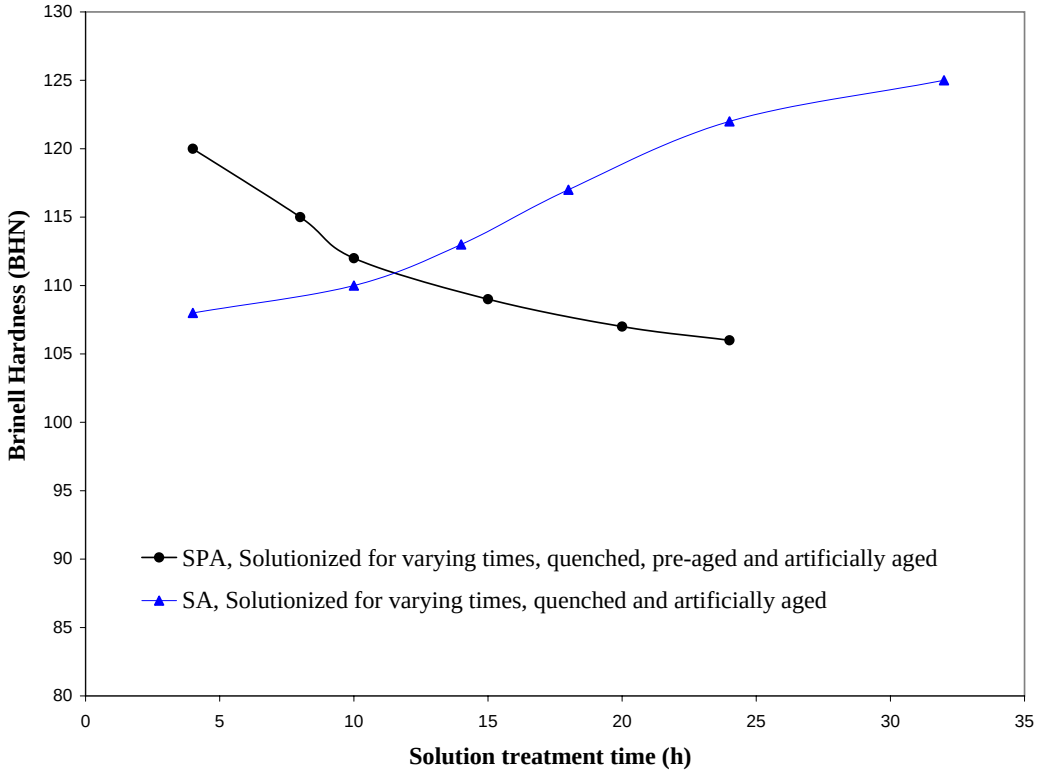

Figure 4.8: Influence of varying solution treatment time on the hardness of 0.005%Na modified secondary Al alloy.

treatment conditions; one was overaged (solution treated for 8 hours at 500^{o}C, quenched, pre-aged for 16 hours at room temperature and artificially aged for 24 hours at 280^{o}C, (SP-OA24 samples)) while the other was naturally aged (solution treated for 8 hours at 500^{o}C, quenched and aged at room temperature for 3 weeks (SNA samples)). The SP-0A24 and SNA samples gave average hardness values of BHN 62 and BHN 102 respectively. 'As cast' samples were not heat treated and gave an average hardness value of BHN 84.

4.5.1.1 Effect of Ageing on Hardness

Varying the ageing time at a constant temperature of 160^{o}C led to a progressive increase in the hardness (Figure 4.7, curve SP-A), with the longest artificially aged sample (32 hours) giving the highest hardness (BHN 129). The samples

Table 4.3: Tensile and hardness properties of 0.005% Na modified overaged and naturally aged aluminium alloy samples.

Alloy Code	Solution Time (h)	Preaging Time (h)	Aging Time (h)	UTS (MPa)	Elongation (%)	Hardness (BHN)
AC*	0	0	0	113	1.3	83.5
SP-OA24**	8	16	24	135	1.8	64.2
SNA***	8	16	504	160	1.6	102

** - Aged at a temperature of 280^{o}C for 24 hours, hence overaged.

*** - Naturally aged at room temperature for 3 weeks

* - Tested in the 'as cast' condition.

that were over aged (24 hours at 280^{o}C) and those that were tested in the 'as cast' condition gave the lowest values of hardness (Table 4.3).

Ageing of Al-Si alloys containing Mg and Cu is carried out to increase the hardness of the alloy through the dispersion of Mg_2Si and Al_2Cu precipitates in the Al matrix. The alloys studied in this case had Mg content of between 0.318wt.% and 0.588wt.% and Cu content of between 3.845wt.% and 4.800wt.% which are within the limits that bring about optimum hardness in Al-Si-Mg-Cu alloys. Mg induces age hardening through the precipitation of Mg/Si precipitates. The hardening effect of Mg occurs upto 0.7wt.% Mg beyond which no further strengthening of Al matrix occurs [94]. A higher Mg content results in a higher yield stress but lower ductility and toughness. Cu and Mg have been found to strengthen the alloy matrix and improve alloy machinability [94].

The hardening of Al-Si alloys containing about 4%Cu during ageing is attributed to the formation of GP1 and GP2 or $\Theta^{"}$ (Al_2Cu) and $\Theta^{'}$ (Al_2Cu) zones and the equilibrium (Al_2Cu) phase. The GP1 zones are two-dimensional Cu-rich regions oriented parallel to {100} planes, while the GP2 zones are considered to be three dimensional regions having an ordered atomic arrangement. The $\Theta^{'}$ phase has

the same composition as the stable phase and exhibits coherency with the solid solution lattice, while the equilibrium Θ is incoherent with the lattice [95]. The composition of the quenched and aged aluminium matrix changes with ageing time due to the precipitation of the Θ' (Al_2Cu) phase, which is responsible for the increase in hardness. The presence of Mg in the Al-Si-Cu alloys accelerates and intensifies the age-hardening process. In these alloy systems, hardening may be caused by precipitation of Al_2Cu, Mg_2Si, Al_2CuMg and $Al_2CuMg_5Si_4$ phases.

The progressive increase in hardness (Figure 4.7, curve SP-A) for the alloy containing 0.325wt.%Mg and 3.493wt.%Cu can be attributed to the precipitation of Al_2Cu, Mg_2Si, Al_2CuMg and/or $Al_2CuMg_5Si_4$ phases in the Al matrix. The presence of both Mg and Cu in sufficient quantities allows the hardness to increase with time as shown in Figure 4.7 (curve SP-A). This trend of results does not agree with the results of previous work by Li et et al. [96] on an Al-Si-Cu-Mg alloy. Li et al. found the hardness of the Al-Si-Cu-Mg alloy at different temperatures (145^oC, 175^oC, 185^oC and 215^oC) to peak after a short ageing time (3 to 15h), after which the hardness started to decrease.

4.5.1.2 Effect of Solution Treatment on Hardness

Varying the solution treatment times in the samples that were not pre-aged progressively increased the hardness with time(Figure 4.8, curve SA). On average, the samples that were solution treated for 8h and aged for varying times had higher hardness (curve SP-A). However, the hardness of the samples that were solution treated for varying times, quenched, pre-aged and artificially aged, curve SPA) decreased with increase in solution time.

Solution treatment of heat treatable Al alloys usually results in certain phases going into solution within the Al matrix. Rapid quenching ensures that the phases are retained in solution. Controlled precipitation through age hardening

or artificial ageing allows a dispersion of precipitates to form in the Al matrix. These precipitates are responsible for the increase in hardness reported in heat treated Al alloys. The process of solutionizing, quenching and artificial ageing allows most of the phases (Al_2Cu, Mg_2Si, Al_2CuMg or $Al_2CuMg_5Si_4$) taken into solution during solutionizing to form hard finely dispersed precipitates. Increasing solutionizing time allows more of each phase to be taken into solution, availing a higher volume fraction of precipitates, hence the increase in hardness with solutionizing time for SA samples. The trend observed for SPA samples could be attributed to loss of solutes during pre-ageing. In addition, the hardening response for most Al-Mg-Si-Cu alloys has been reported to be adversely affected by pre-ageing [97].

The trends observed in Figure 4.7 and Figure 4.8 are further supported by the curves of Figure 4.9 which show that T6 and T4 temper alloys have higher hardness than 'as cast' alloys at all levels of modifier amount. T6 samples, as expected, show higher hardness than T4 temper samples.

4.5.1.3 Effect of Modification on Hardness

Figure 4.9 illustrates the influence of the level of modification on the hardness of the Al-Si secondary foundry alloys used in this study. The modifier content was varied from a minimum of 0.00% Na (unmodified) to a maximum of 0.025% Na. The 'as cast' curve shows the influence of changing the modifier amount on the hardness of samples that were not heat treated. The T4 curve shows the influence of varying the modifier content on the hardness of samples that were solution treated for 8 hours at 540^oC, quenched and naturally aged for four days (T4 temper). The T6 curve shows the influence of varying the modifier content on the hardness of samples that were solution treated for 8 hours at 540^oC, quenched, pre-aged for 16 hours at room temperature and artificially aged for 5

hours at 155^{o}C (T6 temper).

It is observed that the amount of modifier does not significantly affect the hardness of the alloy.

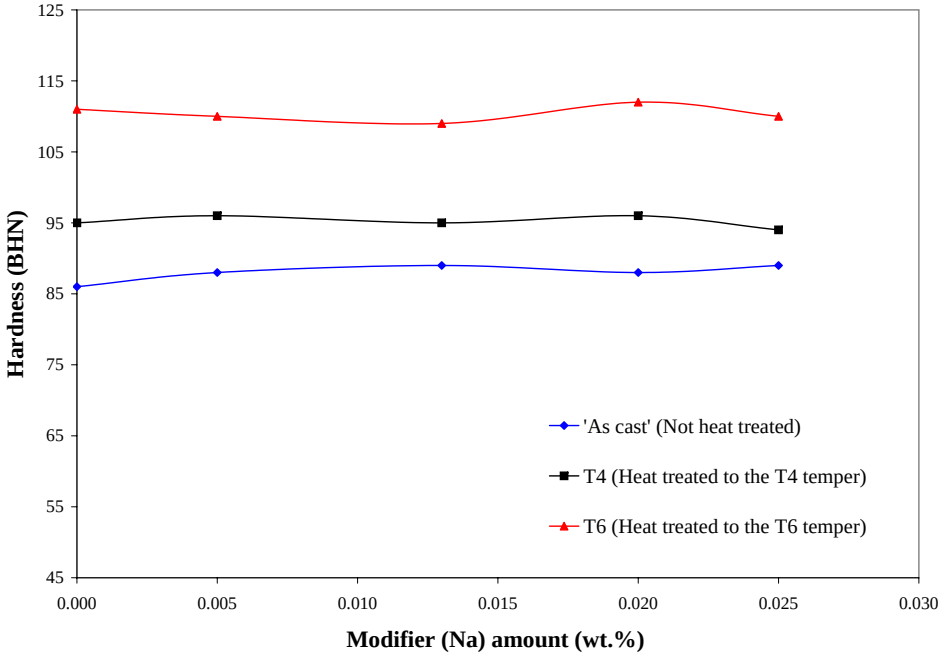

Figure 4.9: Influence of modifier amount on the hardness properties for 'as cast', T4 and T6 heat treated secondary foundry alloy samples.

Hardness in heat treated Al-Si-Cu-Mg alloys is caused by the precipitation of hard Mg/Cu containing precipitates. Modification changes the morphology of eutectic silicon particles from acicular or flaky shape to more rounded or globular shape. This therefore does not affect the precipitation of the Mg/Cu containing precipitates. As a result, it is justified that modification does not affect the hardness of the secondary Al-Si alloys.

Figure 4.9 shows that the T6 heat treated samples had higher hardness than the T4 and 'as cast' samples at all levels of modifier content. This implies that precipitation of hard Mg/Cu containing precipitates is more effective with artificial ageing than with natural ageing, hence the higher hardness of T6 samples.

The low hardness of the 'as cast' samples is characteristic for a material that is not subjected to heat treatment.

4.5.2 Tensile Properties

Figure 4.10 shows the influence of the modifier amount on the tensile strength while Figure 4.11 shows the influence of the modifier amount on the elongation of the Al-Si secondary foundry alloy. In both cases, the 'as cast' curve represents the samples that were not heat treated, T4 and T6 curves represent the samples that were heat treated to the T4 and T6 temper conditions respectively.

4.5.2.1 Effect of Modification on Tensile Strength

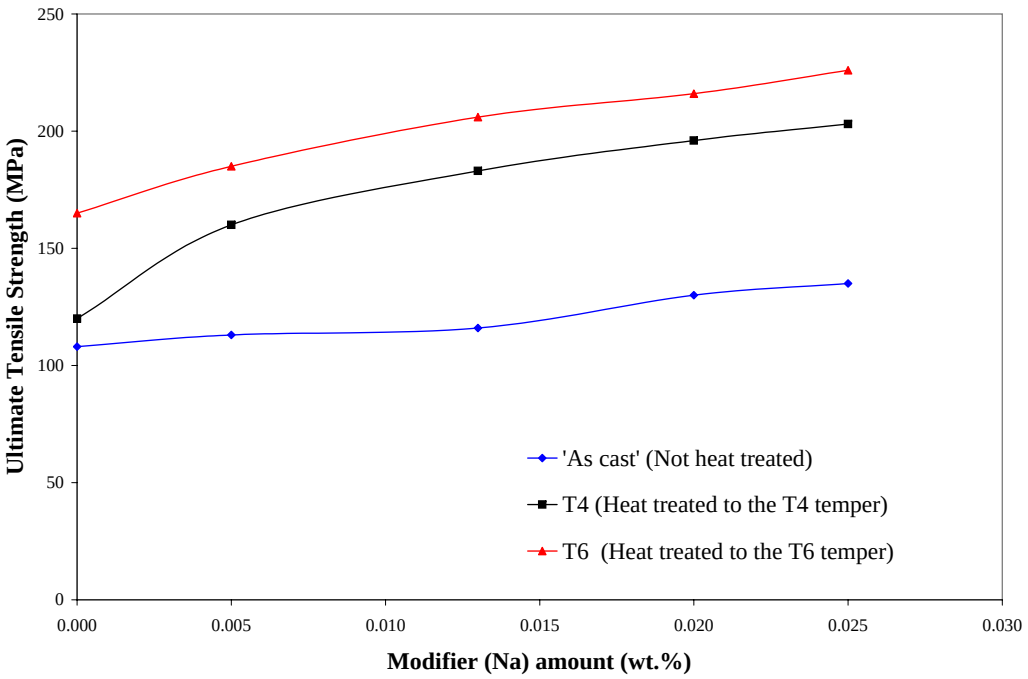

Figure 4.10: Influence of modifier amount on the tensile strength for 'as cast', T4 and T6 heat treated secondary foundry alloy samples.

It can be seen in Figure 4.10 that an increase in modifier amount from 0.00%Na to 0.025% leads to 25%, 69% and 36% increase in tensile strength for 'as cast', T4 and T6 samples respectively. The increase in UTS is less pronounced for

the 'as cast' samples when compared to the T4 and T6 samples. The increase in tensile strength depicted in Figure 4.10 is as a result of a combination of modification and heat treatment.

This combination of modification and heat treatment has been shown to significantly affect the morphology and size of eutectic Si particles, which affects the mechanical properties of Al-Si alloys. Larger Si particles have a higher probability of cracking and hence initiating failure when the alloy is under a tensile load. Gangulee and Gurland [98] found that the fracture probability of an Al-Si alloy increased with increasing Si particle size and increasing volume fraction of Si particles among other factors. Frederick and Bailey [99] also found that fracture is more likely to initiate in large silicon particles present in dendrite cell boundaries. Similar results have also been reported by other researchers [100]. Further work by Caseres et al [101] and Manoharan et al. [102] demonstrated that the fracture process in Al-Si-Mg alloys proceeds by cracking of Si particles ahead of the crack tip. It has also been reported that a low aspect ratio and better circularity of the Si particles (associated with modification and fast cooling rate) can affect the first stage of the crack initiation (void nucleation) owing to an increase in the particles' resistance to fracture [103]. Silicon particle size and shape have been shown to significantly influence the tensile properties of Al-Si alloys [104, 105].

Therefore, it is reasonable to conclude that a combination of increased modification and heat treatment should lead to an improvement in the tensile strength of the alloy as demonstrated in Figure 4.10. The combined effect of modification and heat treatment is to reduce the size of Si particles (low aspect ratio) and to change the shape of the particles (more spheroidized and globular); hence reducing the fracture initiation and failure probability under tensile load.

4.5.2.2 Effect of Modification on Elongation

As shown in Figure 4.11, the tests gave low values of ductility for all the modifier levels and heat treatment tempers; below 2.9% elongation. However, the results show a slight improvement in ductility with increase in modifier amounts and heat treatment. Unmodified Al-Si alloys contain eutectic Si particles that are

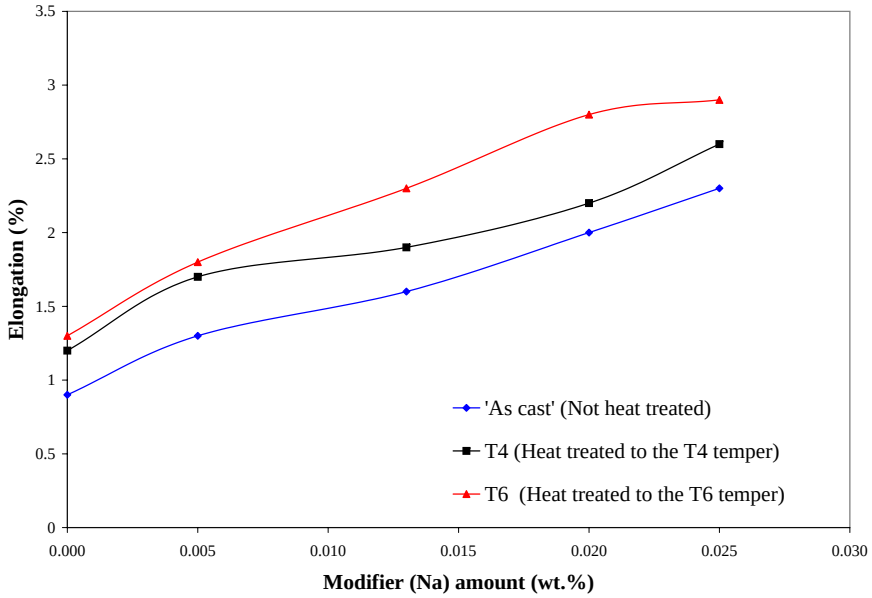

Figure 4.11: Influence of modifier amount on the percent elongation for 'as cast', T4 and T6 heat treated secondary foundry alloy samples.

acicular or flaky in shape. This eutectic Si particle shape has been shown to adversely influence ductility and other mechanical properties of Al-Si alloys. Modification changes the morphology of the eutectic Si to a finer and more globular shape, which results in an improvement in ductility as seen in Figure 4.11.

4.5.2.3 Effect of Solution Treatment on the Tensile Strength

Figure 4.12 shows the influence of varying the solution time (curves SPA and SA) at 500^{o}C on the ultimate tensile strength of the 0.005%Na modified secondary alloy. The SA curve represents the variation of UTS for samples that

were solution treated for different times (4, 10, 14, 18, 24 and 32 hours) at 500^{o}C, quenched in water and artificially aged for 5 hours at 160^{o}C. These samples were not pre-aged. The tensile strength for the SA curve peaks at between 12h and 20h, the tensile values for the other solution treatment times being lower. The SPA curve represents the variation of tensile strength for samples

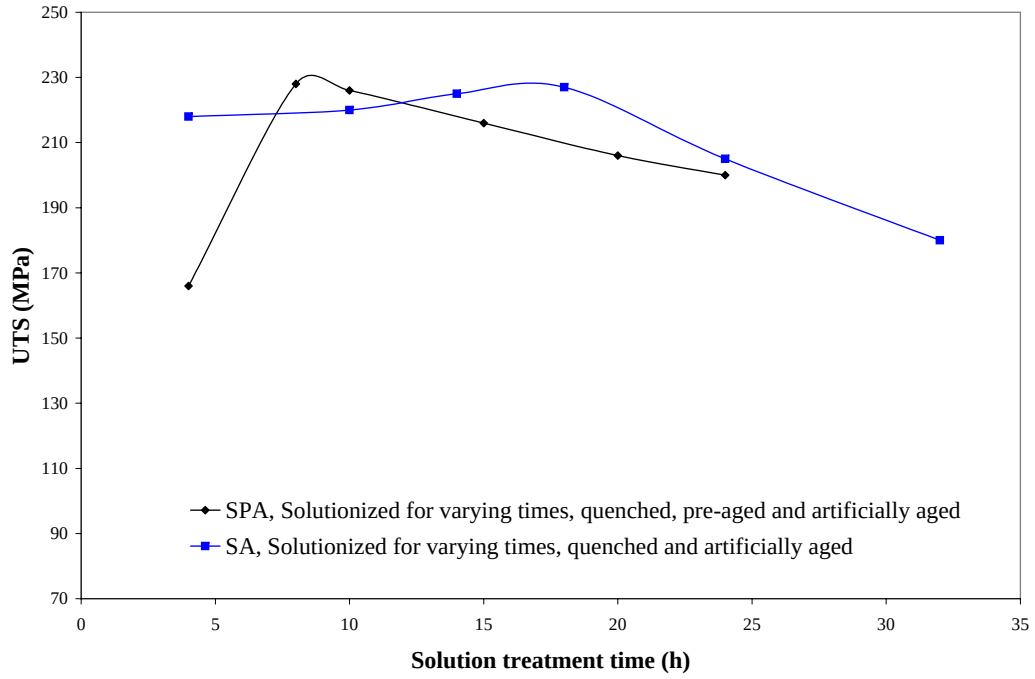

Figure 4.12: The effect of solution treatment time on the ultimate tensile strength for 0.005% Na modified recycled aluminium alloy.

that were solution treated for different times (4, 8, 10, 15, 20 and 24 hours) at 500^{o}C, quenched in water, pre-aged for 16 hours at room temperature and artificially aged for 5 hours at 160^{o}C. The tensile strength of these samples peaked at between 8 hours and 10 hours. The alloy that was not pre-aged (curve SA) has (on average) higher values of tensile strength when compared to the alloy that was pre-aged (curve SPA).

The observed trend does not agree with some of the results found in the literature for alloy A413.1. Moustafa et al. [86] varied the solution heat treatment times for an Al-Si base alloy (A413.1) and found that the tensile strength peaked

at around 4 hours for strontium modified and unmodified alloys. The tensile strength leveled off with a slow decrease up to a solution time of 24 hours. This behaviour may be attributed in part to the difference in composition, the modifier used and possibly the ageing treatment.

4.5.2.4 Effect of Ageing on the Tensile Strength

Figure 4.13 shows the variation of tensile strength with ageing time for the 0.005%Na modified recycled aluminium alloy. The SP-A samples were solution

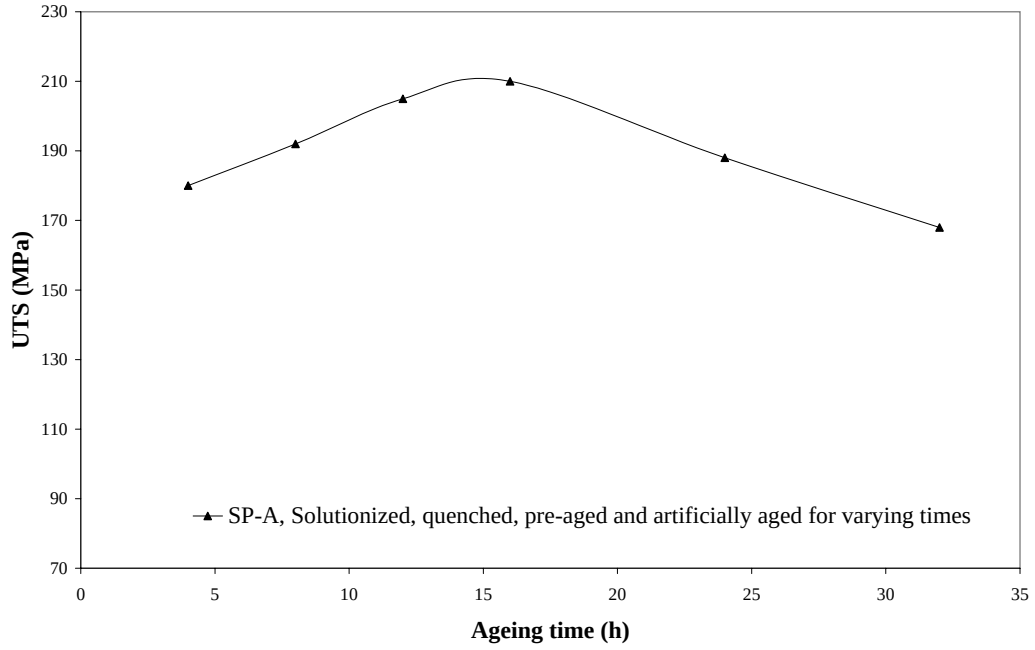

Figure 4.13: The effect of ageing on the ultimate tensile strength of 0.005% Na modified recycled aluminium alloy

treated for 8 hours at 500^{o}C, quenched in water, pre-aged for 16 hours at room temperature and artificially aged for different durations (4, 8, 12, 16, 24 and 32 hours) at 160^{o}C. It is seen that tensile strength values peaked at between 12 and 16 hours. Li et al. [96] in testing the age hardening behaviour of cast Al-Si base alloy, varied the ageing time at 175^{o}C and obtained curves of tensile behaviour generally similar to those illustrated in Figure 4.13. However, the

UTS had two ageing peaks, the first and the second peaks occurring after 6h and 12h respectively.

It can be seen in Table 4.3 that overageing (SP-OA24 samples) and natural ageing (SNA samples) led to a reduction in the tensile strengths of the alloy (135 and 160 MPa respectively). 'As cast' samples had the lowest strength value (113 MPa).

In the age hardening process of Al-Si-Cu-Mg alloy, GP zones and metastable phase can effectively strengthen and lead to ageing peaks. In the early stages of ageing, fine and profuse GP zones homogenously distribute in the matrix, resulting in significant strengthening effect, hence an increase in the tensile strength. The process of precipitation in Al-Si-Cu-Mg alloys is likely to be as follows: supersaturated solid solution → formation of GP zones → dissolution of GP zones → formation of metastable phases → formation of equilibrium phase [96]. It is likely that the peak in the curve of Figure 4.13 is due to strengthening of the alloy as a result of the formation of homogenously distributed GP zones.

4.5.2.5 Quality Index Curves

Figure 4.14 shows the flow curves for the 0.005% Na modified samples aged for different times.

The samples tested were aged for 4, 12, 16, 24 and 32 hours (flow curves SP-A4, SP-A12, SP-A16, SP-A24 and SP-A32 respectively). The SP-OA24 curve represents the samples that were subjected to artificial ageing for 24 hours at 280^{o}C (overaged). It is observed that increasing the ageing time progressively lowers the ductility of the samples with the samples aged for 32 hours (curve SP-A32) giving the lowest ductility while those aged for only 4 hours (curve SP-A4) had comparatively higher ductility. The highest strength samples were those aged for 12 and 16 hours while the lowest strength samples were those

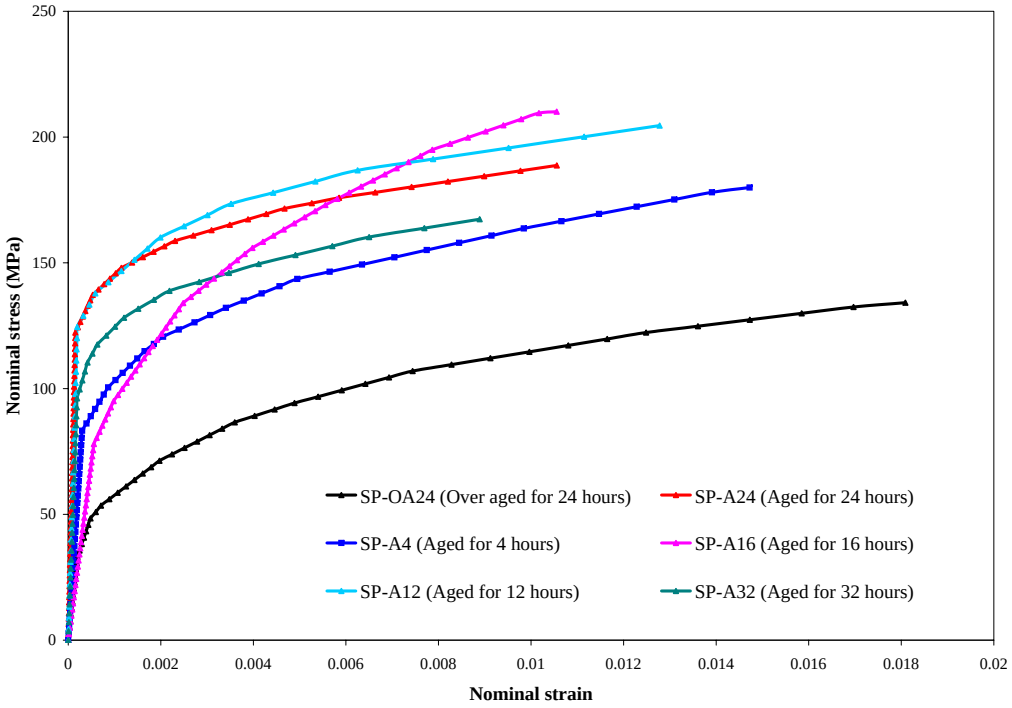

Figure 4.14: Nominal stress - nominal strain flow curves for 0.005% Na modified SPA samples. Solution heat treated for varying times at 500^{o}C, quenched, pre-aged and artificially aged for 5h at 160^{o}C.

aged for 4 hours, however, the ductility of the samples aged for 4 hours was close to that of the overaged samples (curve SP-OA24). Overaged samples have the lowest strength but show an improvement of ductility when compared to the other aged samples.

In order to obtain the quality index curves for the studied alloys, it was necessary to determine the parameters of the flow curves, namely; the strength coefficient, K_q and the strain hardening exponent, n. This was achieved by replotting the flow curves of Figure 4.14 and fitting the function $\sigma = K_q\epsilon^n$ (Equation 2.3) in Figure 4.15.

The fitting parameters are summarized in Table 4.4. It is noted that there is no clear trend on both the strength coefficient and the strain hardening exponent with ageing time. Comparatively, the overaged samples had lower strain hard-

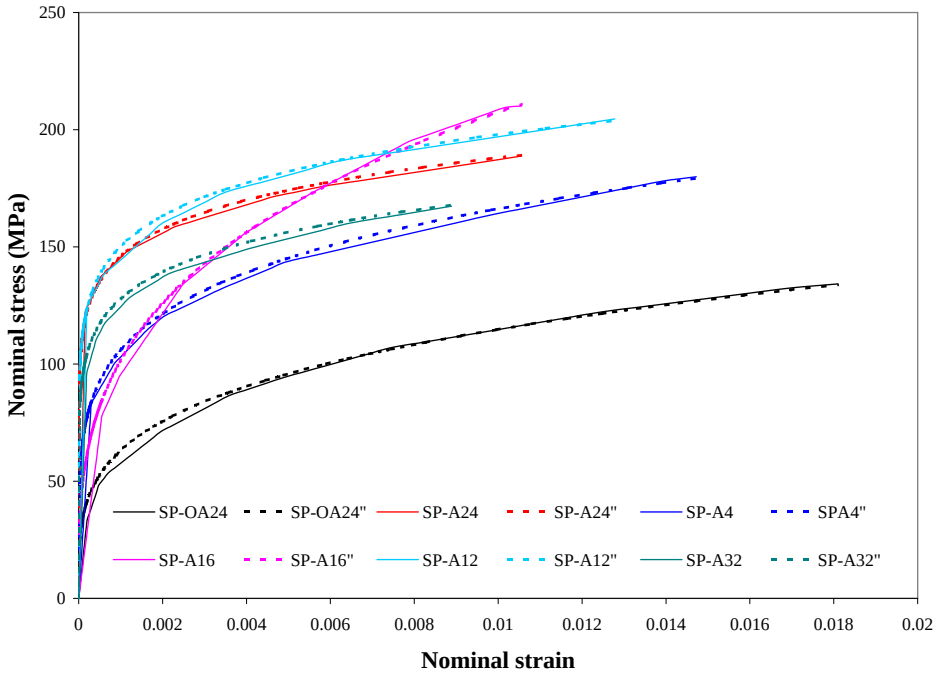

Figure 4.15: Nominal stress - nominal strain flow curves for 0.005% Na modified SP-A samples fitted to the function $\sigma = \mathrm{K}_q\epsilon^n$ (Equation 2.3).

Table 4.4: The strength coefficient, K_q, and the strain hardening exponent, n, of the 0.005% secondary foundry alloy under different ageing conditions.

Alloy Code	Strength Coefficient, K_q (N/mm^2)	Strain hardening exponent, n
SP - A4	408	0.195
SP - A12	344	0.12
SP- A16	243	0.31
SP - A24	311	0.11
SP - A32	303	0.125
SP - OA24	380	0.26

ening rate at all levels of strains tested as opposed to the other samples which had high strain hardening rate at low strains only. Caseres et al. [37] in testing the effect of ageing and Mg content on the quality index of Al-Si-Cu-Mg found overaged samples to have high strain hardening rate at low strains and low strain hardening rate at large strains. The parameters obtained from Figure 4.14 and tabulated in Table 4.4 were then used to create the quality index charts for the

alloy. A single value of the strength coefficient, ($K_q = 350\text{N/mm}^2$), was selected for the range of ageing times used in the test for use in plotting the quality index curves. The single K_q-value was necessary in order to have a common base for plotting the quality index curves. Figure 4.16 was obtained by using the equations $\text{P} \cong K_q \text{s}^n \exp^{-s}$ (Equation 2.4) and $\text{P} = K_q \text{s}^{s/q} \exp^{-s}$ (Equation 2.6) for the n values indicated (in Figure 4.16).

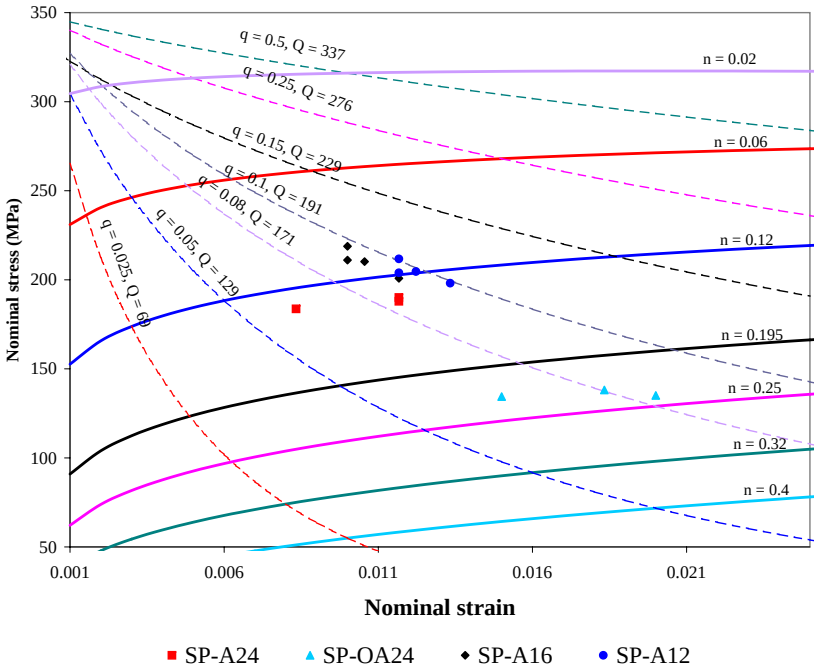

Figure 4.16: A quality index chart for the secondary foundry alloy studied. Solid lines represent the flow curves identified by the respective n-values (n is strain hardening exponent), while the dotted lines are the Iso-q (constant relative ductility parameter) curves identified by the respective q and Q values (Q is the quality index).

The plots of tensile strength-strain data obtained experimentally for selected ageing conditions were also included in Figure 4.16. The Q-values for all the iso-q lines in Figure 4.16 were computed using the equation $\text{Q} = K_q[(\text{qn})^n \text{e}^{-qn} + 0.4\log(100\text{qn})]$ (Equation 2.8) assuming $n = 0.25$. However, it has been reported

that using different values of n in Equation 2.8 has negligible influence on the value of Q [37].

The trend of the tensile strength - strain plots indicates that overageing reduces the quality of the alloy as compared to alloys aged for 12, 16 or 24 hours (aged and peak aged samples). Samples aged for 12 hours have the highest quality, marginally higher than those aged for 16 and 24 hours. A similar observation of a fall in alloy quality due to overageing was reported by Caseres et al. [37] while investigating the influence of ageing and Mg content in Al-Si-Cu-Mg alloys. It is further observed that, alloys aged for 12, 16 and 24 hours fall approximately on the same flow line (flow line with $n = 0.12$ in Figure 4.16) indicating that the strain hardening behaviour in the differently aged samples is not much different. However, overaged samples fall on a separate flow line (flow line with $n = 0.25$ in Figure 4.16), hence overageing affected the strain hardening behaviour of the secondary alloys significantly.

Figure 4.17 gives the quality index, Q, as a function of the strength coefficient, K_q. This illustrates the influence of change in the strength coefficient due to ageing on the quality index. The 'necking control' line gives the Q-values for materials that fail by necking, implying that in tensile deformation, the region above this line cannot be accessed. The data points for the various ageing conditions shown in Figure 4.17 were obtained by using the values of K_q in Table 4.4 in equations Q = UTS + dlog(s_f) (Equation 2.1) and d = -$\frac{dP}{ds} \cong 0.4K_q$ (Equation 2.7). For a given K_q-value, the range of data points represents the differences in ductility caused by the different dendrite arm spacing (DAS), eutectic silicon and Fe-rich intermetallic particle size and/or porosity content [37]. Defect free samples with fine DAS would be expected to have a high ductility and the data points would be placed close to the 'necking control' line in Figure 4.17. The 'necking line' represents the upper bound for microstructural

improvement, in terms of the quality index, for any given K_q-value.

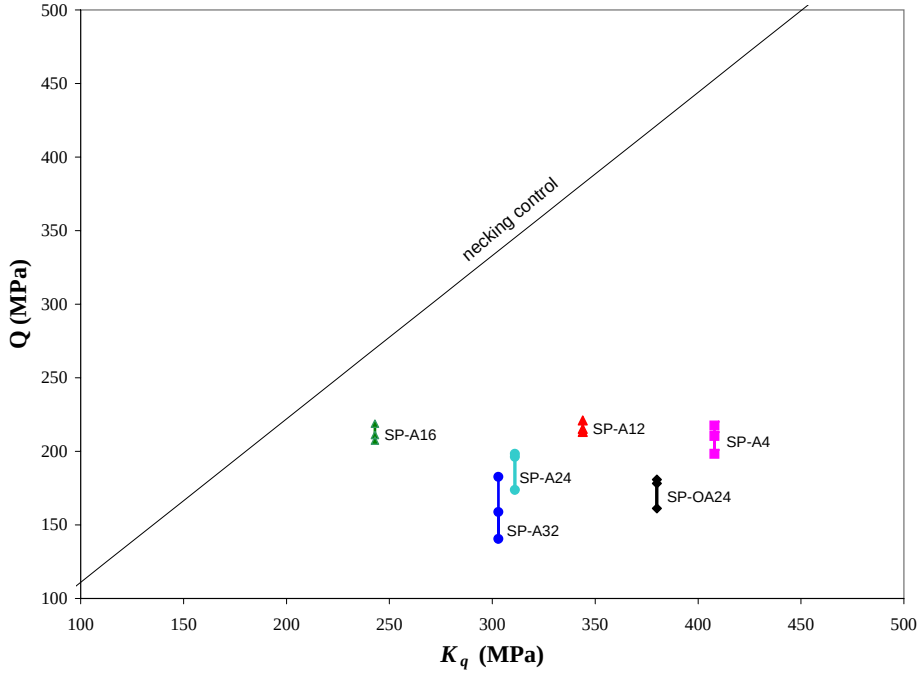

Figure 4.17: The quality index curve as a function of the material strength coefficient, K_q. The 'necking control' line was calculated using $Q = 1.11K_q$ (Equation 2.10).

The data points for the various ageing conditions are all positioned away from the 'necking control' line in Figure 4.17. This indicates that the samples were unlikely to reach the necking stage during tensile deformation. Instead, early brittle fracture is more likely. This behaviour maybe attributed to the fact that the samples were sand cast and hence would have large DAS, porosity and possibly a large number of Fe-rich intermetallics due to the high Fe content.

4.6 Fatigue Life Properties

4.6.1 Introduction

Constant amplitude, fully reversed fatigue life tests under a stress ratio, R = -1 and a frequency, f = 33 Hz were carried out using a rotating bending machine under room temperature conditions. Unmodified, 0.013%Na modified, and

0.020%Na modified samples were subjected to T4 and T6 heat treatment while others were fatigue tested in the 'as cast' condition. The results obtained on the effect of heat treatment and modification on fatigue life properties are presented and discussed in the following section.

4.6.2 Effect of Heat Treatment on Fatigue life Properties

Results of the fatigue tests for unmodified cast recycled aluminium alloys are shown in Figure 4.18 where the alternating stress amplitude, $\sigma_a = 0.5(\sigma_{max} - \sigma_{min})$ is plotted against Log N (N being the number of cycles to fracture).

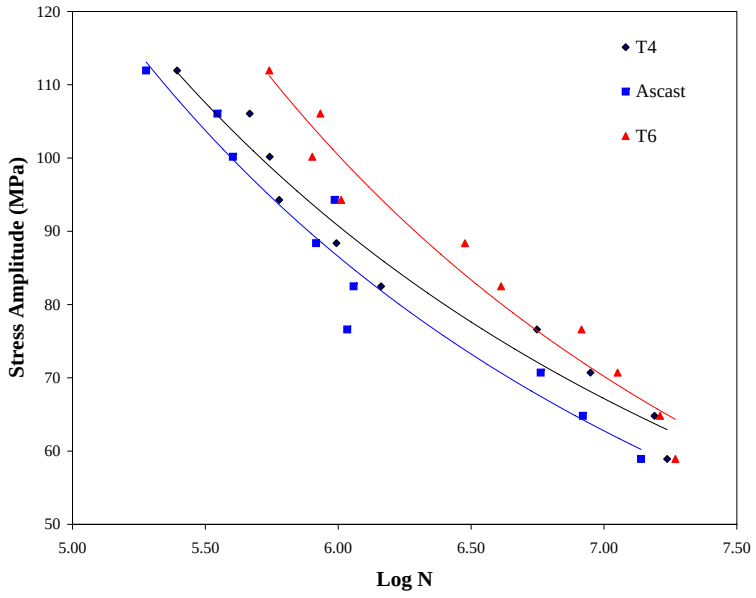

Figure 4.18: Stress amplitude against Logarithm of Cycles to failure (S versus Log N) fatigue curves for unmodified recycled cast aluminium alloy.

The T6 heat treated unmodified recycled aluminium foundry alloys generally had higher fatigue life than the T4 and 'as cast' specimens. In all the temper conditions, the fatigue limit is approximately 60 MN/m^2 where the fatigue life-times were in excess of 10^7. 'As cast' alloys had the lowest fatigue lifetimes in all the levels of applied stresses tested. Weibull statistical analysis was used to examine the effect of heat treatment on the fatigue life properties of the alloys.

The two parameter Weibull plots obtained for the unmodified cast alloys are presented in Figure 4.19.

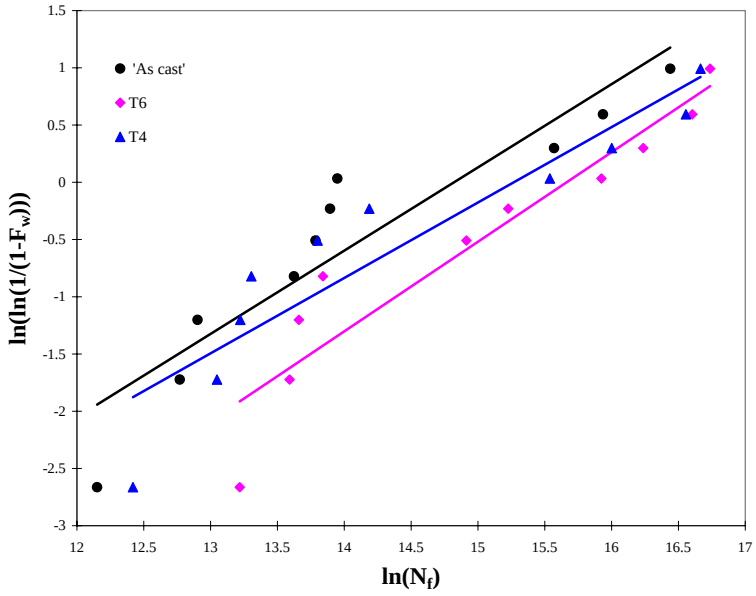

Figure 4.19: Two parameter Weibull plots for unmodified recycled cast aluminium alloy.

Figure 4.20 shows S versus Log N curves for T4 heat treated, T6 heat treated and 'as cast' 0.013% sodium modified specimens. In all the three cases, the fatigue life increases with decreasing stress amplitude. 'As cast' specimens fractured at $3x10^6$ cycles at a stress amplitude of 60 MN/m^2, while T4 and T6 specimens never fractured. Instead the samples showed a fatigue limit of approximately 60 MN/m^2 with fatigue lifetimes in excess of 10^7 for both T6 and T4 specimens. The results show that the T6 heat treated specimens generally had longer fatigue lives compared to T4 and 'as cast' aluminium alloys. 'As cast' 0.013%Na modified recycled aluminium foundry alloys had the lowest fatigue life at the stress levels tested. The two parameter Weibull plots for this case are shown in Figure 4.21.

Fatigue lifetime test results for 0.020%Na modified recycled aluminium foundry alloys are presented in Figure 4.22. Similarly, T6 heat treated samples had

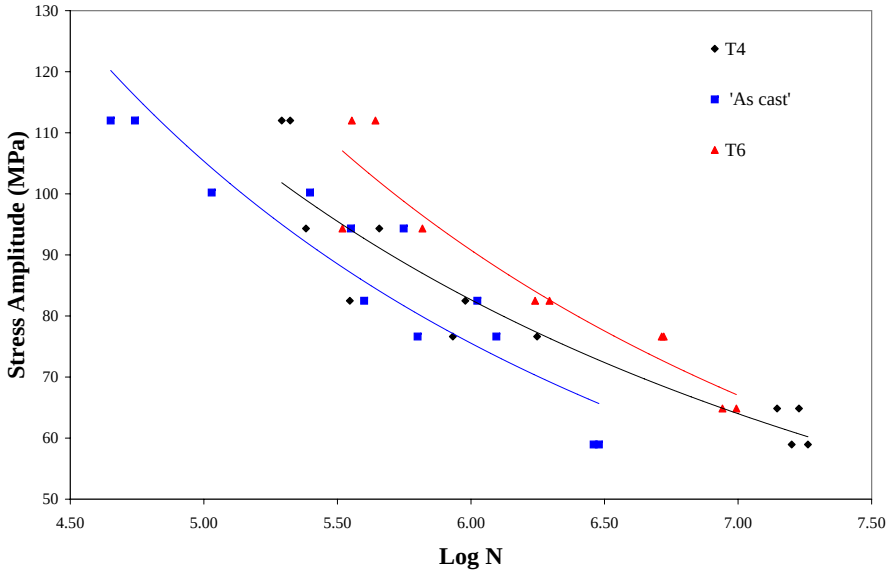

Figure 4.20: S versus Log N fatigue curves for 0.013%Na modified recycled cast aluminium alloy.

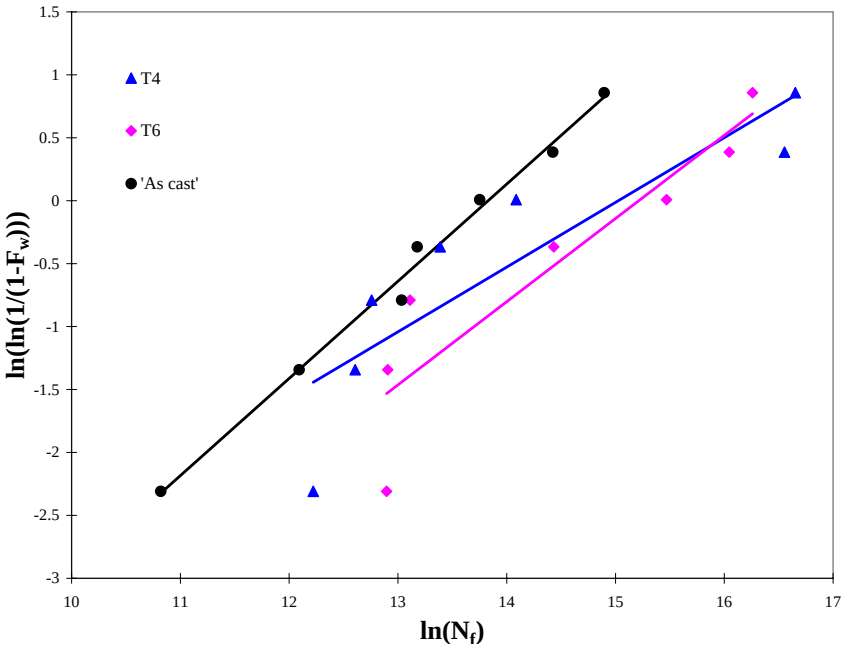

Figure 4.21: Two parameter Weibull plots for 0.013%Na modified recycled cast aluminium alloy.

higher fatigue life than 'as cast' and T4 heat treated samples. In this case however, the T6 samples had a fatigue life in excess of 20^7 cycles, T4 samples had a fatigue life of nearly 15^7 cycles, while 'as cast' samples had a fatigue

life of just over 3.5^6 cycles. The two parameter weibull plots for the 0.020%Na modified alloys are shown in Figure 4.23.

Table 4.5 gives a summary of the shape parameter, β, and the characteristic life, α, obtained from the two parameter Weibull analysis showing the influence of heat treatment on the fatigue life.

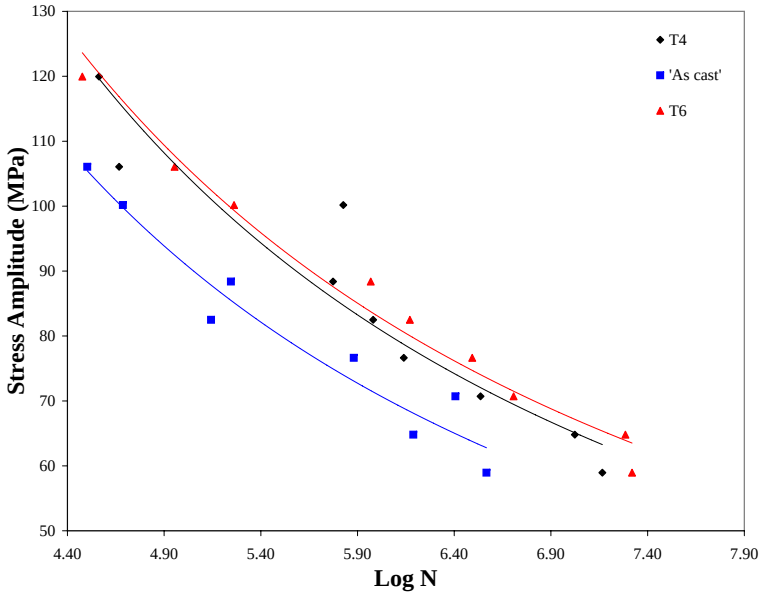

Figure 4.22: S versus Log N fatigue curves for 0.020%Na modified recycled cast aluminium alloy.

Analysis of the fatigue data using Weibull statistics shows that for unmodified alloy, T6 heat treated samples had a characteristic life of $6.34\text{x}10^6$ cycles while T4 and 'as cast' samples had characteristic lives of $4.27\text{x}10^6$ and $2.73\text{x}10^6$ cycles respectively. T6 heat treated samples had over two times the characteristic life 'as cast' samples.

In the case of 0.013%Na modified alloys, at $4.0\text{x}10^6$, the characteristic life of T6 heat treated samples was almost four times higher than 'as cast' samples. 0.013%Na modified T4 heat treated samples had a characteristic life of $3.4\text{x}10^6$ cycles which was close to that of T6 samples.

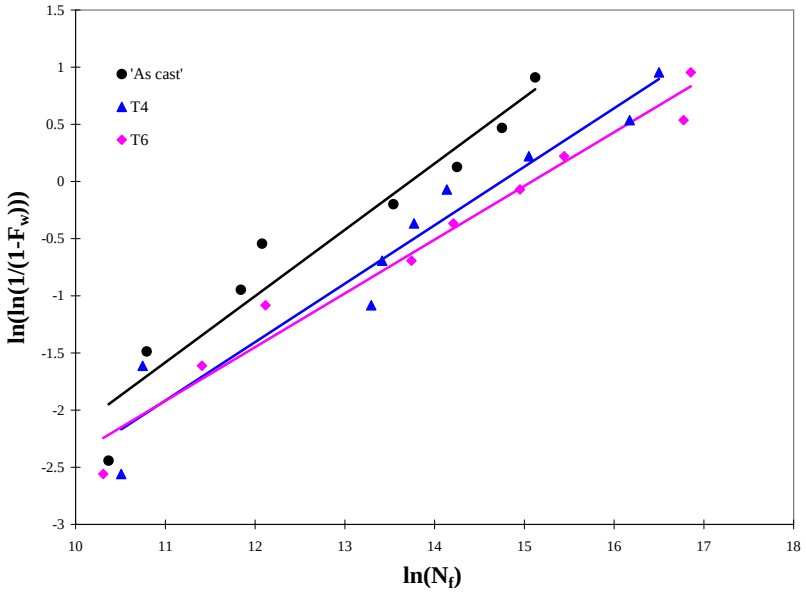

Figure 4.23: Two parameter Weibull plots for for 0.020%Na modified recycled cast aluminium alloy.

Table 4.5: Weibull parameters for the three sets of cast alloys tested showing the influence of heat treatment on the fatigue life.

Modification	Temper	Shape parameter, β	Characteristic life, α
Unmodified	As cast	0.727	2,733,171
	T4	0.659	4,273,738
	T6	0.783	6,345,853
0.013%Na modified			
	As cast	0.722	1,013,228
	T4	0.514	3,355,706
	T6	0.661	4,051,139
0.020%Na modified	As cast	0.580	917,128
	T4	0.511	2,539,775
	T6	0.470	3,550,796

For the 0.020%Na modified T6 heat treated samples, the characteristic life was 3.55×10^6 cycles, which was close to four times that of 'as cast' samples (9.12×10^5 cycles).

This analysis shows that T6 heat treatment improved the fatigue lives of both the modified and unmodified cast samples over samples that were not heat treated.

Although T4 heat treatment similarly improves the fatigue life, the increase was found to be always less than for T6 samples.

Scatter of fatigue life data was exceptionally high in all the cases tested as shown by the low numbers of the shape parameters. This may be attributed to the likelihood of high numbers of different fatigue crack initiators of different sizes and location within the test samples. Due to the casting method used, the melt treatment procedures and filtration method, new and old oxide film films are likely to have found their way into the castings. Other crack initiating sites could have been gas and shrinkage porosity, eutectic silicon and iron intermetallic particles. Examination of the fatigue fracture surfaces to determine the crack initiating sites would have clarified these probabilities. However, this was not possible due to lack of the appropriate equipment for carrying out fracture surface examination.

4.6.3 Effect of Modification on Fatigue Life properties

To assess the effect of modification on the fatigue life time of the cast alloys, the curves in Figures 4.24, 4.26 and 4.28 were plotted representing the different temper conditions. Figures 4.25, 4.27 and 4.29 are the corresponding two parameter Weibull plots obtained for the different temper conditions after analyzing the fatigue life results using Weibull statistical analysis. Table 4.6 gives a summary of the shape parameter, β, and the characteristic life, α, obtained from the two parameter Weibull analysis showing the influence of modification on the fatigue life.

The curves in Figures 4.24, 4.26 and 4.28 show that in the two temper conditions and 'as cast' condition, the fatigue life is consistently higher in unmodified recycled aluminium foundry alloys. In the cases considered, 0.013% modification led to reduced fatigue life properties as opposed to the higher fatigue

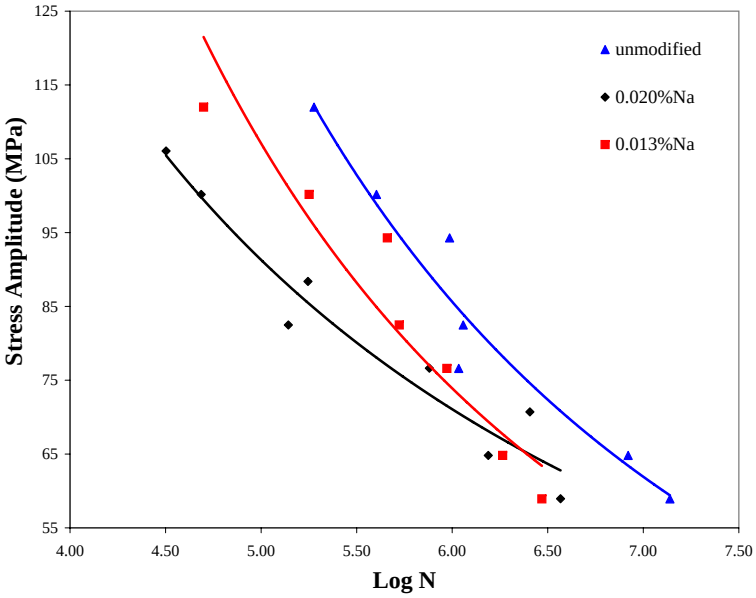

Figure 4.24: Fatigue lifetime curves for 'as cast' recycled aluminium foundry alloy

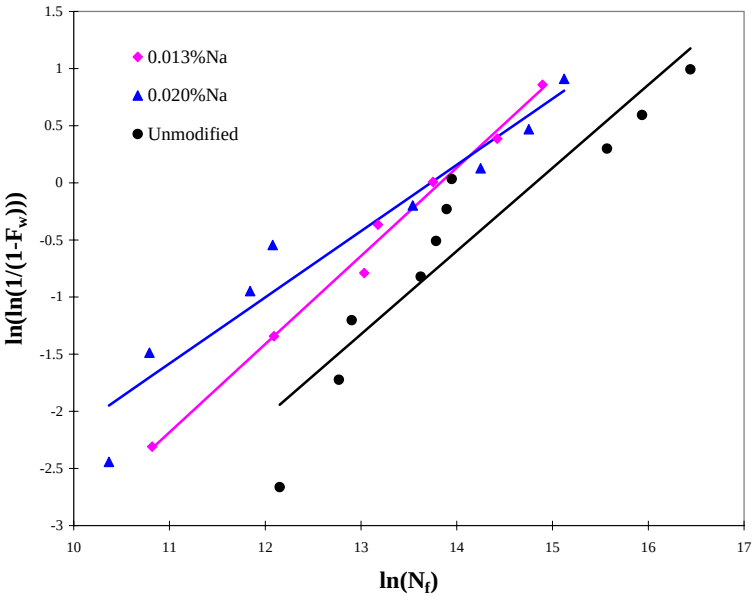

Figure 4.25: Two parameter Weibull plots for 'as cast' recycled aluminium foundry alloy.

properties evident in the unmodified recycled cast aluminium alloys. The fatigue lifetime properties of the unmodified, 0.013% Na and 0.020%Na modified recycled foundry alloys are compared in Figure 4.30. Figure 4.30 shows that

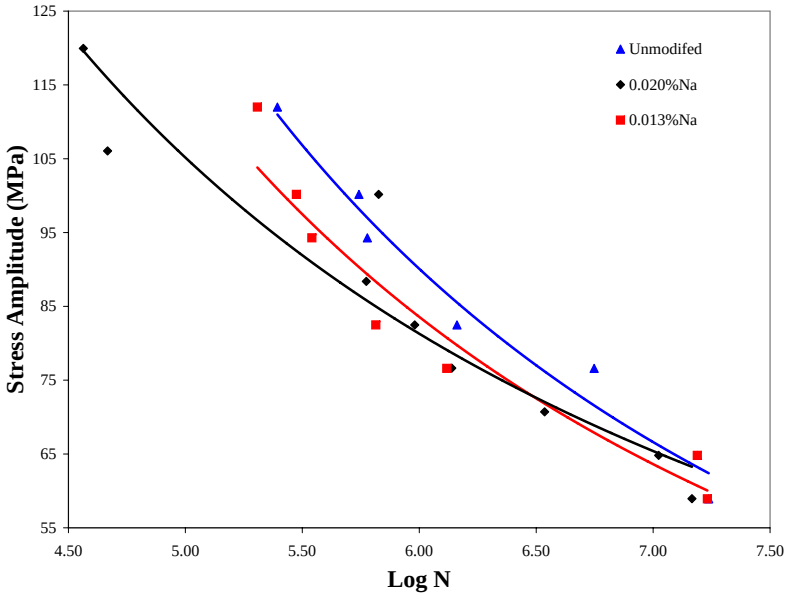

Figure 4.26: Fatigue lifetime curves for T4 heat treated recycled aluminium foundry alloy

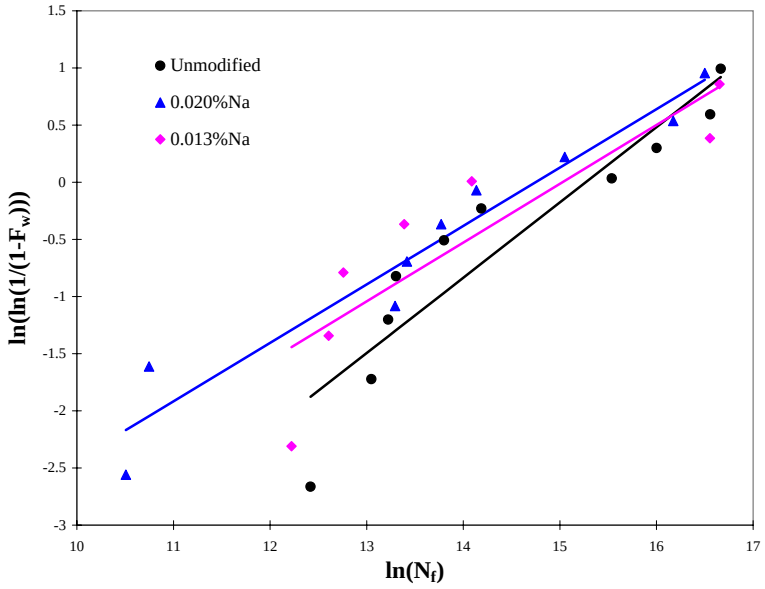

Figure 4.27: Two parameter Weibull plots for T4 heat treated recycled aluminium foundry alloy.

the unmodified T6 treated recycled cast aluminium alloys have the highest fatigue lifetimes while the 0.020% Na modified 'as cast' have the lowest fatigue lifetimes. The results indicate that 0.02%Na modification of the Al secondary

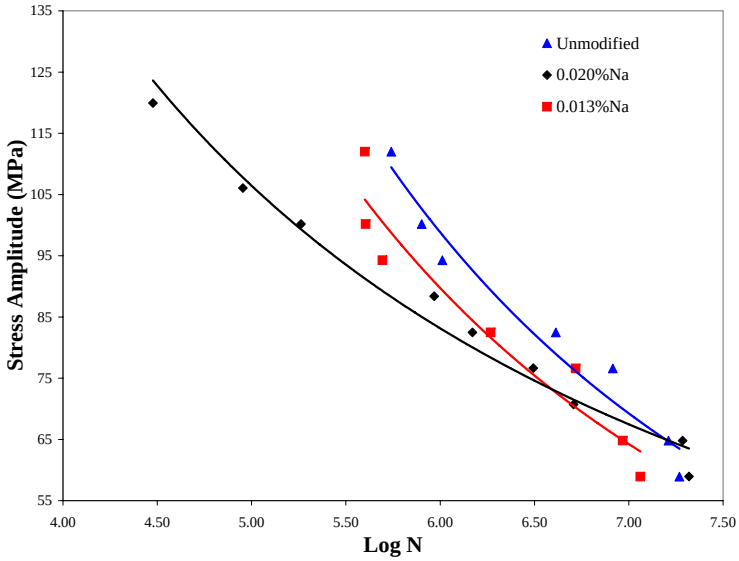

Figure 4.28: Fatigue lifetime curves for T6 heat treated recycled aluminium foundry alloy

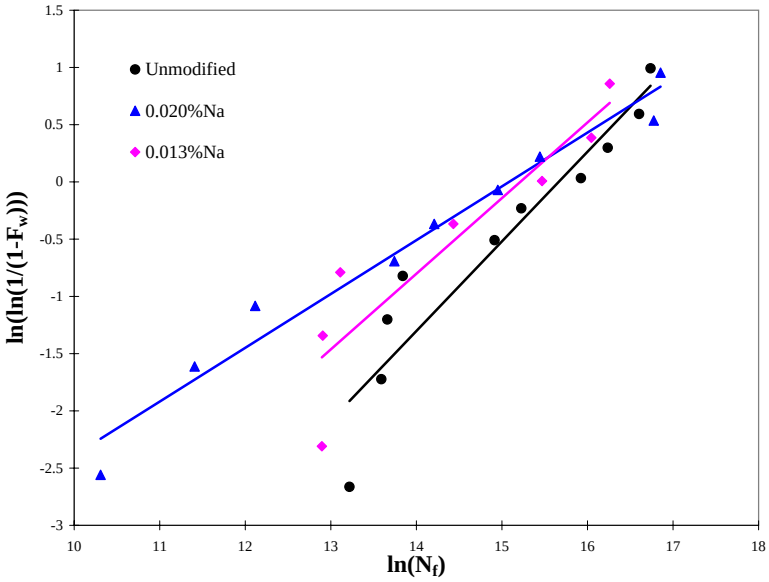

Figure 4.29: Two parameter Weibull plots for T6 heat treated recycled aluminium foundry alloy.

alloy tested in this study leads to a reduction in fatigue life of over 50%.

Weibull statistical analysis was used to investigate the influence of modification on the fatigue life of the 'as cast', T4 and T6 heat treated recycled aluminium

Table 4.6: Weibull parameters for the three sets of cast alloys tested showing the influence of modification on the fatigue life.

Temper condition	Modification	Shape parameter, β	Characteristic life, α
As cast	Unmodified	0.727	2,733,171
	0.013%Na modified	0.722	1,013,228
	0.020%Na modified	0.580	917,128
T4			
	Unmodified	0.659	4,273,738
	0.013%Na modified	0.514	3,355,706
	0.020%Na modified	0.511	2,539,775
T6	Unmodified	0.783	6,345,853
	0.013%Na modified	0.661	4,051,139
	0.020%Na modified	0.470	3,550,796

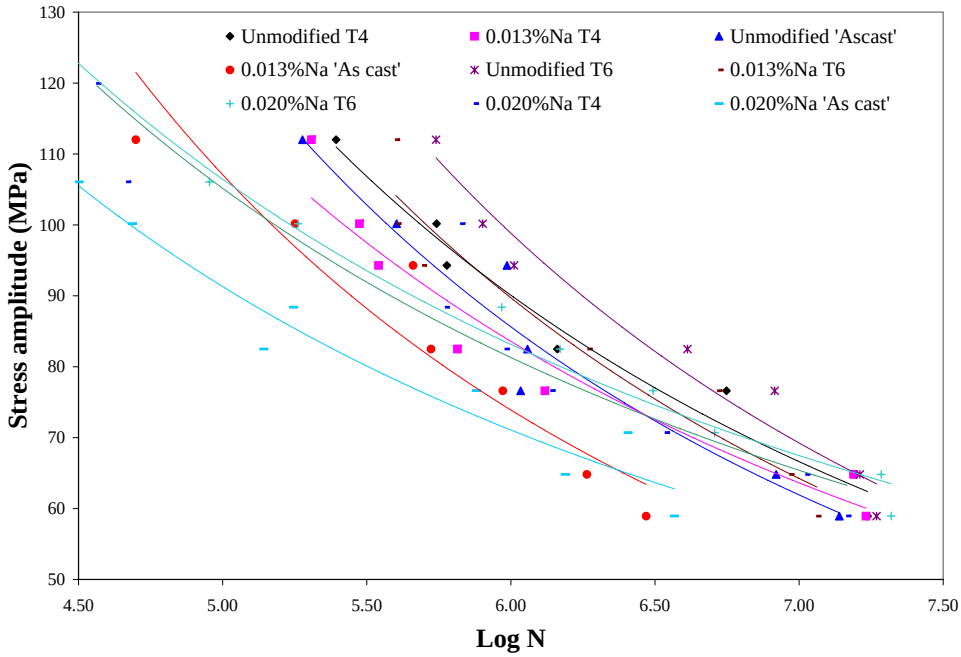

Figure 4.30: Fatigue lifetime curves for unmodified, 0.013% and 0.020%Na modified recycled aluminium foundry alloy

alloys. The summary of the Weibull parameters given in Table 4.6 shows that 'as cast', unmodified samples had a characteristic life of 2.75 x 10^6, while 0.013%Na and 0.020%Na modified had characteristic lives of 1.01 x 10^6 and 9.12 x 10^5 respectively. For this case, 'as cast' had a characteristic life over two times that

of 0.020%Na modified samples.

For the T4 treated samples, the unmodified sample had a characteristic life of 4.27 x 10^6, while the corresponding values for 0.013%Na modified and 0.020%Na modified were 3.34 x 10^6 and 2.54 x 10^6 respectively. In this case, 'as cast' samples had a life almost two times that of 0.020%Na modified samples. Characteristic lives for the T6 heat treated samples were 6.345 x 10^6, 4.05 x 10^6 and 3.55 x 10^6 for the unmodified, 0.013% and 0.020%Na modified alloys respectively. Similarly, the unmodified alloys had a characteristic life that was almost two times higher than that of 0.020%Na modified alloys.

This analysis shows that modification of the recycled aluminium alloys results in reduction in fatigue life by as much as 50%. The severity of reduction in fatigue life increases with increase in modifier level from 0.013%Na to 0.020%Na. A close observation of the fracture surfaces indicate that the cracks are likely to have initiated from high density defect location sites. Microstructural examination of the modified alloys showed a larger size of pores as well as an increase in the number of pores observed when compared to the unmodified alloys. This indicates that addition of modifiers could lead to an increase in the volume and size of porosity in cast aluminium alloys. Ideally, modifier treatment should be done by immersing vacuum packed (in aluminium cans) metallic sodium into the melt. However, in certain cases, it could be stored in paraffin [4] and plunged into the melt using a suitable plunger. The latter method was used in this study because it was not possible to obtain Navac in suitably sized vacuum packed aluminium cans. One major disadvantage of using this method is that sodium packed in this manner still contains some paraffin, which is a source of hydrogen. Consequently, aluminium alloys treated with metallic sodium of this type are usually gassy and castings produced from them are usually highly porous [106]. This could be the reason why there was an increase in the volume

percent and size of porosity and hence the reduction in the fatigue life properties of the recycled aluminium alloys.

Chapter 5

CONCLUSIONS

The influence of modifiers and heat treatment on the mechanical and fatigue properties, microstructure and chemical composition of cast secondary aluminium alloys were investigated in this study. Quality index charts for the recycled aluminium alloys were also developed. The secondary aluminium alloys were cast from selected scrap components. These components were mainly pistons, cylinder heads, gearbox casings and oil sumps. The mechanical properties tested were the ultimate tensile strength, the percent elongation and the hardness. Fatigue properties were also investigated and reported in the form of S versus Log N curves. To investigate the influence of modifiers, five levels of modifier amount were selected; 0.00%Na (unmodified), 0.005%Na, 0.013%Na, 0.020%Na and 0.025%Na. The alloys were then heat treated to the T6 and T4 temper conditions while some were tested in the 'as cast' condition. In order to investigate the influence of heat treatment on mechanical properties and to develop the quality index charts, the 0.005%Na modified alloys were subjected to varying solution treatment and ageing times. The following conclusions can be inferred from the investigation carried out:

- The secondary alloys obtained from the scrap samples are hypoeutectic Al-Si-Cu-Mg based alloys. The alloys had high contents of Cu and Mg compared to the commonly used Al-Si-Mg based alloys.

- The secondary alloys obtained in this study are approximately equivalent to several commercial Al-Si alloys, mainly the British LM4, LM22; the US 319, A319, W319 and the Japanese AC 2A.

- Heat treating the alloy to the T6 condition improves the fatigue life properties over the 'as cast' condition by up to 50%.

- The fatigue life properties obtained for the secondary aluminium alloys are lower than those usually obtained from commercial alloys of similar compositions.

- Modification of the alloys results in the deterioration of fatigue life properties of the cast secondary alloys, for example, increasing the modifier amount to 0.020%Na leads to close to 50% reduction in fatigue life of the secondary alloy.

- Modification increases the influence of heat treatment on the microstructure which leads to greater spheroidisation of the Si eutectic particles.

- The mechanical properties do not correlate well with similar commercial Al-Si alloys. This may be due to the presence of large number of defects and the presence of large Fe-rich intermetallics.

- Hardness of secondary alloys increases with increase in ageing time.

- Heat treatment to the T6 condition increases the ultimate tensile strength and the hardness of the secondary alloy compared to the T4 condition. The effect of T4 heat treatment condition on the ultimate tensile strength and hardness is intermediate between the 'as cast' and the T6 heat treatment condition.

- Modification improves the ultimate tensile strength and the elongation of the secondary aluminium alloys obtained in this study.

Chapter 6

RECOMMENDATIONS

To further clarify certain pertinent issues related to cast recycled aluminium alloys, it is recommended that more work be carried out in the following areas;

- The influence of ageing on the mechanical properties should be investigated further. This would be particulary interesting in cases where pre-ageing of the alloy after quenching is not done.

- The use of a two stage solution treatment has been reported to bring about improved mechanical properties in Cu-containing aluminium alloys. It would be interesting to investigate any influence that a similar treatment would have on the mechanical properties of secondary aluminium alloys similar to the ones studied in this work.

- The quality index curves obtained in this work do not agree with trends obtained elsewhere for similar primary aluminium alloys. Further work in this regard would be necessary to clarify or correct the behaviour obtained in this study.

- The effect of modification on mechanical and fatigue properties, using methods which are in line with modern best practice for melt treatment in the aluminium alloy casting industry, should be investigated further. Further, the possible improvement in mechanical properties by using efficient degassing and inclusion control and removal techniques would be desirable. This would entail using modern equipment such as the rotary impeller degasser and online hydrogen level monitoring using equipments such as the Alcan or the Telegas.

- The failure behaviour of these alloys under thermomechanical loading conditions should be studied. This is necessary to provide insight on their

possible application in high temperature conditions such as for cylinder heads and engine blocks.

REFERENCES

[1] M. J. Caton, *Predicting Fatigue Properties of Cast Aluminium Alloys by Characterizing Small Crack Propagation Behaviour.* Phd., University of Michigan, 2001.

[2] J. A. Taylor, "Metal-related castability effects in aluminium foundry alloys," *Cast Metals*, vol. 8, no. 4, pp. 225–252, 1997.

[3] G. Atxaga, A. Pelayo, and A. M. Irisarri, "Effect of microstructure on fatigue behaviour of cast Al-7Si-Mg alloy," *Materials Science Technology*, vol. 17, no. 4, pp. 446–450, 2001.

[4] J. E. Gruzleski and B. M. Closset, *The treatment of liquid aluminium silicon alloys.* The American Foundrymen's Society, Inc., 1990.

[5] R. Chase, "Aluminium Report - Aluminium's Contribution To Sustainable Modern Living," tech. rep., International Aluminium Institute, 2006.

[6] "Status of Jua Kali sheds in the country," Tech. Rep., Ministry of Research and Applied Technology - Republic of Kenya, 1992.

[7] S. M. Maranga, "Foundry Education and Operations: Aspects for Consideration by the Kenyan Industrial Sector," in *Sixth Mechanical Engineering Seminar - The Focus of Engineering Research for the Industruial Development in the New Millenium, JKUAT, Kenya.*, (JKUAT, Juja, Kenya), 2000.

[8] T. O. Mbuya, *Cast Aluminium Scrap Recycling: Influence of alloy chemistry and process variables on the structure and mechanical properties.* Msc thesis, University of Nairobi, 2003.

[9] F. King, *Aluminium and its Alloys.* Ellis Horwood Limited, 1st ed., 1987.

[10] *A Guide to Melt Treatment in the Aluminium Foundry.* LSM Metallurg Aluminium, 2006.

[11] J. M. Boileau and J. E. Allison, "The effect of porosity on the fatigue properties in a cast 319 aluminium alloy," in *SAE 2001 World Congress*, (Detroit, Michigan), SAE Technical Paper Series, 2001.

[12] L. F. Mondolfo, *Aluminium alloys: structure and properties.* Butterworths, London, 1st ed., 1976.

[13] B. Zhang, W. Chen, and D. R. Poirier, "Effect of solidification cooling rate on the fatigue life of A356.2-T6 cast aluminium alloy," *Fatigue and Fracture Engineering Materials and Structures*, vol. 23, pp. 417–423, 2000.

[14] A. K. Dahle and D. H. StJohn, "Processing from the liquid state," Tech. Rep. CAST/REP/2001139, Cooperative Research Centre for Cast Metals Manufacturing, 2001.

[15] A. K. Dahle, "Casting and solidification of light alloys," Tech. Rep. CAST/REP/2001139, Cooperative Research Centre for Cast Metals Manufacturing, 2001.

[16] J. Campbell, *Castings.* London: Butterworth Publications, 1st ed., 1990.

[17] J. Campbell, ""Ten Rules for Good Castings"," *Modern Casting*, vol. 87, no. 4, pp. 36–39, 1997.

[18] M. Cox, M. Wickins, J. Kuang, R. A. Harding, and J. Campbell, "Effect of top and bottom filling on reliability of investment castings in Al, Fe and Ni based alloys," *Materials Science and Technology*, vol. 16, pp. 1445–1452, 2000.

[19] M. Avalle, G. Belingardi, M. P. Cavartota, and R. Doglione, "Casting defects and fatigue strength of a die cast aluminium alloy: a comparison between standard specimens and production components," *International Journal of Fatigue*, vol. 24, pp. 1–9, 2002.

[20] K. Shiozawa, Y. Tohda, and S.-M. Sun, "Crack initiation and small fatigue crack growth behaviour of squeeze-cast Al-Si alloys," *Fatigue and Fracture Engineering Materials and Structures*, vol. 20, no. 2, pp. 237–247, 1997.

[21] S. Ishihara and A. J. McEvily, "Analysis of short fatigue crack growth in cast aluminium alloys," *International Journal of Fatigue*, vol. 24, no. 11, pp. 1169–1174, 2002.

[22] *Modification of Aluminium Silicon Foundry alloys.* LSM, 2006.

[23] *Heat Treatable Aluminium Alloys.* Key to Metals, www.key-to-metals.com, 2006.

[24] F. Paray and J. E. Gruzleski, "Microstructure - Mechanical property relationships in a 356 alloy. Part I - Microstructure," *Cast Metals*, vol. 7, no. 1, pp. 29–40, 1994.

[25] S. Kumai, S. Aoki, S.-W. Han, and A. Sato, "Effects of dendrite cell size and eutectic Si particle morphology on fatigue crack growth in cast HIPed AC4CH alloys," *Materials Transactions, JIM*, vol. 40, no. 7, pp. 685 – 691, 1999.

[26] T. Kobayashi, T. Ito, and N. Fatahalla, "Fatigue properties and microstructure of Al-Si-Cu system casting alloys," *Materials Science and Technology*, vol. 15, pp. 1037–1043, 1999.

[27] S. G. Shebastari, S. M. Miresmaeli, and S. M. A. Boutorabi, "Effect of Sr modification and melt cleanliness on melt hydrogen absorption of 319 Al alloy," *Journal of Materials Science*, vol. 38, pp. 1901–1907, 2003.

[28] Y. C. Cho, Y. R. Im, S. Kwon, and H. C. Lee, "The effect of alloying elements on the microstructure and mechanical properties of Al-12Si cast alloys," *Materials Science Forum*, vol. 426-432, pp. 339–344, 2003.

[29] Q. G. Wang, C. H. Caseres, and J. R. Griffiths, "Cracking of Fe-rich intermetallics and eutectic Si particles in an Al-7Si-0.7Mg casting alloy," *AFS Transactions*, vol. 32, pp. 131–136, 1998.

[30] F. Lee, J. Major, and F. Samuel, "Fracture behaviour of Al-12Si-0.35Mg-0.02Sr casting alloy under fatigue testing," *Fatigue and Fracture Engineering Materials and Structures*, vol. 18, no. 3, pp. 385–396, 1995.

[31] Q. G. Wang, D. Apelian, and J. R. Griffiths, "Microstructural effects on the fatigue properties of aluminium castings," in *Advances in Aluminium Casting Technology* (M. T. and J. Campbell, eds.), (Rosemont, Illinois), pp. 217–223, ASM International, 1998.

[32] M. Drouzy, S. Jacob, and M. Richard, "Interpretation of tensile results by means of Quality Index and probable yield strength," *AFS International Cast Metals Journal*, vol. 5, pp. 43–50, 1980.

[33] C. H. Caseres, M. Makhlouf, D. Apelian, and L. Wang, "Quality Index chart for different alloys and temperatures: a case study on aluminium die-casting alloys," *Journal of Light Materials*, vol. 1, pp. 51–59, 2001.

[34] F. Paray and J. E. Gruzleski, "Microstructure - Mechanical property relationships in a 356 alloy. Part II - Mechanical Properties," *Cast Metals*, vol. 7, pp. 153–163, 1994.

[35] C. H. Caseres and J. Barresi, "Selection of temper and Mg content to optimise the Quality Index of Al-7Si-Mg casting alloys," *International Journal of Cast Metals Research*, vol. 12, pp. 377–384, 2000.

[36] C. H. Caseres, "A rationale for the Quality Index of Al-Si-Mg casting alloys," *International Journal of Cast Metals Research*, vol. 10, pp. 293–299, 1998.

[37] C. H. Caseres, J. Sokolowski, and P. Gallo, "Effect of ageing and Mg content on the Quality Index of two model Al-Cu-Si-Mg alloys," *Materials Science and Engineering A*, vol. 127, pp. 53–61, 1999.

[38] C. H. Caseres, "A phenomenological approach to the Quality Index of Al-Si-Mg casting alloys," *International Journal of Cast Metals Research*, vol. 12, pp. 367–375, 2000.

[39] C. H. Caseres, T. Din, A. Rashid, and J. Campbell, "Effect of ageing on the Quality Index of an Al-Cu alloy," *Materials Science Technology*, vol. 15, pp. 711–716, 1999.

[40] T. Din, A. Rashid, and J. Campbell, "High strength aerospace casting alloys: quality factor assessment," *Materials Science Technology*, vol. 12, pp. 269–273, 1996.

[41] G. E. Dieter, *Mechanical Metallurgy*. Butterworth Publishers, London, metric ed., 1990.

[42] J. F. Major, "Porosity control and fatigue behaviour in A356-T61 Alloy," *AFS Transactions*, vol. 94, pp. 901–906, 1997.

[43] M. J. Couper, A. E. Neeson, and J. R. Griffiths, "Casting defects and the fatigue behaviour of an aluminium casting alloy," *Fatigue and Fracture Engineering Materials and Structures*, vol. 13, no. 3, pp. 213–227, 1990.

[44] C. M. Sonsino and J. Ziese, "Fatigue strength and applications of aluminium alloys with different degrees of porosity," *International Journal of Fatigue*, vol. 2, pp. 75–84, 1993.

[45] Q. G. Wang, D. Apelian, and D. A. Lados, "Fatigue behaviour of A356-T6 aluminium cast alloys. Part I - Effect of casting defects," *Journal of Light Materials*, vol. 1, pp. 73–84, 2001.

[46] B. Zhang, P. K. Sung, D. R. Poirier, and W. Chen, "Effects of Strontium modification and Hydrogen content on fatigue behaviour of A356.2 al alloy," *AFS Transactions*, vol. 42, pp. 383–389, 2000.

[47] D. A. Lados, D. Apelian, and A. M. de Figueredo, "Fatigue performance of high integrity cast aluminium components," in *International Casting Technology Symposium*, (Columbus, OH.), ASM International, 2002.

[48] B. Skallerud, T. Iveland, and G. Harkegard, "Fatigue life assessement of aluminium alloys with casting defects," *Engineering Fracture Mechanics*, vol. 44, no. 6, pp. 857–874, 1993.

[49] J. A. Odegard and K. Pedersen, "Fatigue properties of an A356(AlSi7Mg) aluminium alloy for automotive applications - fatigue life prediction," *SAE Technical Series Papers*, pp. 25 – 31, 1994.

[50] S. E. Stanzl-Tschegg, H. R. Mayer, E. K. Tschegg, and A. Beste, "In-service loading of AlSi11 aluminium cast alloy in the very high cycle regime," *International Journal of Fatigue*, vol. 15, no. 4, pp. 311–316, 1993.

[51] H. Mayer, M. Papakyriacou, B. Zettl, and S. E. Stanzl-Tschegg, "Influence of porosity on the fatigue limit of die cast magnesium and aluminium alloys," *International Journal of Fatigue*, vol. 25, pp. 245–256, 2003.

[52] C. T. Jason and V. L. Frederick, "Modeling of long life fatigue behaviour of a cast aluminium alloy," *Fatigue and Fracture Engineering Materials and Structures*, vol. 16, no. 6, pp. 631–647, 1993.

[53] J.-Y. Buffiere, S. Savelli, P. H. Jouneau, E. Maire, and R. Fougeres, "Experimental study of porosity and its relation to fatigue mechanisms of model Al-7Si-0.3Mg cast Al alloys," *Materials Science and Engineering A*, vol. 316, pp. 115–126, 2001.

[54] Y. X. Gao, J. Z. Yi, P. D. Lee, and T. C. Lindley, "The effect of porosity on the fatigue life of cast Al-Si alloys," *Fatigue and Fracture Engineering Materials and Structures*, vol. 27, pp. 559–570, 2004.

[55] S. Savelli, J.-Y. Buffiere, P. H. Jouneau, and R. Fougeres, "Fatigue mechanisms of a model Al-7Si-0.3Mg cast Aluminium alloy," *Materials Science Forum*, vol. 331-337, pp. 203–208, 2000.

[56] Q. G. Wang, P. E. Jones, and M. Osborne, "Effect of Iron on the microstructure and mechanical properties of an Al-7Si-0.4Mg casting alloy," in *Proceeding from the 2nd International Aluminum Casting Technology Symposium 79 October 2002, Columbus*, 2002.

[57] Y. Kuroki, T. Tanaka, T. Sato, and A. Kamio, "Effects of defects and Fe intermetallic compounds on fatigue properties of Al-Si-Cu-Mg alloy castings," *Materials Transactions, JIM*, vol. 42, no. 11, pp. 2339–2344, 2001.

[58] Y.-H. Tan, S.-L. Lee, and H.-Y. Wu, "Effects of Be on fatigue crack propagation of A357 alloys containing iron," *International Journal of Fatigue*, vol. 18, no. 2, pp. 137–147, 1996.

[59] *ASTM E 155 Standard Reference Radiographs for Inspection of Aluminum and Magnesium Castings.*

[60] M. J. Caton, J. W. Jones, J. M. Boileau, and J. E. Allison, "The effect of solidification rate on the growth of small fatigue cracks in a cast 319-type Al alloy," *Metallurgical and Materials Transactions A*, vol. 30A, pp. 3055–3068, 1999.

[61] B. Zhang, D. R. Poirier, and W. Chen, "Effects of HIPping and Sr modification on the fatigue behaviour of A356.2 aluminium alloy," *AFS Transactions*, vol. 02, no. 123, pp. 1–13, 2002.

[62] S. E. Stanzl-Tschegg, H. R. Mayer, A. Beste, and S. Kroll, "Fatigue and fatigue crack propagation in AlSi7Mg cast alloys under service loading conditions," *International Journal of Fatigue*, vol. 17, no. 2, pp. 149–155, 1995.

[63] M. H. Lee, J. J. Kim, H. K. Kyung, J. K. Nack, L. Sunghak, and W. L. Eui, "Effects of HIPping on high-cycle fatigue properties of investment cast A356 aluminium alloys," *Materials Science and Engineering A*, vol. A00, pp. 1–7, 2002.

[64] S. Mashl, J. C. Hebeisen, D. Apelian, and Q. Wang, "Hot Isostatic Pressing of A356 and 380/383 Aluminium Alloys: An Evaluation of Porosity, Fatigue Properties and Processing Costs," in *SAE 2000 World Congress*, (Detroit, Michigan), pp. 1–6, 2000.

[65] J. Campbell, C. Nyahumwa, and N. R. Green, "The concept of the fatigue potential of cast alloys," in *Materials Solutions Conference '98 on Aluminium Casting Technology* (M. Tiryakioglu and J. Campbell, eds.), (Rosemont, Illinois), pp. 225–233, 1998.

[66] C. Nyahumwa, J. Campbell, and N. R. Green, "Effect of mold filling turbulence on fatigue properties of cast aluminium alloys," *AFS Transactions*, vol. 58, pp. 215–223, 1998.

[67] N. R. Green and J. Campbell, "Influence of oxide film filling on the strength of Al-7Si-Mg Alloy Castings," *AFS Transactions*, vol. 114, pp. 341–347, 1994.

[68] M. Avalle, G. Belingardi, M. P. Cavartota, and R. Doglione, "Static and fatigue strength of a die cast aluminium alloy under different feeding conditions," *Proceedings of the Institution of Mechanical Engineers*, vol. 216, no. Part L, pp. 25–30, 2002.

[69] H. Jiang, P. Bowen, and J. F. Knott, "Fatigue performance of a cast aluminium alloy Al-7Si-Mg with surface defects," *Journal of Materials Science*, vol. 34, pp. 719–725, 1999.

[70] R. E. Spear and G. R. Gardner, "Dendrite Cell Size," *Transactions of the American Foundrymen's Society*, vol. 71, pp. 209–215, 1964.

[71] A. Wickberg, G. Gustafsson, and L. E. Larsson, "Microstructural effects on the fatigue properties of a cast Al-7Si-Mg alloy," *SAE Technical Series Papers*, pp. 729–735, 1985.

[72] Q. G. Wang, D. Apelian, and D. A. Lados, "Fatigue behaviour of A356/357 Aluminium cast alloys. Part II - Effect of microstructural constituents," *Journal of Light Materials*, vol. 1, pp. 85–97, 2001.

[73] D. A. Lados and D. Apelian, "Fatigue crack growth characteristics in cast Al-Si-Mg alloys - Part I: Effect of processing and microstructure," *Materials Science and Engineering A*, vol. A385, pp. 200–211, 2004.

[74] C. J. Davidson, J. R. Griffiths, and A. S. Machin, "The effect of solution heat treatment time on the fatigue properties of Al-Si-Mg casting alloy," *Fatigue and Fracture of Engineering Materials and Structures*, vol. 25, pp. 223–230, 2001.

[75] K. Togho and M. Oka, "Influence of coarsening treatment on fatigue strength and fracture toughness of Al-Si-Mg casting alloy," *Key Engineering Materials*, vol. 261-263, pp. 1263–1268, 2004.

[76] F. Lee, J. Major, and F. Samuel, "Effect of Si particles on the fatigue crack growth characteristics of Al-12Si-0.5Mg-Sr casting alloys," *Metallurgical and Materials Transactions A*, vol. 26A, pp. 1553–1571, 1995.

[77] C. M. Styles and P. A. S. Reed, "Fatigue of an Al-Si gravity die casting alloy," *Materials Science Forum*, vol. 331-337, pp. 1457–1462, 2000.

[78] C. H. Caseres, C. Davidson, J. R. Griffiths, L. Hogan, and Q. G. Wang, "Hypoeutectic Al-Si-Mg foundry alloys," *Materials Forum*, vol. 21, pp. 27–43, 1997.

[79] G. E. Dieter, *Engineering Design.* McGraw Hill, 1982.

[80] D. A. Lados and D. Apelian, "The Effect of Residual Stress on the Fatigue Crack Growth Behavior of Al-Si-Mg Cast Alloys: Mechanisms and Corrective Mathematical Models," *Metallurgical and Materials Transactions A*, vol. 37A, pp. 133–145, 2006.

[81] X. Dai, X. Yang, J. Campbell, and J. Wood, "Effects of runner design on the mechanical strength of Al-7Si-Mg alloy castings," *Materials Science and Engineering A*, vol. 354, pp. 315–325, 2003.

[82] S. Guleyupoglu, "Casting process design guidelines," *AFS Transactions*, vol. 105, pp. 465–471, 1997.

[83] M. Cox, R. A. Harding, and J. Campbell, "Optimized running system design for bottom filled aluminium alloy 2L99 investment castings," *Materials Science and Technology*, vol. 19, pp. 613–625, 2003.

[84] H. Joseph, P. Cleary, V. Alguine, and T. Nguyen, "Simulation of die filling in gravity die casting using SPH and MAGMAsoft," in *Second International Conference on CFD in the Materials and Process Industries*, (CSIRO, Melbourne, Australia), pp. 423–428, 1999.

[85] G. Wang, X. Bian, W. Wang, and J. Zhang, "Influence of Cu and minor elements on the solution treatment of Al-Si-Cu-Mg cast alloys," *Materials Letters*, vol. 57, pp. 4083–4087, 2003.

[86] M. Moustafa, F. Samuel, and H. Doty, "Effect of solution heat treatment and additives on the hardness, tensile properties and fracture behaviour of Al-Si of Al-Si (A413.1) automotive alloys," *Journal of Materials Science*, vol. 38, pp. 4523–4534, 2003.

[87] *General Rules for Fatigue Testing of Metals - JIS Z 2273.* Tokyo: Hohbunsha Co., Ltd., 1st ed., 1978.

[88] *Methods of Rotating Bending Fatigue Testing of Metals - JIS Z 2274.* Tokyo: Hohbunsha Co., Ltd., 1st ed., 1978.

[89] *Method for Brinell Hardness Test; testing of metals, B.S. 240: Part 1: 1962.* London: British Standards Institution, 1962.

[90] M. Schaefer and R. Fournelle, "Effect of Strontium modification on near-threshold fatigue crack growth in an Al-Si-Cu die cast alloy," *Metallurgical and Materials Transactions A*, vol. 27A, pp. 1293–1301, 1996.

[91] L. Wang, M. Makhlouf, and D. Apelian, "Aluminium die casting alloys: alloy composition, microstructure, and properties-performance relationships," *International Materials Reviews*, vol. 40, no. 6, pp. 221–238, 1995.

[92] P. Ouillet and F. H. Samuel, "Effect of Mg on the ageing behaviour of Al-Si-Cu 319 type aluminium casting alloys," *Journal of Materials Science*, vol. 34, pp. 4671–4697, 1999.

[93] A. M. Samuel, P. Ouellet, and F. Samuel, "Microstructural interpretation of thermal analysis of commercial 319 Al alloy with Mg and Sr additions," *AFS Transactions*, vol. 105, pp. 951–962, 1997.

[94] Q. G. Wang and C. H. Caseres, "Mg effects on the eutectic structure and tensile properties of Al-Si-Mg alloys," *Materials Science Forum*, vol. 242, pp. 159–164, 1997.

[95] M. Tash, F. H. Samuel, F. Mucciardi, and H. W. Doty, "Effect of metallurgical parameters on the hardness and microstructural characterization of as cast and heat treated 356 and 319 aluminium alloys," *Materials Science and Engineering A*, vol. A, no. 443, pp. 185–201, 2007.

[96] R. X. Li, R. Li, Y. Zhao, L. He, C. Li, H. Guan, and Z. Hu, "Age-hardening behaviour of cast Al-Si base alloy," *Materials Letters*, vol. 58, pp. 2096–2101, 2004.

[97] W. Miao and D. Laughlin, "Effects of Cu content and Pre-aging on precipitation characteristics in Aluminium alloy 6022," *Metallurgical and Materials Transactions A*, vol. 31A, 2000.

[98] A. Gangulee and J. Gurland, "On the fracture of Silicon particles in Al-Si alloys," *Transactions of the Metallurgical Society of AIME*, vol. 239, pp. 269–273, 1967.

[99] S. F. Frederick and W. A. Bailey, "The relation of ductility to dendrite cell size in a cast Al-Si-Mg alloy," *Transactions of the Metallurgical Society of AIME*, vol. 242, pp. 2063–2067, 1968.

[100] C. Verdu, H. Cercueil, S. Communal, P. Sainfort, and R. Fougeres, "Microstructural aspects of damage mechanisms of cast Al-7Si-Mg alloys," *International Journal of Fatigue*, vol. 19, pp. 729–729(1), 1997.

[101] C. H. Caseres and J. R. Griffiths, "Damage by cracking of Si particles in an Al-7Si-0.4Mg casting alloy," *Acta Matellurgica Materiala*, vol. 44, no. 1, pp. 25–33, 1996.

[102] M. Manoharan, J. J. Lewandowski, and W. H. J. Hunt, "Fracture characteristics of an Al-Si-Mg model composite system," *Materials Science and Engineering A*, vol. 172, pp. 63–69, 1993.

[103] F. Mahmoud and K. Toshiro, "A study of the microstructure and fracture behaviour relations in Al-Si casting alloys," *Scripta Metallurgica*, vol. 30, no. 6, pp. 475–480, 1994.

[104] C. H. Caseres, C. Davidson, and J. R. Griffiths, "The deformation and fracture behaviour of an Al-Si-Mg casting alloy," *Materials Science and Engineering A*, vol. 197, pp. 171–179, 1995.

[105] F. Mahmoud and K. Toshiro, "Tensile properties influencing variables in eutectic Al-Si casting alloys," *Scripta Metallurgica*, vol. 31, no. 6, pp. 701–705, 1994.

[106] J. R. Brown, *Foseco Foundryman's Handbook*. London: Pergamon Press plc., 9 ed., 1986.

Appendix A

Tabulated Results

Table A.1: Tensile properties of unmodified, 0.013% and 0.020% Na modified 'as cast', T4 and T6 recycled aluminium alloy samples

Na (Modifier)	UTS ($MN/m^{2)}$			Elongation (%)			Hardness (BHN)		
Amount(%)	As cast	T4	T6	As cast	T4	T6	As cast	T4	T6
0.000	108	120	165	0.9	1.2	1.3	86	95	111
0.005	113	160	185	1.3	1.7	1.8	88	96	110
0.013	116	183	206	1.6	1.9	2.3	89	95	109
0.020	130	196	216	2	2.2	2.8	88	96	112
0.025	135	203	226	2.3	2.6	3.2	89	94	110

Table A.2: Tensile and hardness properties of 0.005% Na modified solution heat treated and artificially aged recycled aluminium alloy samples. The solution treatment times were varied at a constant temperature of 500^{o}C without pre-ageing.

Alloy Code	Solution Time (h)	Preaging Time (h)	Aging Time (h)	UTS (MPa)	Elongation (%)	Hardness (BHN)
SA-4	4	0	5	218	1.8	108
SA-10	10	0	5	220	2.1	110
SA-14	14	0	5	225	2.3	113
SA-18	18	0	5	227	2.2	117
SA-24	24	0	5	205	2.1	122
SA-32	32	0	5	180	2.0	125

Table A.3: Tensile and hardness properties of 0.005% Na modified solution heat treated, pre-aged and artificially aged recycled aluminium alloy samples. The solution heat treatment times were varied at a constant temperature of 500^{o}C. The samples were pre-aged for 16 hours at room temperature.

Alloy Code	Solution Time (h)	Preaging Time (h)	Aging Time (h)	UTS (MPa)	Elongation (%)	Hardness (BHN)
AC*	0	0	0	113	1.3	83.5
SPA-4	4	16	5	166	1.5	120
SPA-8	8	16	5	228	1.8	115
SPA-10	10	16	5	226	1.8	112
SPA-15	15	16	5	216	1.6	109
SPA-20	20	16	5	206	1.5	107
SPA-24	24	16	5	200	1.5	106

* - Tested in the 'as cast' condition.

Table A.4: Tensile and hardness properties of 0.005% Na modified solution heat treated, pre-aged and artificially aged recycled aluminium alloy samples. The ageing times were varied at a constant temperature of 160^{o}C.

Alloy Code	Solution Time (h)	Preaging Time (h)	Aging Time (h)	UTS (MPa)	Elongation (%)	Hardness (BHN)
SP-A4	8	16	4	180	1.5	106
SP-A8	8	16	8	192	1.4	111
SP-A12	8	16	12	205	1.3	114
SP-A16	8	16	16	210	1.1	118
SP-A24	8	16	24	188	1.1	125
SP-A32	8	16	32	168	0.9	129

Appendix B

Brinell Hardness Table

Table B.1: Table of Brinell Hardness values (HB) used to obtain hardness of the test specimens [89]

DIAMETER OF BALL = 10 mm LOAD = 1 000 kgf $F/D^2 = 10$

Diameter of impression	0·00	0·01	0·02	0·03	0·04	0·05	0·06	0·07	0·08	0·09
mm										
2·50	200	199	197	196	194	193	191	190	188	187
2·60	185	184	182	181	179	178	177	175	174	173
2·70	171	170	169	168	166	165	164	163	162	160
2·80	159	158	157	156	155	154	152	151	150	149
2·90	148	147	146	145	144	143	142	141	140	139
3·00	138	137	136	135	135	134	133	132	131	130
3·10	129	128	128	127	126	125	124	123	123	122
3·20	121	120	120	119	118	117	117	116	115	114
3·30	114	113	112	112	111	110	110	109	108	108
3·40	107	106	106	105	104	104	103	102	102	101
3·50	101	100	99·5	98·9	98·3	97·7	97·2	96·6	96·1	95·5
3·60	95·0	94·4	93·9	93·3	92·8	92·3	91·8	91·2	90·7	90·2
3·70	89·7	89·2	88·7	88·2	87·7	87·2	86·8	86·3	85·8	85·3
3·80	84·9	84·4	83·9	83·5	83·0	82·6	82·1	81·7	81·3	80·8
3·90	80·4	80·0	79·5	79·1	78·7	78·3	77·9	77·5	77·1	76·7
4·00	76·3	75·9	75·5	75·1	74·7	74·3	73·9	73·5	73·2	72·8
4·10	72·4	72·0	71·7	71·3	71·0	70·6	70·2	69·9	69·5	69·2
4·20	68·8	68·5	68·2	67·8	67·5	67·1	66·8	66·5	66·2	65·8
4·30	65·5	65·2	64·9	64·6	64·2	63·9	63·6	63·3	63·0	62·7
4·40	62·4	62·1	61·8	61·5	61·2	60·9	60·6	60·4	60·1	59·8
4·50	59·5	59·2	59·0	58·7	58·4	58·1	57·9	57·6	57·3	57·1
4·60	56·8	56·5	56·3	56·0	55·8	55·5	55·3	55·0	54·8	54·5
4·70	54·3	54·0	53·8	53·5	53·3	53·0	52·8	52·6	52·3	52·1
4·80	51·9	51·6	51·4	51·2	51·0	50·7	50·5	50·3	50·1	49·8
4·90	49·6	49·4	49·2	49·0	48·8	48·6	48·3	48·1	47·9	47·7
5·00	47·5	47·3	47·1	46·9	46·7	46·5	46·3	46·1	45·9	45·7
5·10	45·5	45·3	45·1	45·0	44·8	44·6	44·4	44·2	44·0	43·8
5·20	43·7	43·5	43·3	43·1	42·9	42·8	42·6	42·4	42·2	42·1
5·30	41·9	41·7	41·5	41·4	41·2	41·0	40·9	40·7	40·5	40·4
5·40	40·2	40·0	39·9	39·7	39·6	39·4	39·2	39·1	38·9	38·8
5·50	38·6	38·5	38·3	38·2	38·0	37·9	37·7	37·6	37·4	37·3
5·60	37·1	37·0	36·8	36·7	36·5	36·4	36·3	36·1	36·0	35·8
5·70	35·7	35·6	35·4	35·3	35·1	35·0	34·9	34·7	34·6	34·5
5·80	34·3	34·2	34·1	33·9	33·8	33·7	33·6	33·4	33·3	33·2
5·90	33·1	32·9	32·8	32·7	32·6	32·4	32·3	32·2	32·1	32·0
6·00	31·8	—	—	—	—	—	—	—	—	—